Role of chemotaxis, cyclic-di-GMP and type 1 fimbriae in *Escherichia coli* surface attachment

Dissertation

Zur Erlangung des Doktorgrades der Naturwissenschaften

(Dr. rer. nat.)

Dem Fachbereich Biologie

der Philipps-Universität Marburg vorgelegt

von

María Esteban López

aus Madrid, Spain

Marburg, 2020

Die Untersuchungen zur vorliegenden Arbeit wurden von October 2016 bis April 2020 am Max-Planck-Institut für terrestrische Mikrobiologie in Marburg unter der Leitung von Prof. Dr. Victor Sourjik durchgeführt.

Vom Fachbereich Biologie der Philipps Universität Marburg (HKZ: 1180)

als Dissertation angenommen am: 2.06.2020

Erstgutachter: Prof. Dr. Victor Sourjik

Zweitgutachter: Dr. Simon Ringgaard

Weitere Mitglieder der Prüfungskommission:

Prof. Dr. Martin Thanbichler

Prof. Dr. Knut Drescher

Tag der mündlichen Prüfung: 28.08.2020

Die während der Promotion erzielten Ergebnisse wurden in folgender Originalpublikationen veröffentlicht:

Laganenka, L., **Esteban-Lopez, M**., Colin, R., & Sourjik, V. (2020). Flagellum-Mediated Mechanosensing and RflP Control Motility State of Pathogenic *Escherichia coli*. *mBio, 11*(2).

Suchanek, V. M*., **Esteban-Lopez, M***., Colin, R., Besharova, O., Fritz, K., & Sourjik, V. (2020). Chemotaxis and cyclic-di-GMP signalling control surface attachment of *Escherichia coli*. *Mol Microbiol.* 113(4):728-739.

*These authors contributed equally to this work.

“Nothing in life is to be feared, it is only to be understood. Now is the time to understand more, so that we may fear less.”

Marie Skłodowska-Curie

Content

Abbreviations

GFP	Green fluorescent protein
CFP	Cyan fluorescent protein
YFP	Yellow fluorescent protein
OD	Optical density
ddH_2O	Sterile ultra-pure water
DNA	Deoxyribonucleic acid
dNTP	Deoxyribonucleotide triphosphate
IPTG	Isopropyl-β-D-1-thiogalactopyranoside
rpm	Revolutions per minute
PCR	Polymerase chain reaction
c-di-GMP	Bis-(3′-5′)-cyclic dimeric guanosine monophosphate

Abstract

Bacteria are commonly found in their natural environments not as single cells, but as part of communities called biofilms. For biofilm formation, bacteria typically have to attach to a surface. This attachment is also important for the establishment of infections. In order to interact with the surfaces, bacteria have a series of appendages usually known as adhesins. Biofilm formation, as well as attachment, have been extensively studied. However, the role of each adhesins in attachment to different surfaces and the signaling involved in surface sensing is not fully understood.

This work aims to further understand the roles of motility and the main adhesins present in *E. coli* in attachment to both hydrophobic and hydrophilic surfaces under static conditions and under flow. Furthermore, the influence of chemotaxis and the second messenger bis-(3′-5′)-cyclic dimeric guanosine monophosphate (c-di-GMP) in the bacterial initial attachment was also studied.

In this work, motility mediated by the flagella was shown to be essential for cells to reach the surface and non-motile bacteria showed an impaired surface attachment and colonization. However, though flagella have been reported to play a role on attachment beyond motility, their relevance in attachment was strongly dependent on the experimental setup and phase of attachment. Thus, they were shown to be important as secondary adhesins for attachment to mannosylated surfaces and for attachment under flow. However, flagella did not improve the attachment to abiotic surfaces and, under certain conditions, the presence of a non-rotating flagella did impair attachment instead of favoring it. Motility in *E. coli* is controlled by the chemotaxis machinery and the second messenger c-di-GMP. The role of chemotaxis was studied by using chemotaxis deficient strains and chemoattractant stimulation and was shown to improve attachment by reducing the tumbling and increasing smooth swimming near the surface.

In the case of c-di-GMP, mutants of diguanylate cyclases and phosphodiesterases that are responsible for the c-di-GMP pool in the cell, as well as strains lacking the flagellar brake YcgR, were used. Though c-di-GMP is normally considered a biofilm promoting signal, the results presented in this work show that lower levels of this second messenger improve bacterial surface attachment and colonization by increasing bacterial swimming speed. Furthermore, type 1 fimbriae were found to mediate the increased attachment of these fast swimming bacteria. Both the effect of chemotaxis and c-di-GMP were observed on abiotic and mannosylated, biomimetic surfaces.

In the last part of these work, type 1 fimbriae were also observed to be crucial for long term surface attachment and growth on the surface. The need for fimbriae at later time points of attachment is abolished in the absence of protein synthesis and cell division.

Though differences in flagella expression were hypothesized to be responsible for these fimbrial requirement, flagella were shown to not be able to compensate for the lack of fimbriae. However, fimbriae were not essential for growth on the surface in the absence of motility. Non-motile flagellated cells were shown to be capable of attachment and growth at the surface. Although whole proteome analysis revealed an increased in fimbrial proteins upon attachment of motile cells, indicating a possible downstream effect of flagella surface sensing, it failed to explain the difference between attachment phenotype of wild-type and motility deficient but flagellated cells. Therefore, possible explanations of how lack of motility could bypass the need for fimbriae in long term attachment were proposed.

Zusammenfassung

Bakterien kommen in ihrer natürlichen Umwelt normalerweise nicht als einzelne Zellen vor, sondern als Teil von Gemeinschaften, die als Biofilme bezeichnet werden. Um solche Biofilme zu etablieren, müssen sich Bakterien typischerweise an Oberflächen anheften. Die Fähigkeit sich an verschiedene Oberflächen anzuheften spielt zudem eine wichtige Rolle bei bakteriellen Infektionen. Hierbei vermitteln bakterielle Zellanhänge, auch bekannt als Adhäsine, die Interaktion zwischen Bakterium und Oberfläche. In der Vergangenheit wurden zahlreiche Studien zur Entstehung von Biofilmen und bakterieller Adhäsion durchgeführt. Welche Rolle die einzelnen Adhäsine bei der Anhaftung und Erkennung von verschiedenen Oberflächen einnehmen bleibt jedoch noch immer unklar.

In dieser Arbeit wurde untersucht welche Rolle Motilität und die wichtigsten Adhäsine von *E. coli* auf die Anhaftung an hydrophobe und hydrophile Oberflächen bzw. in fließenden und nicht fließenden Flüssigkeiten, hat. Darüber hinaus wurde untersucht welchen Einfluss Chemotaxis und der Second Messenger bis-(3',5')-zyklischem di-Guanosinmonophosphat (c-di-GMP) auf die erste Phase der bakteriellen Anheftung hat.

In dieser Arbeit wurde gezeigt, dass die durch Flagellen vermittelte Motilität für das Erreichen der Oberfläche essenziell ist. Wobei nicht bewegliche Bakterien eine beeinträchtigte Oberflächenanhaftung und -besiedlung zeigten. Obwohl berichtet wurde, dass Flagellen eine Rolle bei der Anheftung spielen, die über Motilität hinausgeht, war ihre Relevanz für die Anheftung stark vom Versuchsaufbau und der Anheftungsphase abhängig. Es konnte jedoch gezeigt werden, dass sie als sekundäre Adhäsine für die Anhaftung an mannosylierten Oberflächen und für die Anhaftung in fließenden Flüssigkeiten wichtig sind. Flagellen verbesserten jedoch nicht die Anhaftung an abiotische Oberflächen. Unter bestimmten Bedingungen beeinträchtigten nicht rotierenden Flagellen die Anhaftung, anstatt sie zu begünstigen. Die Motilität in *E. coli* wird durch das Chemotaxis-System und den Second-Messenger c-di-GMP gesteuert. Die Rolle von Chemotaxis wurde mittels Chemotaxis-defizienten Stämmen und deren Stimulation mit Lockstoffen untersuch und zeigte, dass durch eine Verringerung des Taumelns die Zellen länger in geraden Bewegungen an der Oberfläche schwimmen und dadurch die Anheftung begünstigt wird. In Bezug auf c-di-GMP wurden Mutanten von Diguanylatcyclasen und Phosphodiesterasen, die für den c-di-GMP-Pool in der Zelle verantwortlich sind, sowie Stämme ohne Flagellenbremse YcgR verwendet. Obwohl c-di-GMP normalerweise als ein Biofilm förderndes Signal angesehen wird, zeigen die in dieser Arbeit vorgestellten Ergebnisse, dass ein niedrigerer c-di-GMP Spiegel die Anhaftung und Besiedlung von Oberflächen verbessern, indem die

Schwimmgeschwindigkeit der Bakterien erhöht wird. Darüber hinaus wurde festgestellt, dass Typ-1-Fimbrien die erhöhte Anhaftung dieser schnell schwimmenden Bakterien vermitteln. Sowohl der Effekt von Chemotaxis als auch von c-di-GMP wurden auf abiotischen und mannosylierten biomimetischen Oberflächen beobachtet.

Im letzten Teil dieser Arbeit wurde zudem beobachtet, dass Typ-1-Fimbrien für die langfristige Anhaftung und das Wachstum auf Oberflächen entscheidend sind. In der Abwesenheit von Proteinsynthese und Zellteilung ist die Notwendigkeit von Fimbrien zu späteren Zeitpunkten der Anhaftung vernachlässigbar.

Obwohl angenommen wurde, dass Unterschiede in der Flagellenexpression für die Notwendigkeit von Fimbrien für die Anheftung verantwortlich sind, konnte gezeigt werden, dass Flagellen das Fehlen von Fimbrien nicht kompensierten können. In der Abwesenheit von Motilität waren Fimbrien jedoch nicht essenziel für das Wachstum an Oberflächen. Nicht motile begeißelte Zellen konnten sich an Oberflächen anheften und wachsen. Die Analyse des gesamten Proteoms zeigte einen Anstieg von Fimbrien-Proteinen beim Anheften von motilen Zellen, was auf einen möglichen Downstream-Effekt, der durch Fimbrien vermittelte Erkennung von Oberflächen hinweist. Dies konnte jedoch nicht den phänotypischen Unterschied zwischen Wildtyp- und nicht motilen aber begeißelten Zellen erklären. Daher wurden mögliche Erklärungen vorgeschlagen, wie das Fehlen von Motilität die Notwendigkeit von Fimbrien bei langfristiger Anheftung umgehen kann.

1. Introduction

1.1. Bacterial attachment

In their natural environment, bacteria often live attached to surfaces, both biotic and abiotic. Attachment to these surfaces can be important for the establishment of a bacterial infection. It can also lead to the formation of biofilms. Biofilms can be defined as communities of microorganisms that are attached to a surface or to each other and embedded in an extracellular matrix. Living as part of these communities make bacteria more resistant to environmental factors, antimicrobials and the immune system. In fact, most bacteria can be found not as single cells but as part of these communities in their natural environment. Biofilms are responsible for many problems in the medical setting causing hospital-acquired infections by colonizing medical devices and implants for example. Furthermore, they are an issue for many industries where they do not only represent a health hazard, but can cause important economical loses (Abdallah *et al.*, 2014; Monroe, 2007; O'Toole *et al.*, 2000).

The first step for infection or biofilm formation is often attachment. Surface adhesion has been proposed as a two-phase process. The first step is a reversible attachment ruled by hydrodynamic and electrostatic forces. The second is slower and it involves Van der Waals interactions between the surface and the bacterial cell wall (Anderson *et al.*, 2007; Tuson & Weibel, 2013). The transition from reversible to irreversible attachment involves short range forces like hydrophobic interactions and covalent or hydrogen bonds (Kumar & Anand, 1998). Bacteria possess certain cell structures that are important for this transition often referred to as adhesins.

E. coli is able to adhere to a wide variety of abiotic materials, including glass, aluminum, stainless steel and various organic polymers (Chao & Zhang, 2011). However, surface characteristics determine the bacterial attachment. In general, *E. coli* cells have a negative net charge on their surface at a neutral pH, due to the lipopolysaccharides and carboxylate and phosphate groups in their peptidoglycan. Therefore, they will attach better to positively charged surfaces and be repelled from negatively charged ones (Bolster *et al.*, 2009; Dickson & Koohmaraie, 1989). Nonetheless, this depends on the ionic strength and pH of the medium (Dai *et al.*, 2004; Husmark & Ronner, 1990).

As it was mentioned before, hydrophobic interactions between bacteria and substrate are important for irreversible attachment. Bacteria generally prefer hydrophobic surfaces.

Furthermore, the presence of cell structures on the surface of *E. coli*, such as curli fibers, increase their hydrophobicity, further favoring their attachment (Boyer *et al.*, 2007; Y. Liu *et al.*, 2004; Zita & Hermansson, 1997). However, it is not clear to what extent the hydrophobicity of the cells plays a role on attachment and it seems that, besides the surface as previously mentioned, it varies between bacterial species (Bolster *et al.*, 2009; Gannon *et al.*, 1991).

Another important feature that influences attachment, is the surface roughness and microtopography. Normally, on a microscale, rougher surfaces favor the attachment of bacteria for a number of reasons: bacteria are more protected from shear forces and other environmental unfavorable conditions, rougher surfaces offer more area for attachment and it allows bacteria to locally condition the surface which, as it will be shown, can improve further attachment (Arnold & Bailey, 2000; Zoltai *et al.*, 1981). However, the role of nanoscale roughness is not clear and seemingly it is highly dependent on the bacterial species (Hsu *et al.*, 2013; S. Sharma *et al.*, 2016).

Additionally, molecules present in the bulk tend to be carried to the surface (Kumar & Anand, 1998). This deposit of molecules on the surface is referred to as conditioning film. These molecules could alter the properties of the surface such as hydrophobicity or electrostatic charges, thus affecting bacterial attachment (Dickson & Koohmaraie, 1989). Even though it is generally understood to favor attachment, like in the case of a nutrient deposit, it is not clear how important the presence of a conditioning film is for initial attachment. Furthermore, some molecules have been reported to inhibit it and their use has been proposed as a method for suppressing bacterial contamination (Bernbom *et al.*, 2009; Fletcher, 1976; He *et al.*, 2015; Wong, 1998). In addition, the attachment of some bacteria may allow others to colonize surfaces which they could not otherwise in a process called co-aggregation (Whittaker *et al.*, 1996).

1.2. Motility and flagella

Motility, mediated by the bacterial flagella, is important for the cell attachment, since it increases the probability of random collisions with a given surface and helps the bacteria to overcome the repulsive electrostatic forces that it faces when approaching a surface, due to the negative charge of their cell envelope (Berne *et al.*, 2015; Tuson & Weibel, 2013). Furthermore, the flagellum itself has been reported to play a direct role on

attachment and has been shown to be actively expressed in attached cells within the biofilm (Besharova *et al.*, 2016; Friedlander *et al.*, 2013; Friedlander *et al.*, 2015; Haiko & Westerlund-Wikstrom, 2013).

1.2.1. Flagellar structure and regulation

E. coli is a peritrichously flagellated bacterium with several flagella distributed on the surface. Each flagellum is about 10 µm long and is a complex structure with over 60 proteins involved in its assembly and function. It is composed of a basal body, a hook and a filament (Figure 1). The filament is the longest part of the flagellum, it is mainly composed of around 20000 flagellin proteins (FliC) and works as a helical propeller (Berg, 2003; Chevance & Hughes, 2008; Turner *et al.*, 2000). Connecting the filament and the basal body is the hook. This part of the flagellum is characterized for its flexibility and allows the different flagella to form a bundle and propel the bacterium optimally (Samatey *et al.*, 2004).

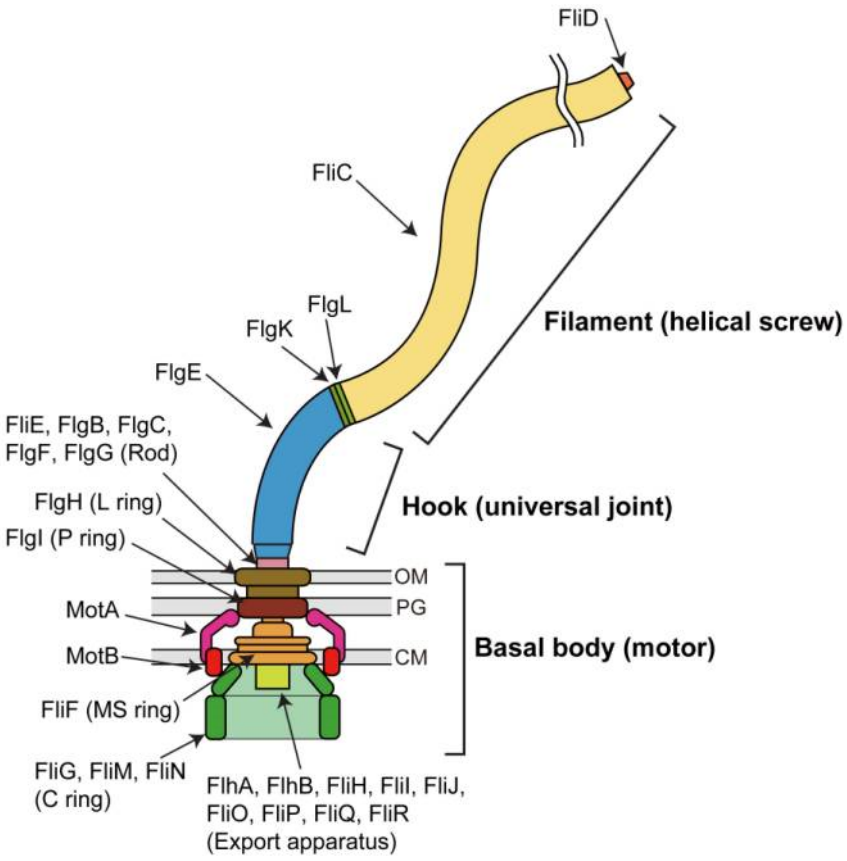

Figure 1. Flagellar structure. Proteins forming the basal body, hook and filament of the *E. coli* flagellum are depicted (Morimoto & Minamino, 2014).

The basal body is embedded in the cell membrane and is composed of the stator and rotor. The stator is formed by the ion-conducting MotA and MotB proteins. The rotor is composed of FliG, FliM and FliN. FliG is responsible for the interaction with MotA, and therefore the communication between rotor and stator (Berg, 2003; Khan *et al.*, 1988; Ridgway *et al.*, 1977; Zhao *et al.*, 1996a; Zhao *et al.*, 1996b). FliM plays an important role in the switching of the flagellar rotation direction by coupling the flagellum with the chemotaxis machinery as it will be discussed later on (Berg, 2003; Morimoto & Minamino, 2014). The force generation required for flagella rotation is given by the proton-motor force, the dispersal of the proton potential across the membrane (Larsen *et al.*, 1974; Lloyd *et al.*, 1996; Manson *et al.*, 1977).

The regulation of flagella expression is a very complex process that involves several genes. Flagellar genes are expressed following a hierarchy: first expressed are class I, then class II and finally class III genes. Class I genes are *flhD* and *flhC*, that encode for the master regulator of flagella expression $FlhD_4C_2$. It induces the expression of class II genes including those that encode for the basal body and for the export apparatus. Also, among class II genes, is the sigma factor *fliA* (σ^{28}) and its anti-σ factor, *flgM*. When the basal body secretion-system is functional, FlgM gets secreted and FliA is released and can transcribe of class III genes that encode for the rest of the structural components of the flagella, the chemotaxis machinery, and motor (Aldridge *et al.*, 2006; Chilcott & Hughes, 2000; Karlinsey *et al.*, 2000; McCarter, 2006).

As it was mentioned before, motility is important for bacteria, allowing them to swim in their planktonic state and promoting bacterial attachment. In *E. coli*, motility is controlled by the chemotaxis pathway (Sourjik & Wingreen, 2012; Wadhams & Armitage, 2004), as well as by the biofilm-associated second messenger c-di-GMP (Guttenplan & Kearns, 2013; Hengge, 2009; Jenal & Malone, 2006; Romling, 2013).

1.2.2. Chemotaxis

Chemotaxis allows *E. coli* to react to compounds present in their environment in order to find favorable conditions. *E. coli* can follow gradients of nutrients, chemicals or signal molecules among others.

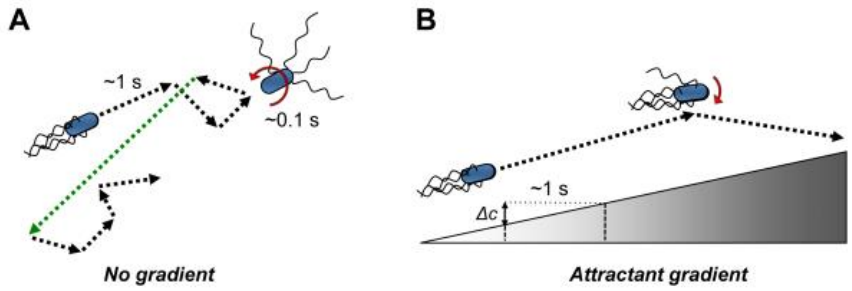

Figure 2. Swimming behavior of *E. coli* in the absence and presence of a gradient (Sourjik & Wingreen, 2012)**.**

In a homogeneous environment, *E. coli* explores its surrounding in a random walk manner: when the flagella are rotating counterclockwise (CCW), they form a bundle and propel the bacterium, which swims in straight runs of around 1 s. When at least one of the motors switches its rotation to clockwise (CW), a rapid reorientation of the flagella bundle occurs, which leads to the cell to tumble (0.1 s) (Figure 2). In the presence of favorable or harmful compounds, the direction of swimming gets biased by increasing the length of runs and reducing the frequency of tumbles, in order to find optimal conditions (Larsen *et al.*, 1974; Macnab & Koshland, 1972; Tindall *et al.*, 2012; Wadhams & Armitage, 2004). *E. coli* does so by making temporal comparisons of its environment, which allows it to detect changes in concentration of chemoeffectors (Darnton *et al.*, 2007; Segall *et al.*, 1986).

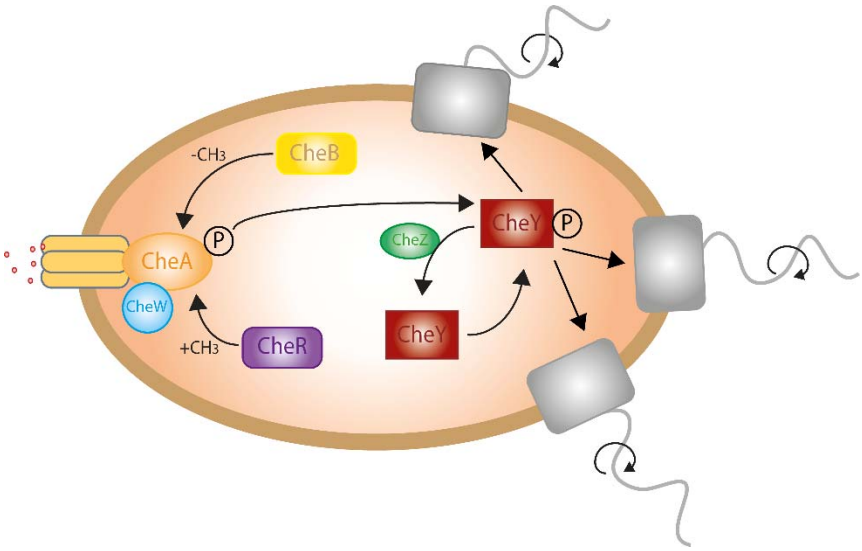

Figure 3 .Schematic representation of the chemotaxis pathway.

This behavior is possible thanks to the chemotaxis machinery. *E. coli* has 5 different receptors (Tar, Tsr, Tap, Trg and Aer) which are ligand specific and cluster in the membrane (Briegel *et al.*, 2012; Hazelbauer *et al.*, 2008). Associated with the receptors through the adaptor protein CheW, is the chemotactic signaling histidine kinase CheA. CheA phosphorylates the response regulator CheY, which – in its phosphorylated state – binds to FliM at the flagellar motor. This induces a switch in the direction of flagellar rotation from the default CCW to CW resulting in a tumble and therefore, in the reorientation of the cell swimming direction (Hazelbauer *et al.*, 2008; Hazelbauer & Lai, 2010; Segall *et al.*, 1982). CheY is subsequently dephosphorylated by the phosphatase CheZ. *E. coli*, also possesses an adaptation system based on the methylation/demethylation enzymes CheB and CheR. The activity of these enzymes serves as a short-term memory that enables bacteria to adapt to constant stimulation and allows them to detect further changes in their environment as it follows up a gradient (Alon et al., 1999; Amin & Hazelbauer, 2010) (Figure 3).

1.2.3. C-di-GMP signaling

Bis-(3′-5′)-cyclic dimeric guanosine monophosphate (c-di-GMP) is a second messenger in charge of coordinating many cellular functions such as virulence, motility, biofilm formation, cell cycle progression and development, since it is bound by a large diversity of effector components (Jenal *et al.*, 2017; Romling *et al.*, 2013). In general, it is considered a biofilm promoting signal because it stimulates the synthesis of extracellular matrix components such as curli fibers and cellulose. It also plays a role in motility, helping cells transition to a sessile life style (Pesavento *et al.*, 2008; Sommerfeldt *et al.*, 2009; Tagliabue *et al.*, 2010).

The c-di-GMP pool in the cells is controlled by the activity of diguanylate cyclases (DGC) and phosphodiesterases (PDE). The GGDEF (Gly-Gly-Asp-Glu-Phe) domain of the DGC catalyzes the c-di-GMP formation from two guanosine triphosphates (GTPs). The phosphodiesterase activity in PDE is provided by EAL (Glu-Ala-Leu) or HD-GYP (His-Asp, Gly-Tyr-Pro) domains which catalyze the c-di-GMP degradation into phosphoguanylyl-guanosine (pGpG) and guanosine monophosphate (GMP) (Jenal & Malone, 2006; R. Paul *et al.*, 2004; Ryjenkov *et al.*, 2006; Schirmer & Jenal, 2009). 29 genes that encode for GGDEF/EAL proteins can be found in *E. coli* K-12 (Boehm *et al.*, 2010; Hengge *et al.*, 2016). Two of the proteins involved in the control of motility and the

production of matrix proteins are DgcE and PdeH. This DGC/PDE pair has been shown to act upstream of PdeR that, together with DgcM, regulate MlrA activity. MlrA modulates *csgD* expression and therefore, curli production (Lindenberg *et al.*, 2013; Pesavento *et al.*, 2008; Serra & Hengge, 2019). Furthermore, the activity of PdeH maintains a low c-di-GMP level in the cell even under conditions in which c-di-GMP-dependent processes are activated. In fact, the deletion of any DGC does not have an effect on the cellular concentration of c-di-GMP in the presence of PdeH. However, if absent, the bigger effect on the total pool of c-di-GMP is due to the activity of DgcE (Sarenko *et al.*, 2017).

These proteins have also been reported to antagonistically control motility in post-exponentially growing cells (Pesavento *et al.*, 2008). *pdeH* is under class III flagellar control and is expressed predominantly during exponential phase while *dgcE* expression is induced during stationary phase (Pesavento *et al.*, 2008; Sommerfeldt *et al.*, 2009). Deletion of *pdeH* leads to a nonmotile phenotype and further deletion of *dgcE* restores motility (Girgis *et al.*, 2007; Pesavento *et al.*, 2008; Sarenko *et al.*, 2017). They both act via YcgR, a protein commonly known as flagellar brake.

YcgR possesses a PilZ domain that allows it to bind c-di-GMP (Ryjenkov *et al.*, 2006). However, it is not clear if YcgR requires c-di-GMP binding to influence motility or if the binding enhances its activity (Fang & Gomelsky, 2010; K. Paul *et al.*, 2010). It has been shown that YcgR is capable of interacting with the flagellar motor, though it is not clear exactly how. However, there have been mechanisms proposed. It has been suggested that YcgR binds to MotA in the flagellar motor in a c-di-GMP dependent manner. Higher levels of this second messenger would therefore, enhance the interaction of these proteins (Boehm *et al.*, 2010). However, other models point to the interaction of YcgR with FliG or FliG and FliM in the rotor, biasing the flagella rotation (Fang & Gomelsky, 2010; K. Paul *et al.*, 2010). A more recent study seemingly unifies both models and proposes that YcgR interacts with MotA at the MotA-FliG interface. This decreases the energy transfer from the stator to the rotor and therefore reduces the bacterial swimming speed (Hou *et al.*, 2020).

1.3. Bacterial adhesins

Once bacteria reach the surface, cellular appendages can mediate their irreversible attachment. These structures are referred to as adhesins. In addition to flagella, two other major adhesins present in *E. coli* are type 1 fimbriae and curli fibers.

1.3.1. Type 1 fimbriae

Type 1 fimbriae or type 1 pili are filamentous protein structures expressed in both commensal and pathogenic strains. 100-500 fimbriae with a length of 0.2-2 μm can be found on the bacterial surface (Beloin *et al.*, 2008).

The structural proteins and those involved in its biogenesis are encoded in the *fimAICDFGH* operon. The main structural component is the major subunit FimA, which forms the fimbrial rod. Each rod has around 1000 FimA copies. The fimbrial tip, located at the end of the rod, is comprised of FimF, FimG and FimH at the end of the tip (Hahn *et al.*, 2002; Per Klemm & Schembri, 2000). The export of the pilus is mediated by a chaperone-usher pathway. FimC interacts with the fimbrial subunits, facilitating their folding, stabilizing them and preventing premature interactions in the periplasm. It targets them to the usher protein FimD, which helps the assembly and export through the outer membrane (Du *et al.*, 2018) (Figure 4). FimI is essential for fimbriation but its exact function is unknown (Valenski *et al.*, 2003).

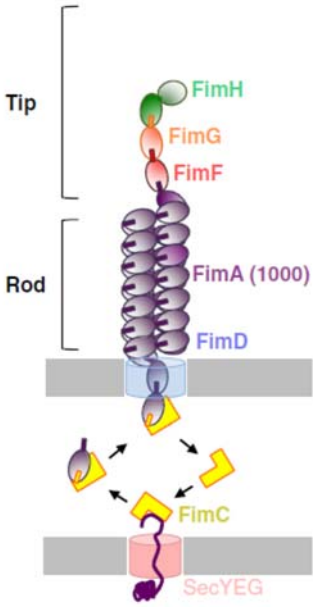

Figure 4. Type 1 fimbriae structure. Proteins forming the chaperone-usher pathway, rod and tip. (Lillington et al., 2014).

Type 1 fimbriae have been reported to play a role in adhesion to some abiotic surfaces acting as adhesins (Beloin *et al.*, 2008). In addition, fimbriae have been reported to influence the attachment to abiotic surfaces non-specifically, by affecting the outer membrane composition (Orndorff *et al.*, 2004; Otto *et al.*, 2001).

However, type 1 fimbriae are crucial for the attachment of *E. coli* to epithelial cells. These organelles, or more precisely the protein found on the fimbrial tip FimH, are capable of binding glycoproteins with one or many D-mannose residues, which are expressed in eukaryotic cells. This adhesion, when cells are exposed to none or low flow rates, is weak and allows bacteria to roll across the surface leading to an increase of colonization (Anderson *et al.*, 2007). However, it has been shown that the fimbrial tip undergoes a conformational change under high shear flow. This change decreases the flexibility of the fimbrial tip, which becomes more rigid, strengthening the attachment to the substrate. These kinds of interactions are referred to as catch-bonds. In the case of type 1 fimbriae, two different conformational states of the fimbrial tip can be found, one of low and one of high affinity for the substrate. This, in a urinary infection setting would allow bacteria to stay attached to urinary epithelial cells (that present a mannosylated surface) where they are exposed to high shear stress (Aprikian *et al.*, 2011; Feenstra *et al.*, 2017; Reisner *et al.*, 2014; Sauer *et al.*, 2016). This process is of such importance, that FimH has been proposed as a new target for drug development against urinary tract infections (Mydock-McGrane *et al.*, 2016).

The expression of type 1 fimbriae is regulated by phase variation. This leads to a mixture of cells expressing and non-expressing fimbriae. Phase variation occurs through the inversion of a DNA element upstream of *fimA* called *fim* switch or *fimS.* When *fimS* is in its ON orientation the fimbrial genes are transcribed while when *fimS* is in OFF, fimbriae are not produced. The switch from one state to the other is mediated by the recombinases FimB and FimE which can bind to inverted repeats flanking *fimS* (Abraham et al., 1985; Olsen & Klemm, 1994). The genes encoding for these recombinases are located upstream of *fimA*. FimB can perform ON to OFF and OFF to ON switch at a low frequency ($\sim 10^{-3}$ *per* cell *per* generation) while FimE is responsible only for ON to OFF switch but does so in a high frequency (up to 0.7 *per* cell *per* generation) and with great specificity (Gally *et al.*, 1993; McClain *et al.*, 1993). There are other recombinases capable of mediating the phase variation of *fimS*. However, these are not present in *E. coli* K-12 and have only been found in pathogenic strains (Xie *et al.*, 2006).

The actions of these recombinases are dependent on multiple environmental cues such as temperature, pH, osmolarity or oxygen availability. They are also regulated by the availability of branched chain aminoacids, alanine, N-acetylglucosamine and sialic acid (Aberg *et al.*, 2006; El-Labany *et al.*, 2003; Gally *et al.*, 1993; Olsen *et al.*, 1998; Schwan *et al.*, 2002; Sohanpal *et al.*, 2004). In addition, some regulators also play a key role in the regulation of fimbriae expression like the integration host factor (IHF), the leucine-responsive regulatory protein (Lrp) or the DNA binding transcriptional dual regulator (H-NS) (Dorman & Higgins, 1987; Gally *et al.*, 1993; Olsen *et al.*, 1998; Roesch & Blomfield, 1998). These responses to environmental cues can affect the recombinases expression or the switch itself allowing the bacteria to respond to their surroundings. This leads, for example, to the upregulation of fimbria expression at 37°C, the human body temperature or their inhibition in the face of an immune response (El-Labany *et al.*, 2003; Olsen *et al.*, 1998).

1.3.2. Curli fibers

Another adhesin present in *E. coli* are curli fibers. Curli are 0.5-1 µm long amyloid fibers composed of the structural components CsgA and CgsB which are encoded in the *csgBAC* operon (Hammar *et al.*, 1995; P. Klemm & Schembri, 2004). CsgA constitutes the main subunit of curli fibers, while CsgB functions as a nucleator in the assembly of curli on the cell surface (Barnhart *et al.*, 2006; Beloin *et al.*, 2008). The expression of

curli fibers is controlled by the curli master regulator CsgD. In general, sigma S is responsible for its translation when cells enter stationary phase (Arnqvist *et al.*, 1994; Hengge, 2009). However, many factors influence the expression of *csgD* which makes curli expression a process with a complex regulation (Ogasawara *et al.*, 2010). Curli expression is downregulated by several sRNAs, H-NS and the two-component system CpxR-CpxA. On the other hand, curli expression is upregulated by IHF, the two-component system EnvZ-OmpR and, as mentioned earlier, c-di-GMP via MlrA (Brown *et al.*, 2001; Jubelin *et al.*, 2005; Michaux *et al.*, 2014; Mika & Hengge, 2014; Ogasawara *et al.*, 2010).

Curli fibers are a major component of the extracellular matrix at growth temperatures of 30ºC or below, though clinical isolates have been reported to express curli at 37°C (Bian *et al.*, 2000). These adhesins are important for cell-surface interactions, cell-cell interactions and biofilm development (McCrate *et al.*, 2013; Ogasawara *et al.*, 2010; Romling *et al.*, 1998). In addition, it has been shown that curli fibers can be important on attachment to abiotic surfaces (Austin *et al.*, 1998; Pawar *et al.*, 2005; Vidal *et al.*, 1998). In fact, curli overproduction has been shown to improve adhesion especially to hydrophobic surfaces (Oh *et al.*, 2012; Pawar *et al.*, 2005). Furthermore, they have been reported to play a role on attachment to biotic surfaces. One example is their involvement in plant leaves colonization which has been linked to food poisoning cases (Fink *et al.*, 2012; Macarisin *et al.*, 2012). They are also involved in the attachment to epithelial cell lines and invasion of host tissues (Gebbink *et al.*, 2005; Gophna *et al.*, 2001; Gophna *et al.*, 2002; Henderson *et al.*, 2011; van der Velden *et al.*, 1998).

1.3.3. Other adhesive components

Other adhesive structures can be found in *E. coli* K-12. Some of them belong to the chaperone usher protein (CUP) family in which type 1 fimbriae is found. In fact, 38 different CUP have been found in *E. coli* (Wurpel *et al.*, 2013). Some of them have been described and seem to play a role in attachment to abiotic surfaces (Korea *et al.*, 2011). However, their expression is low or even cryptic and could important adhesins in other conditions different than the experimental settings used for these studies (Korea *et al.*, 2010). This suggest that *E. coli* possess a large arsenal of adhesins which allows it to attach to various surfaces under different environmental conditions.

There are other adhesion components involved at later stages of attachment and biofilm maturation that are also produced by commensal strains of *E. coli*. Some of these belong

to the family of autotransporters and have been shown to be involved in cell aggregation and biofilm formation. The most prominent example is antigen 43 (Ag43) (Danese *et al.*, 2000; Hasman *et al.*, 1999; van der Woude & Henderson, 2008).

The production of extracellular polymeric substances (EPS) is involved in maintaining the cells attached to the surface, promoting cell-cell and cell-surface interactions and in the maturation of biofilms. (Beloin *et al.*, 2008; G. Sharma *et al.*, 2016). As part of the extracellular matrix, β-1,6-N-acetyl-D-glucosamine polymer (PGA) (Itoh *et al.*, 2008; X. Wang *et al.*, 2005), colonic acid and cellulose (Saldana *et al.*, 2009) are secreted and too contribute to attachment and biofilm maturation. However, though commensal strains of *E. coli* can produce cellulose, *E. coli* K-12 strain does not (Z. Wang *et al.*, 2011).

Finally, pathogenic strains of *E. coli* possess many other adhesins that are absent in commensal lab strains. Examples of these are P pilus, F1C fimbriae, S fimbriae, aggregative adherence fimbriae (AAF), long polar fimbriae (LPF), CS1-CFA/I or the autotransporters AIDA and TibA (Sherlock *et al.*, 2004; Sherlock *et al.*, 2005; Wurpel *et al.*, 2013).

1.4. Surface sensing

The previous chapters described the changes that bacteria experience when approaching a surface, the adhesins that are involved in bacterial attachment and the overall regulation involved in the transition between planktonic and sessile cells. For these regulatory changes to occur, bacteria must sense the surface, though not much is known about how bacteria accomplish it, likely because of the complexity of this process. Differences between the bulk and the surface, cell envelope stress or the attachment via appendages are signals which could trigger bacterial surface sensing.

In the first case, bacteria can sense differences in pH, osmolarity, ionic strength and nutrient availability between the bulk and the surface (Berne *et al.*, 2018). For example, when surfaces are negatively charged, which are the most common, counter ions accumulate in the surface-bulk interface which, in turn, lowers the pH and can affect the proton-motor force of the bacteria (Hong & Brown, 2009). Another example is the enrichment of nutrients near the surface that can be sensed by the cells via changes in their metabolism (Marshall, 1988; Samuelsson & Kirchman, 1990). These differences in

the environment are sensed by bacteria via two-component systems. In the case of *E. coli*, those involved in attachment and biofilm formation are CpxAR (Raivio, 2014; Raivio *et al.*, 2013), EnvZ/OmpR (Clarke & Voigt, 2011; Prigent-Combaret *et al.*, 1999) and RcsCDB (Francez-Charlot *et al.*, 2005; Majdalani & Gottesman, 2006).

However, these physicochemical properties mentioned above are not restricted to surfaces so it is unlikely that these cues are exclusively responsible for the regulatory changes involved in the transition to a sessile life style.

Bacteria can interact directly with the surface via their cell body. This can be sensed by the cell as envelope stress through the CpxAR two-component system (Busscher & van der Mei, 2012; Harapanahalli *et al.*, 2015; Lejeune, 2003). As it was previously mentioned, CpxAR is involved in the control of flagellar expression and regulation by, among other things, upregulating c-di-GMP production which is important for the transition to a sessile lifestyle (Dudin *et al.*, 2014; Otto & Silhavy, 2002; Raivio *et al.*, 2013; Tschauner *et al.*, 2014). In addition, this system also responds to changes in pH and osmolarity (Otto & Silhavy, 2002; Raivio *et al.*, 2013).

Another way for cells to sense the surface is through their adhesive appendages. When attaching via flagella, bacteria have been reported to sense the hindered rotation (Lele *et al.*, 2013). The mechanosensing part of the flagella is the stator, which can sense and adapt to changes in flagellar load. When the load is low, it is believed that binding sites in the stator involved in their remodeling, are inaccessible. However, as the load on the flagellum increases so does the torque generated by the stator (Nord *et al.*, 2017; Tipping *et al.*, 2013). This affects the peptidoglycan which leads to conformational changes of the stator making these binding sites available (Chawla *et al.*, 2017; Lele *et al.*, 2013; Nord *et al.*, 2017). This increases the probability of new stator elements being incorporated leading to stator remodeling. Furthermore, attachment via type 1 fimbriae has been reported to alter gene expression in *E. coli* affecting some genes involved in attachment. Nonetheless, the genes affected are controlled by different regulators. Thus, these gene expression changes might be a result of multiple signals (Bhomkar *et al.*, 2010; Otto *et al.*, 2001). Therefore, it cannot be determined which pathways are affected by type 1 fimbriae attachment specifically.

Overall, bacteria seem to be able to sense the surface by the interplay of multiple signals that can trigger the transition to a sessile lifestyle. It is therefore difficult to establish the

direct implication of one appendage or a single two-component system for initiating this transition.

1.5. Aims

Early attachment is important for biofilm formation and for the establishment of bacterial infections. Though biofilm formation and attachment have been extensively studied, it is still unclear how exactly motility and each adhesin contributes to bacterial attachment to different surfaces and previous studies have shown contradictory results.

This work aims to have a closer look at the attachment of *E. coli* W3110 (and W3110 *rpoS*$^{+}$) to abiotic and biomimetic surfaces. Firstly, this study focuses on the role of motility and its regulation by the chemotaxis pathway and c-di-GMP. C-di-GMP is a second messenger which promotes biofilm formation in *E. coli* and inhibits motility via the flagellar brake YcgR. In this work, both the general levels and the influence of c-di-GMP in flagellar rotation are assessed. Another goal of this work is the study of different adhesins, especially type 1 fimbriae, and their importance for surface attachment. Curli fibers have been reported to play a role in surface attachment as well as cell-cell interactions while flagella have been hypothesized to favor attachment beyond motility. Type 1 fimbriae are known to be important virulence factors and adhesins, being present in many commensal and pathogenic *E. coli* strains. They have been shown to be crucial for the establishment of various infections, such as urinary tract ones. However, their implication in attachment to abiotic surfaces is not as clear. In this study, the importance of flagella, curli fibers and type 1 fimbriae for early and late attachment and their interplay with motility and other adhesins in this process are investigated. Finally, this study aims to further understand how *E. coli* senses the surface after attachment and changes its gene expression to transition into a sessile state.

2. Results

2.1. Bacterial attachment under static conditions

As it was mentioned in the first chapter, *E. coli* is capable of attaching to a variety of surfaces. This attachment depends on several external factors, such as temperature (Figure 5) or the surface chemistry (Figure 6). As it was previously mentioned, sigma S is the master transcriptional regulator of the stationary phase and the general stress response and is important for biofilm development. In this screening two different strains, W3110 *rpoS*$^{+}$ and W3110 *rpoS*$^{-}$, expressing or not a functional *rpoS,* respectively, were used. W3110 *rpoS*$^{-}$ is thus suitable to evaluate the early stages of biofilm formation. Furthermore, *E. coli* possesses different structures called adhesins involved in the attachment to specific surfaces. In order to understand the importance of adhesins, the attachment to hydrophobic and hydrophilic surfaces of different knockouts was tested. For this purpose, cells were harvested in exponential (OD_{600} 0.5) or stationary (OD_{600} 1.2) phase and seeded in hydrophobic or hydrophilic 24 or 8-well plates. After one hour at 30°C, wells were washed, imaged and the number of attached cells was quantified.

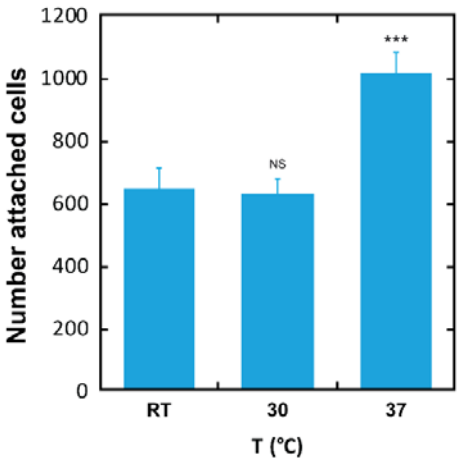

Figure 5. Attachment of W3110 *rpoS*$^{+}$ at different temperatures to hydrophobic surfaces plates. Unattached cells were removed by washing. Shown are mean and standard error of three replicates. Statistical analysis was performed using a two-sample t-test with unequal sample size and unequal variance, with $P < 0.0005$ (***), NS, not significant.

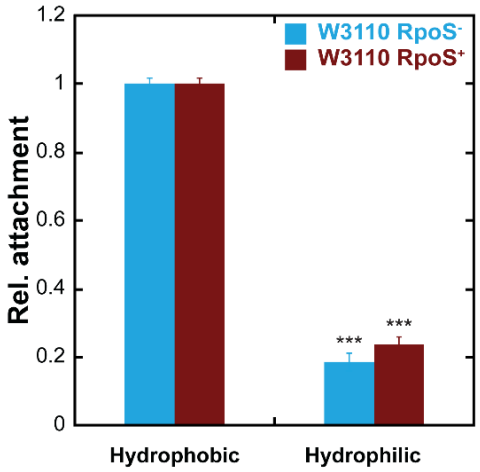

Figure 6. Relative number of cells attached to hydrophobic and hydrophilic surfaces. Relative attachment of W3110 *rpoS*- and W3110 *rpoS*+ after 1 hour incubation at 30°C. Attached cells of each strain were normalized to the number of cells attached of the same strain to hydrophobic plates. Shown are mean and standard error of three to five replicates. Statistical analysis was performed using a two-sample t-test with unequal sample size and unequal variance, with $P < 0.0005$ (***).

Firstly, when evaluating the attachment to hydrophobic ibidi uncoated plates, motility was shown to be important for the cells to reach the surface, since cells lacking flagella (*ΔfliC*) and cells that possess non-rotating flagella (*ΔmotA*) showed a significant decrease in the attachment, especially when cells were harvested in the exponential phase (Figure 7A, B). *ΔfliC and ΔmotA* cells in both backgrounds showed a similar attachment when harvested in the exponential and stationary phase thus, flagella did not play a direct role on attachment beyond motility in this setup. *ΔfliC and ΔmotA* cells in both backgrounds showed a similar attachment when harvested in the exponential and stationary phase thus, flagella did not play a direct role on attachment beyond motility in this setup. Lack of motility had a most dramatic effect on cells that did not express an active sigma S transcription factor (Figure 7A, C). Interestingly, only in this background (W3110 *rpoS*-), cells lacking the flagellar brake, *ΔycgR,* showed an increased attachment (Figure 7A, C). These cells mimicked low c-di-GMP levels, as this second messenger cannot influence the flagellar rotation. This process is normally understood to be important in biofilm formation since it helps the cells transition from a motile to a sessile state. However, contrary to what was expected, under these experimental conditions a low c-di-GMP concentration seemed to benefit the attachment rather than inhibiting it, which will be further explored later on. In fact, this was observed in the case of *rpoS* positive cells (Figure 7B, D). On the other hand, in W3110 *rpoS*+ cells, which possess sigma S, together with the absence of motility, *ΔycgR* showed the highest effect on attachment

indicating that high levels of c-di-GMP are indeed important for initial attachment at least under certain conditions (Figure 7B, D).

Curli fibers did not seem to be important for attachment to hydrophobic plates in cells growing exponentially since *ΔcsgA* attached to these plates similar to the wild-type in both backgrounds studied (Figure 7A, B). However, these adhesins became more relevant in later growth rates (Figure 7C, D). These results agree with the fact that curli fibers are only expressed during stationary phase.

Lastly, *ΔfimA,* which lacks type 1 fimbriae, showed a reduced attachment to hydrophobic plates of W3110 *rpoS*$^{-}$ cells (Figure 7A, C). On the other hand, type 1 fimbriae did not affect the attachment of W3110 *rpoS*$^{+}$, which express a functional sigma S (Figure 7B, D). In both W3110 *rpoS*$^{-}$ and W3110 *rpoS*$^{+}$, *ΔfimA* showed a higher effect on attachment when cells were harvested in the stationary phase (Figure 7C, D). This was an unexpected finding since the expression levels of fimbriae has been reported to be higher in the exponential phase (Schembri *et al.*, 2003). In addition, as it was mentioned before, sigma S is involved in the downregulation of fimbriae. This could explain why the influence of fimbriae on attachment of W3110 *rpoS*$^{+}$ cells was limited, as type 1 fimbriae levels would be already lower in wild-type cells.

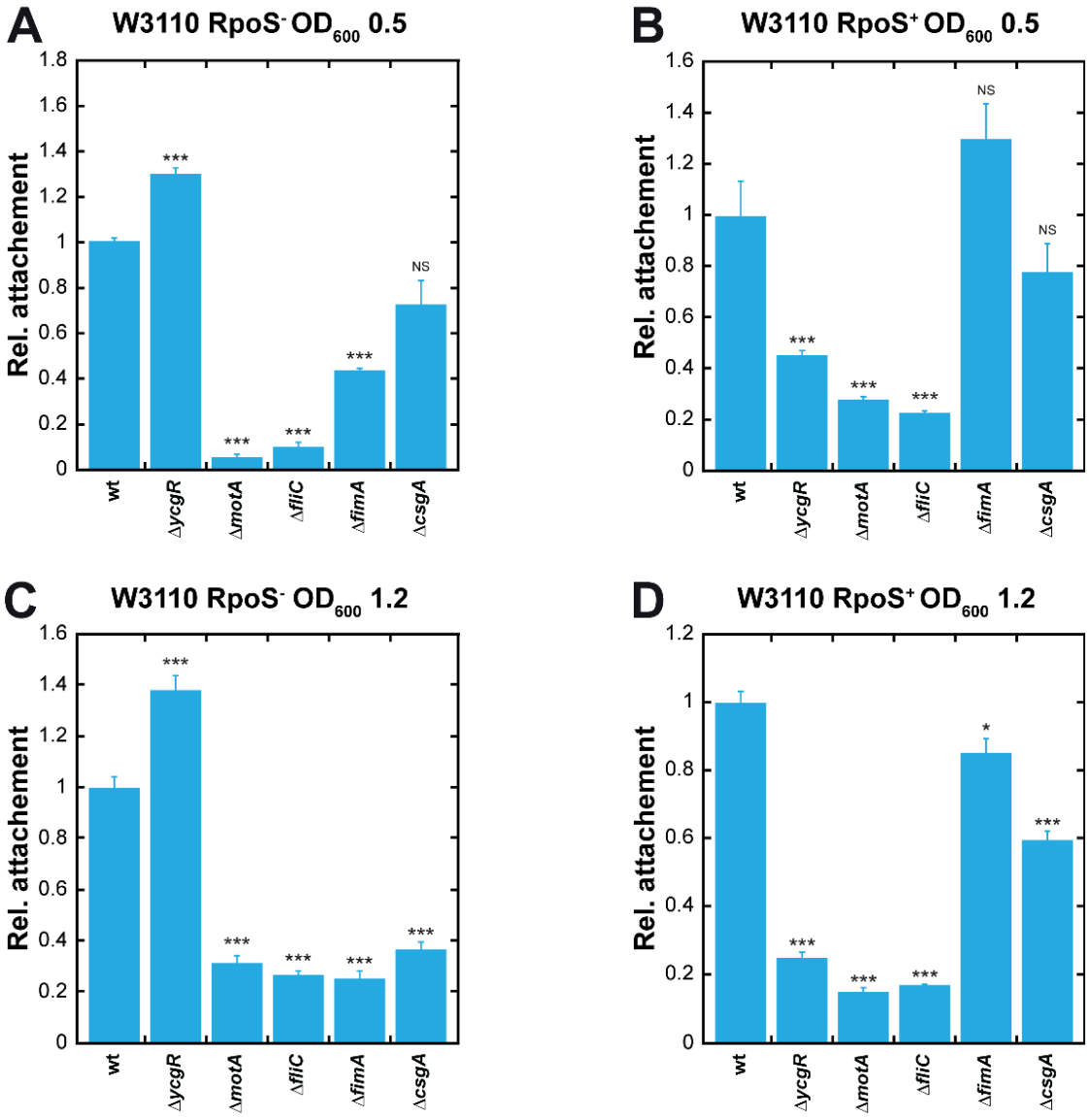

Figure 7. Attachment to hydrophobic surfaces. Relative number of cells attached after 1 hour of incubation at 30°C to ibidi uncoated plates. W3110 *rpoS*⁻ **(A, C)** or W3110 *rpoS*⁺ **(B, D)** cells were grown until OD_{600} 0.5 **(A, B)** or 1.2 **(C, D)**, harvested, washed in motility buffer and diluted in fresh motility buffer until OD_{600} 0.05. Statistical analyses were performed here and throughout using a two-sample t-test with unequal sample size and unequal variance, with $P < 0.05$ (*), $P < 0.0005$ (***), NS, not significant.

In the case of the hydrophilic Corning Costar glass plates, motility seemed to be important for the cells to reach the surface as it was seen for hydrophobic surfaces. *ΔmotA and ΔfliC* W3110 *rpoS*⁻ cells showed a significant reduction in attachment when compared to wild-type when harvesting both in the exponential or stationary phase (Figure 8A, C). In the case of W3110 *rpoS*⁺ cells, similar results were obtained when cells were harvested in the stationary phase (Figure 8D). In addition, flagella do not seem to act as an adhesin in the absence of motility in exponentially growing W3110 *rpoS*⁻ and

stationary phase W3110 *rpoS*$^{-}$ and W3110 *rpoS*$^{+}$ cells since *ΔmotA* and *ΔfliC* showed a similar attachment (Figure 8A, B, D). However, in the case of W3110 *rpoS*$^{+}$ cells harvested during exponential phase, the results were quite different to the ones seen before. For these cells, no significant differences in attachment were found between *ΔfliC* and wild-type (Figure 8B). Thus, motility does not seem to be relevant for attachment in these experimental conditions. Nevertheless, attachment of non-motile flagellated cells (*ΔmotA*) was almost abolished (Figure 8B). Therefore, in this case, instead of acting as adhesin, the stopped flagella might be hindering the attachment, not allowing the rest of the adhesins or the bacterial body to interact with the surface.

On hydrophilic surfaces, a similar pattern could be observed when it comes to *ΔycgR,* curli fibers and type 1 fimbriae as seen for hydrophobic plates. The deletion of the flagellar brake, *ΔycgR,* led to an increased attachment when compared to wild-type cells only in a sigma S deficient background (W3110 *rpoS*$^{-}$) (Figure 8A, C). Curli fibers were only relevant for attachment when cells were harvested in the stationary phase (Figure 8C, D) and *ΔcsgA* attached similar to wild-type when harvested in the exponential phase (Figure 8A, B). This was observed for both W3110 *rpoS*$^{-}$ and W3110 *rpoS*$^{+}$. Type 1 fimbriae were only important for the attachment of sigma S deficient cells (W3110 *rpoS*$^{-}$) (Figure 8A, C) and *ΔfimA* reduced the attachment to hydrophilic cells especially when cells were harvested in the stationary phase (Figure 8C, D).

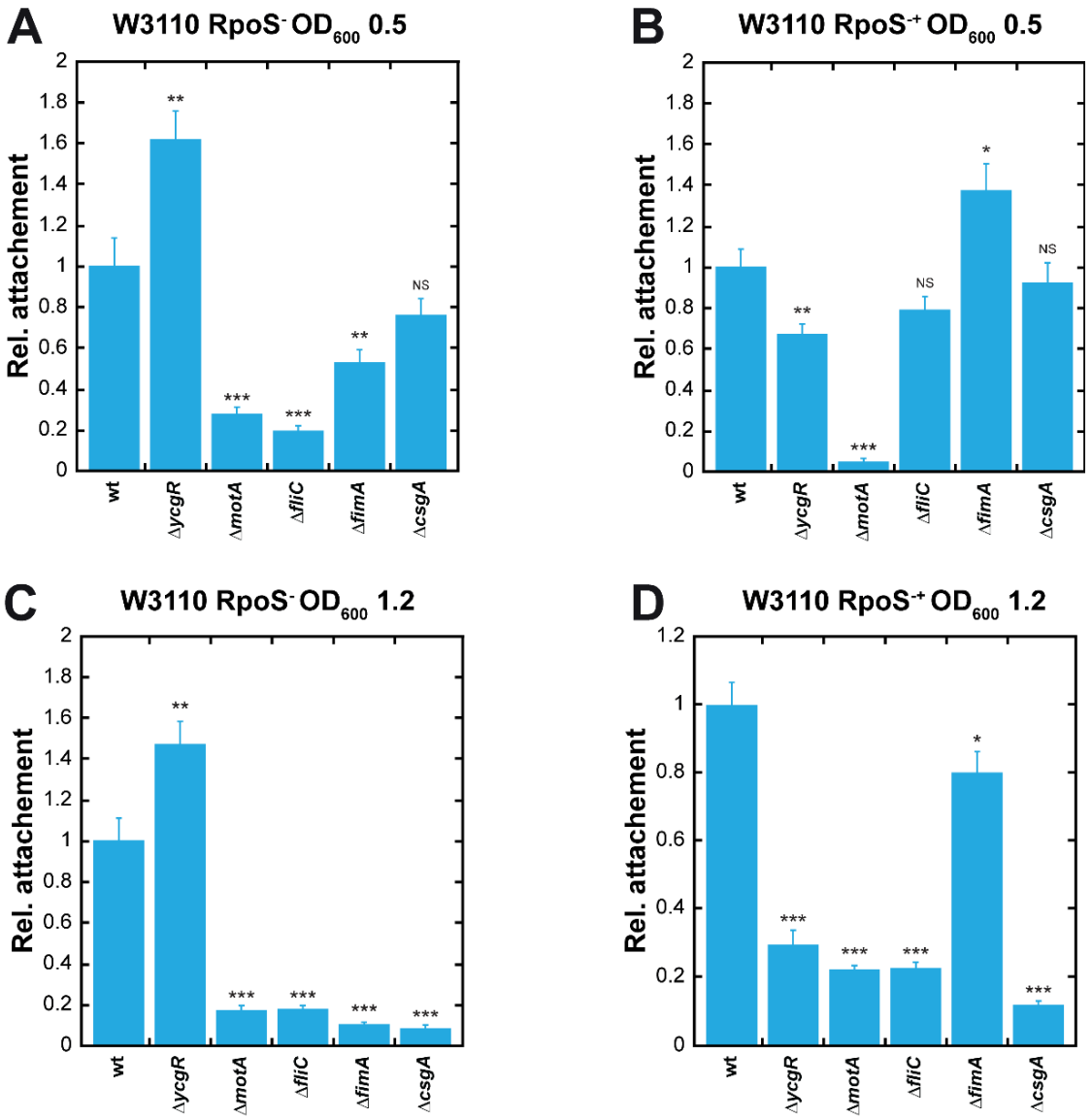

Figure 8. Attachment to hydrophilic surfaces. Relative number of cells attached after 1 hour of incubation at 30°C to Greiner Bio-One glass-bottom plates. W3110 *rpoS*$^-$ (A, C) or W3110 *rpoS*$^+$ (B, D) cells were grown until OD_{600} 0.5 (A, B) or 1.2 (C, D), harvested, washed in motility buffer and diluted in fresh motility buffer until OD_{600} 0.05. Statistical analyses were performed using a two-sample t-test with unequal sample size and unequal variance, with $P < 0.05$ (*), $P < 0.005$ (**), $P < 0.0005$ (***), NS, not significant.

In general, regardless of the surface, motility seemed to be crucial for attachment since it allows cells to reach the surface. However, the importance of flagella in attachment seems to be strain and surface specific. Furthermore, these results indicate that not only one adhesin is responsible for the attachment to a specific surface and it is more likely that the interplay between them is more relevant for attachment.

2.2. Chemotaxis and cyclic-di-GMP signaling control surface attachment

Besides possessing adhesive structures, planktonic bacteria need to establish contact with the surface in order to attach. Flagella-driven motility could contribute to attachment. Motility in *E. coli* is controlled by the chemotaxis pathway as well as by the biofilm-associated second messenger c-di-GMP. Thus, the importance of motility during surface attachment and colonization was assessed.

2.2.1. Smooth swimming promotes surface attachment

To investigate possible functions of motility and its regulation in surface attachment of *E. coli* W3110 *rpoS*$^-$, first the biomass of cells attached on microtiter plates after 24 h incubation was quantified using crystal violet (CV) staining (Figure 9A). In line with previous studies, *ΔfliC* strain that lacks flagella and *ΔmotA* strain that has paralyzed flagella showed strongly reduced surface colonization under these conditions. Biomass of surface-attached cells was also reduced for *ΔcheZ* strain that has an increased level of tumbling, but not for the smooth-swimming *ΔcheY* and *ΔcheA* strains. Defects in motility apparently impair surface colonization by reducing initial attachment, as time-resolved microscopy showed a steady increase in the number of attached wild-type cells during the first 12 hours of incubation but nearly no surface attachment for *ΔfliC*, *ΔmotA* or *ΔcheZ* cells (Figure 9B, C). Confirming that under these conditions motility rather than flagella themselves are required for attachment, similar numbers of flagella-less and wild-type cells attached when bacteria were artificially forced to the surface using mild centrifugation (Figure 10A, B).

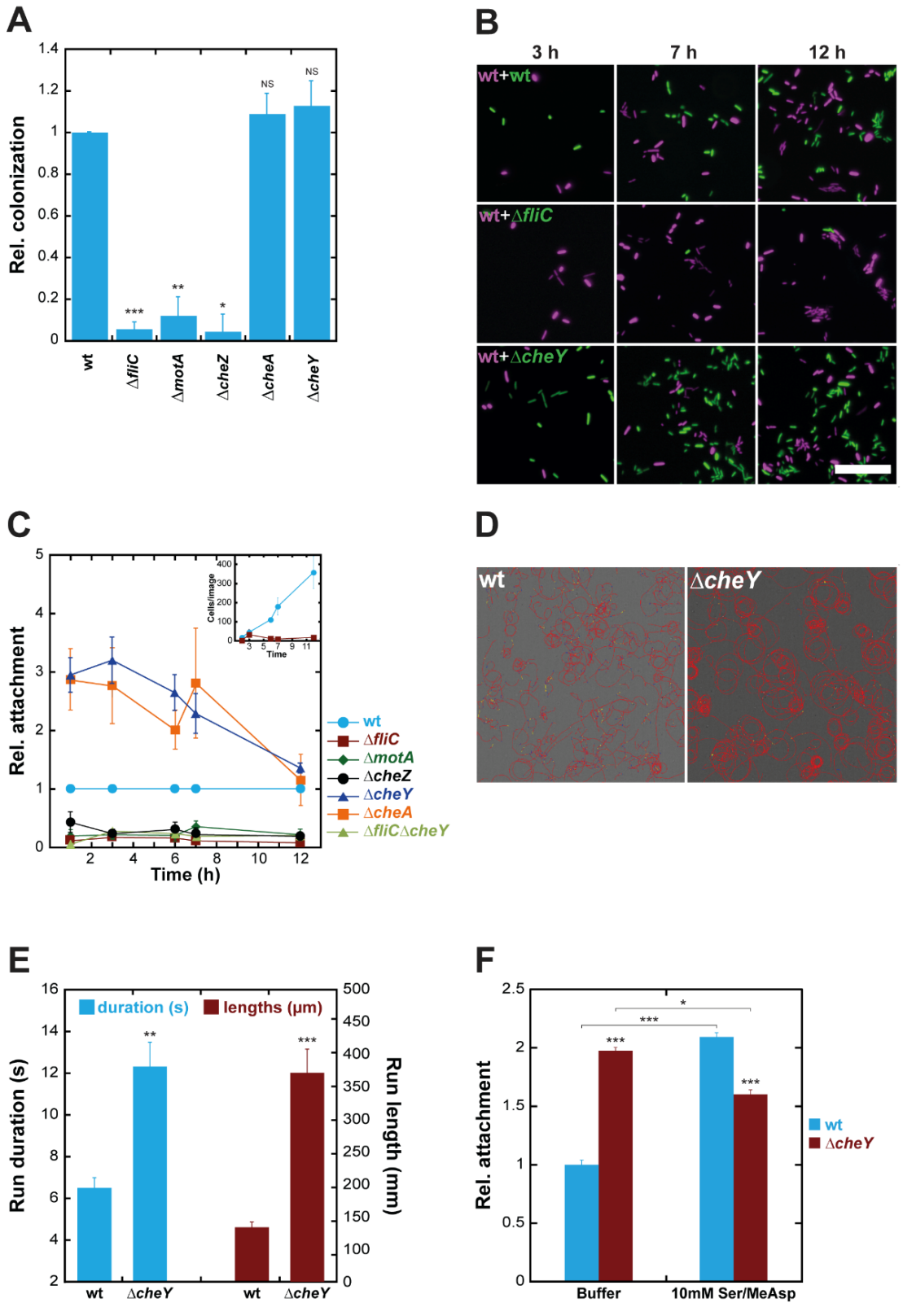

Figure 9. Motility and chemotaxis regulate *E. coli* surface attachment. A. Relative surface colonization by motility and chemotaxis mutants. *E. coli* cultures were incubated on polystyrene Corning Costar tissue culture TC-treated plates for 24 in M9 medium at 30°C. *(Continued on the following page).*

Figure 9. *(continued from the previous page)* Colonization was quantified using staining with crystal violet (CV) and normalized to the CV value of the wild-type (wt). Shown are mean and standard error of three to eight replicates. **B, C.** Time course of the relative surface attachment of indicated motility and chemotaxis mutants. Wild-type cells labeled with cyan fluorescent protein (CFP) or with mCherry were mixed 1:1 with wild-type or mutant cells labeled with yellow or green fluorescent protein (YFP or GFP) and incubated for indicated time in M9 medium at 30°C on polystyrene BD Falcon TC-treated plates. **B**. Exemplary images of mixed cultures of wild-type cells labeled in magenta and wild-type or mutants in green. Scale bar: 25 µm. **C**. Relative numbers of attached cells at different time points. The number of attached cells in each image was normalized to the number of wild-type cells, and the values were normalized again to the wild-type/wild-type ratio in the same experimental series. *Inset* shows absolute numbers of attached wild-type and Δ*fliC* cells. Shown are mean and standard error of three replicates. **D**, **E**. Swimming behavior at the surface of a glass slide. **D**. Exemplary images of tracks of wild-type and Δ*cheY* cells. **E**. Cells were grown in planktonic cultures to postexponential phase and trajectory durations and lengths were quantified. Shown are mean and standard error of three replicates. **F**. Relative surface attachment in the presence of chemoattractants. Attachment of wild-type and Δ*cheY* cells in motility buffer with and without 10 mM of methyl aspartate and serine to ibidi uncoated imaging plates was quantified after 20 minutes incubation and normalized to the number of wild-type cells that were attached without chemoattractants. Shown are mean and standard error of six replicates. Statistical analyses were performed here and throughout using a two-sample t-test with unequal sample size and unequal variance, with $P < 0.05$ (*), $P < 0.005$ (**), $P < 0.0005$ (***), NS, not significant.

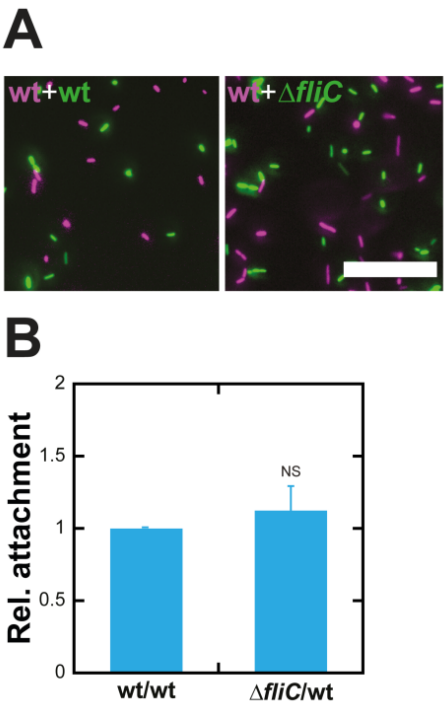

Figure 10. Flagella are dispensable for attachment to surfaces. A, **B**. Relative attachment of wild-type and Δ*fliC* cells in M9 medium after centrifugation to BD falcon TC-treated imaging plates. Wild-type cells labeled with mCherry were mixed 1:1 with wild-type and Δ*fliC* cells labeled with GFP. **A**. Exemplary images of mixed cultures of wild-type cells (magenta) and wild-type, Δ*fliC* (green). Scale bar: 25 µm. **B**. The number of attached cells in each image was normalized to the number of wild-type cells in the same image, and the values were normalized again to the wild-type/wild-type ratio in the same experimental series. Shown are mean and standard error of four to five experiments. Statistical analysis was performed using a two-sample t-test with unequal sample size and unequal variance, with NS, not significant.

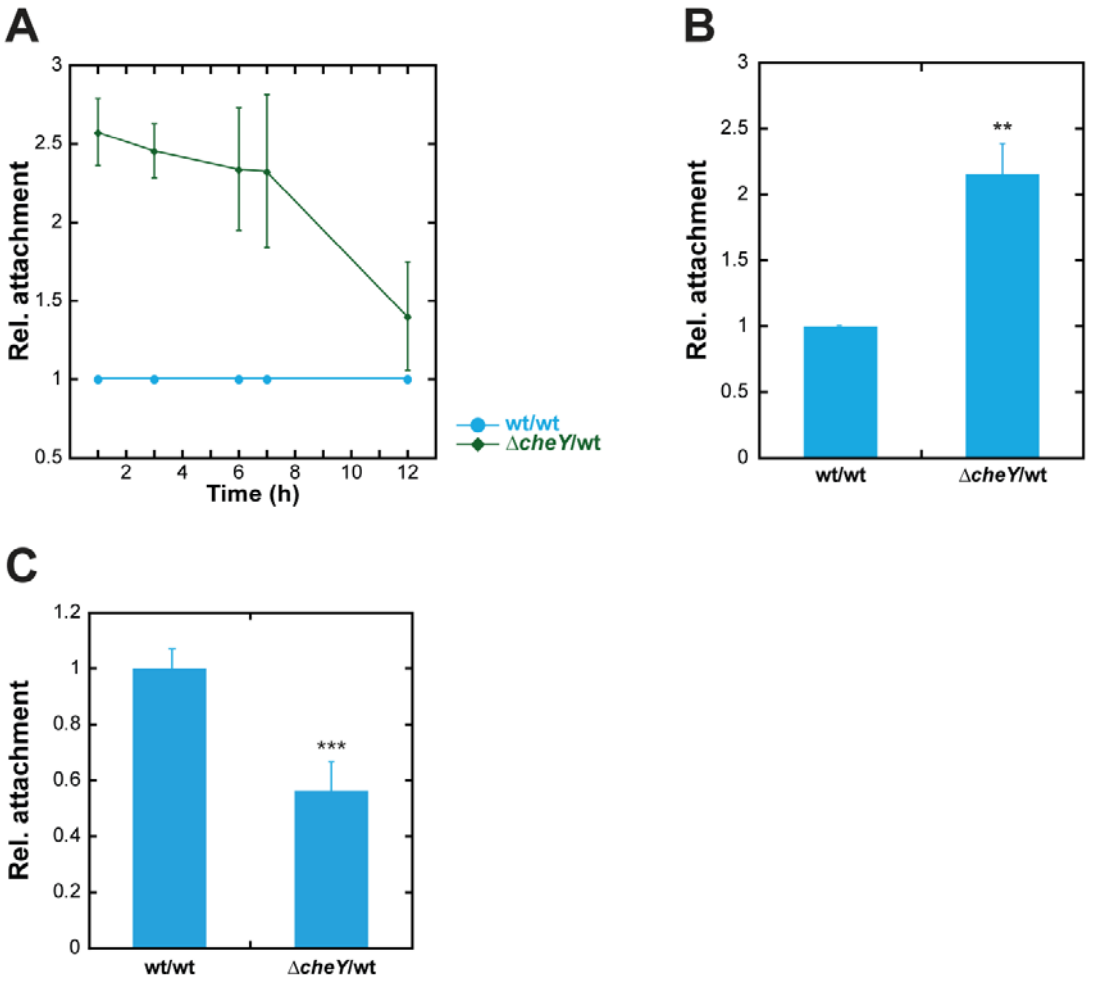

Figure 11. Smooth swimming promotes attachment. A, **B**. Time course of the relative surface attachment of wild-type and Δ*cheY* cells to ibidi uncoated imaging plates. **A**. Relative surface attachment in M9 medium at 30°C. Wild-type cells labeled with mCherry were mixed 1:1 with wild-type and Δ*cheY* cells labeled with GFP. Attached cells were quantified and normalized as in Fig. 9C. Shown are mean and standard error of three replicates. **B**. Relative attachment in motility buffer after 1 h incubation. **C**. Relative attachment of wild-type and Δ*cheY* cells after mild centrifugation. Experiments were performed and analyzed as in Fig. 10B. Shown are mean and standard error of three to six replicates. Statistical analysis was performed using a two-sample t-test with unequal sample size and unequal variance, with $P < 0.0005$ (***), $P < 0.005$ (**).

Interestingly, in contrast our results based on CV staining of cell biomass at the late stages of attachment and biofilm formation (Figure 9A), a much better attachment of *ΔcheA* and *ΔcheY* strains at the early time points of incubation was observed (Figure 9B, Figure 11A, B). These results indicate that cell attachment may be directly related to the ability of bacteria to make smooth runs, which is strongly reduced in *ΔcheZ* but is increased in *ΔcheA* and *ΔcheY* strains. Confirming that the enhanced attachment of *ΔcheY* is motility dependent, no increase in attachment was observed upon deletion of *ΔcheY* in *ΔfliC* background (Figure 9C). Moreover, adhesiveness of *ΔcheY* cells seemed to be even lower than that of the wild-type, judging by their poorer attachment in the

centrifugation assay (Figure 11C). Smooth swimming may lead to trapping of cells in the proximity of the surface, and indeed *ΔcheY* cells spend more time swimming at the surface than wild-type cells (Figure 9E) and their trajectories are longer (Figure 9D, E). Both measures confirm entrapment of Δ*cheY* cells at the surface, which means that the smooth swimming mutants sample a larger surface area than wild-type cells and therefore have an increased probability of attachment.

Since stimulation with chemoattractants transiently inhibits CheA activity and therefore reduces cell tumbling, it was expected to enhance attachment similar to the effects of *cheA* and *cheY* knockouts. Indeed, stimulation with 10 mM of α-metyl-DL-aspartate and L-serine, strong chemoattractants sensed by two major *E. coli* chemoreceptors, elevated attachment of the wild-type cells to the levels similar to, and even slightly higher than that of Δ*cheY* strain (Figure 9F). The origins of this slightly better attachment of the attractant-stimulated wild-type compared to Δ*cheY* mutant needs further investigation. The generally reduced attachment of stimulated cells, apparent for Δ*cheY* but also presumably true for the wild-type cells, is likely to be non-specifically caused by high millimolar levels of amino acids.

2.2.2. Low levels of c-di-GMP enhance surface attachment

Next, it was observed that colonization of microtiter plate surface by *E. coli* is also affected by c-di-GMP signaling. Deletion of the gene encoding DgcE, the dominant c-di-GMP cyclase under our growth conditions and the major cyclase controlling motility via c-di-GMP in *E. coli* (Pesavento *et al.*, 2008)(Pesavento *et al.*, 2008)(Pesavento *et al.*, 2008)(Pesavento *et al.*, 2008), led to increased biomass of surface-associated cells (Figure 12A). Inversely, the deletion of the major diesterase PdeH markedly reduced colonization (Figure 12A). These effects were mediated by the motility control via YcgR, because Δ*ycgR* showed similar increase in the colonization as Δ*dgcE*, and no additional increase was observed for Δ*ycgR*Δ*dgcE* strain (Figure 12A). Consistently, deletion of *ycgR* also abolished the effect of the *pdeH* deletion (Figure 12A). Deletion of other cyclases with lesser contributions to the global cellular c-di-GMP pool showed weaker or no increase in attachment (Figure 13A). Furthermore, overexpression of DgcE that is expected to globally elevate the cellular level of c-di-GMP has reduced attachment, again in the YcgR-dependent manner (Figure 13B).

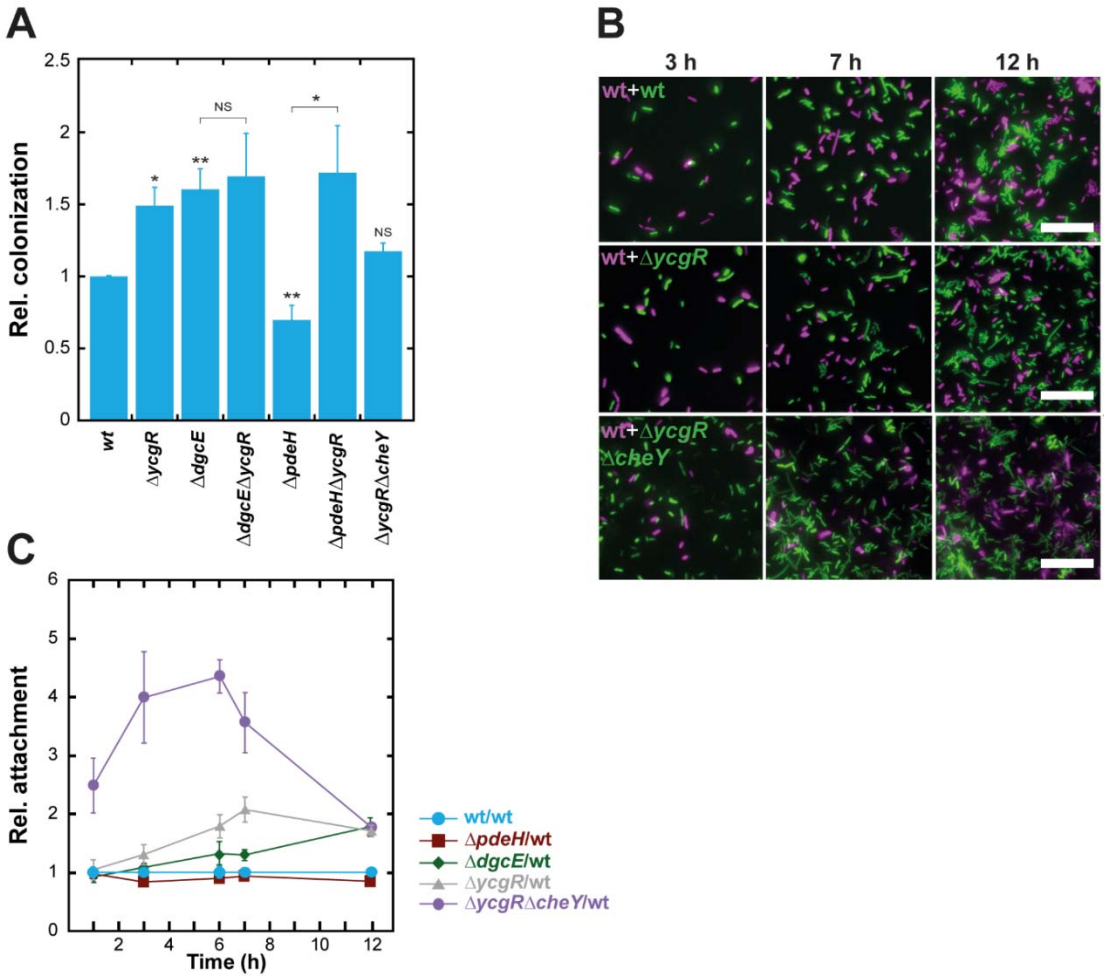

Figure 12. Regulation by c-di-GMP alters surface attachment of *E. coli*. A. Relative surface colonization by indicated mutants with perturbed c-di-GMP regulation. Experiments were performed and analyzed as in Fig. 9A. Shown are mean and standard error for eight or more replicates. **B**, **C**. Time course of the relative surface attachment of indicated mutants with perturbed c-di-GMP regulation. Experiments were performed and analyzed as in Fig. 9B, C. Shown are mean and standard error for three to eight replicates. Scale bar: 25 µm. Statistical analyses were performed here and throughout using a two-sample t-test with unequal sample size and unequal variance, with $P < 0.05$ (*), $P < 0.005$ (**), NS, not significant.

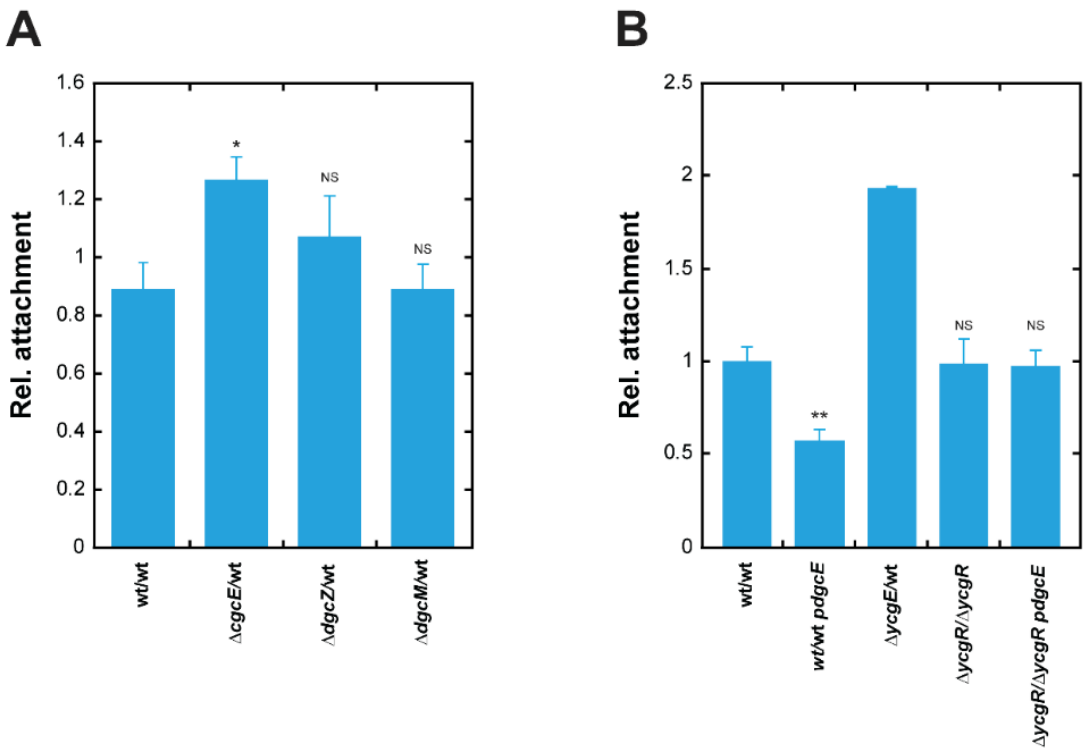

Figure 13. Effect of other diguanylate cyclases and overexpression of *dgcE* on attachment. **A**. Relative attachment by wild-type and the indicated diguanylate cyclase knockouts regulation to the surface of ibidi uncoated imaging plates in motility buffer after 1 h incubation. Wild-type cells labeled with mCherry were mixed 1:1 with wild-type and Δ*dgcE,* Δ*dgcZ* or Δ*dgcM* cells labeled with GFP. Attached cells were quantified and normalized as in Fig. 9C. Shown are mean and standard error of three to five replicates. **B**. Relative attachment of wild-type and Δ*ycgR* cells transformed with an inducible plasmid encoding DgcE. Experiments were performed in motility buffer and with ibidi uncoated imaging plates with 1 h incubation. Cells carrying an empty vector were mixed with ones carrying the plasmid encoding *dgcE*. Attached cells were quantified and normalized as in Fig. 9C. Shown are mean and standard error of three to six replicates. Statistical analysis was performed using a two-sample t-test with unequal sample size and unequal variance, with $P < 0.005$ (**), $P < 0.05$ (*), NS, not significant.

Although Δ*dgcE* and Δ*pdeH* strains showed similar surface attachment after one hour of incubation in the microscopy assay, which might be due to inherently low c-di-GMP levels at the early phase of culture growth, the effects of the deletions become visible between 3 and 6 h and further increased up to 12 h of attachment (Figure 12B, C). At this time point, the results of microscopy and CV staining became comparable, and no further enhancement in the differences between strains was observed until 24 h (Figure 14). Interestingly, the attachment of Δ*ycgR* cells could be further strongly enhanced during the early stage of incubation by deleting *cheY* in this background (Figure 12C), suggesting that effects of *ycgR* and *cheY* mutations are multiplicative.

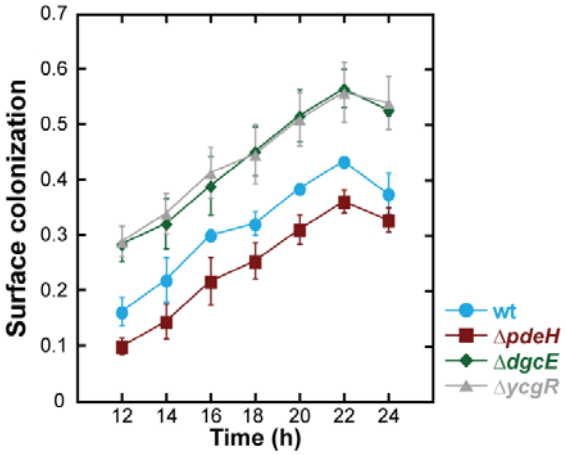

Figure 14. Regulation by c-di-CMP alters surface colonization. Time course of the relative surface colonization by the wild-type and indicated mutants in M9 medium at 30°C of Corning Costar TC- treated plates assayed using crystal violet staining. Error bars indicate standard errors of five to eight replicates.

To rule out that the effect of *ycgR* deletion on attachment is due to altered adhesiveness, again centrifugation assay was again performed. Indeed, no differences in adhesion were observed between wild-type and Δ*ycgR* cells (Figure 15). Interestingly, the relative attachment of Δ*dcgE* cells was mildly reduced, whereas that of Δ*pdeH* cells was increased (Figure 15), which could be explained by involvement of c-di-GMP in the production of extracellular matrix. Since these effects are opposite to the differences in attachment observed for the swimming cells, they do not appear to play major role in attachment under these experimental conditions. Finally, when compared to the wild-type, not only the number of attached Δ*ycgR* cells but also the strength of attachment apparently increased (Figure 16).

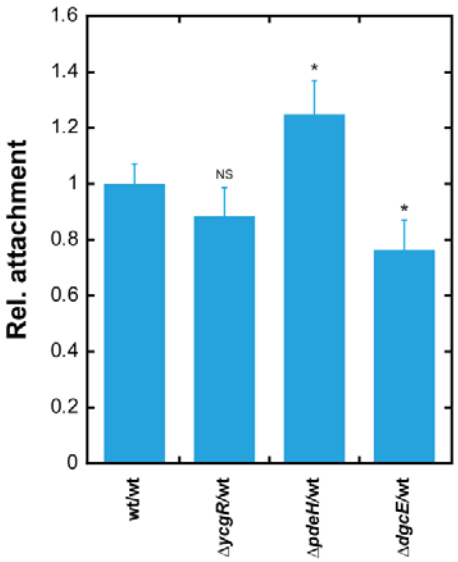

Figure 15. Adhesiveness is not responsible for the effect of c-di-GMP levels on attachment. Relative attachment by indicated mutants with perturbed c-di-GMP regulation after mild centrifugation. Experiments were performed and analyzed as in Fig. 10B. Shown are mean and standard error of four to eight replicates. Statistical analysis was performed using a two-sample t-test with unequal sample size and unequal variance, with $P < 0.05$ (*), NS, not significant.

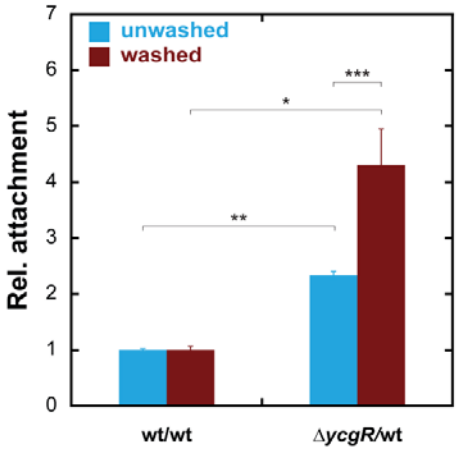

Figure 16. Fast swimming strengthens surface attachment. Relative attachment of wild-type and Δ*ycgR* cells in motility buffer to the surface of ibidi uncoated imaging plates after 1 h incubation. Attached cells were quantified and normalized as in Fig. 9C. Shown are mean and standard error of three replicates. Statistical analysis was performed using a two-sample t-test with unequal sample size and unequal variance, with $P < 0.0005$ (***), $P < 0.005$ (**), $P < 0.05$ (*).

2.2.3. C-di-GMP controls swimming speed via YcgR

To get insights into the mechanism of YcgR-mediated reduction of surface attachment by c-di-GMP, surface attachment and motility of wild-type and Δ*ycgR* cells was directly compared. Even when pre-grown in a shaking culture to OD_{600} of 0.5 and subsequently imaged in the motility buffer (i.e., in absence of further growth), Δ*ycgR* cells showed pronouncedly enhanced surface attachment compared to the wild-type (Figure 17A). Thus, the enhanced attachment of Δ*ycgR* cells does not require growth or differentiation on the surface. Among the analyzed motility parameters, differences in swimming speed between mutants were consistent with the previous report (Wood *et al.*, 2006), with cells swimming faster at low c-di-GMP levels (Figure 17B). In contrast, no differences in cell tumbling rates could be detected under our conditions (Figure 17C). These results indicate the increased swimming speed of Δ*ycgR* and Δ*dgcE* cells as the cause of their more efficient attachment to surfaces. Although swimming speed could in principle also influence surface trapping of cells, no significant differences between trajectory lengths on the surface for Δ*ycgR,* Δ*dgcE* or Δ*pdeH* cells were observed (Figure 17D). This invariance of trajectory length in spite of increased swimming speed could be explained by the compensating shortening of trajectory durations at low levels of c-di-GMP (Figure 18). Thus, swimming speed rather than the trajectory length seems to correlate with enhanced attachment.

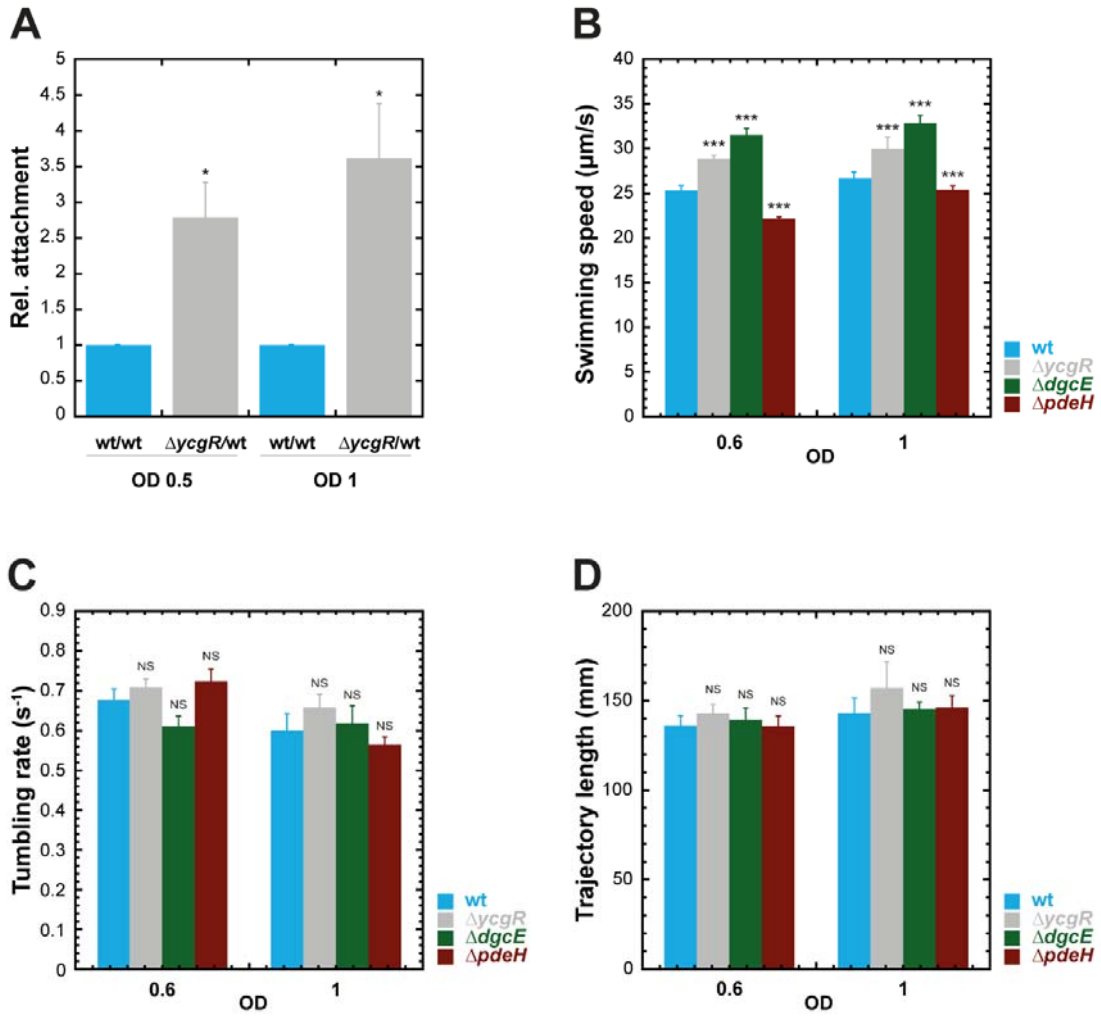

Figure 17. Faster swimming of Δ*ycgR* cells promotes attachment to surfaces. A. Relative surface attachment of wild-type and Δ*ycgR* cells in motility buffer. Planktonic cultures were grown to the indicated OD_{600}. Wild-type cells labeled with mCherry were mixed 1:1 with wild-type or Δ*ycgR* cells labeled with YFP and incubated in ibidi uncoated imaging plates at room temperature for 1 h. Attached cells were quantified and normalized as in Fig. 9C. Shown are mean and standard error of five to six replicates. **B-D**. Swimming behavior at the surface of a glass slide. Planktonic cultures were grown to the indicated OD_{600}, and swimming speed **(B)**, tumbling rate **(C)**, and trajectory lengths **(D)** of wild-type, Δ*ycgR*, Δ*dgcE* and Δ*pdeH* cells swimming at the surface were quantified. Shown are mean and standard error of three replicates. Experiments performed by Dr. Remy Colin. Statistical analyses were performed here and throughout using a two-sample t-test with unequal sample size and unequal variance, with $P < 0.05$ (*), $P < 0.0005$ (***), NS, not significant.

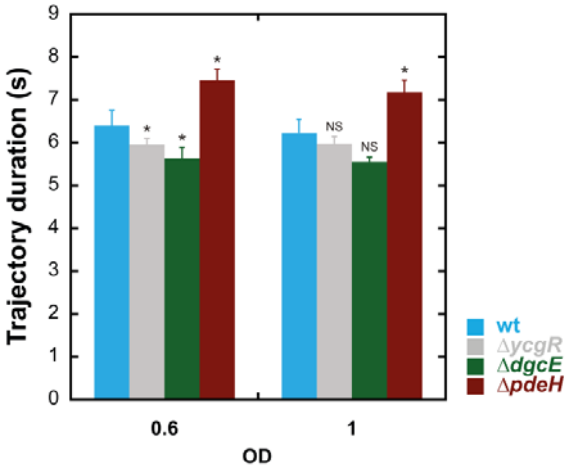

Figure 18. Trajectory duration is shortened at low c-di-GMP levels. Trajectory durations of wild-type and indicated mutants cells swimming at the surface of a glass slide. Cells were grown in planktonic cultures to the indicated OD_{600}. Experiment performed by Dr. Remy Colin. Shown are mean and standard error of three replicates. Statistical analysis was performed using a two-sample t-test with unequal sample size and unequal variance, with $P < 0.05$ (*), NS, not significant.

2.2.4. Type 1 fimbriae mediate swimming-speed dependence of surface attachment

Since flagella apparently have only a minor role in attachment under our conditions, the potential involvement of type 1 fimbriae, one of the major and best characterized adhesins of *E. coli,* was tested. Indeed, Δ*fimA* strain that lacks a major subunit of fimbria showed clearly reduced attachment (Figure 19A, B). In contrast, deletion of *csgA* encoding the subunit of curli fibers, major component of *E. coli* biofilm matrix, had no significant effect on attachment under our conditions (Figure 19A, B). Same results were observed when the surface colonization was assessed for these strains after 24 hours (Figure 20), which is consistent with the previously observed higher importance of type 1 fimbriae for early biofilm formation (Monteiro *et al.*, 2012).

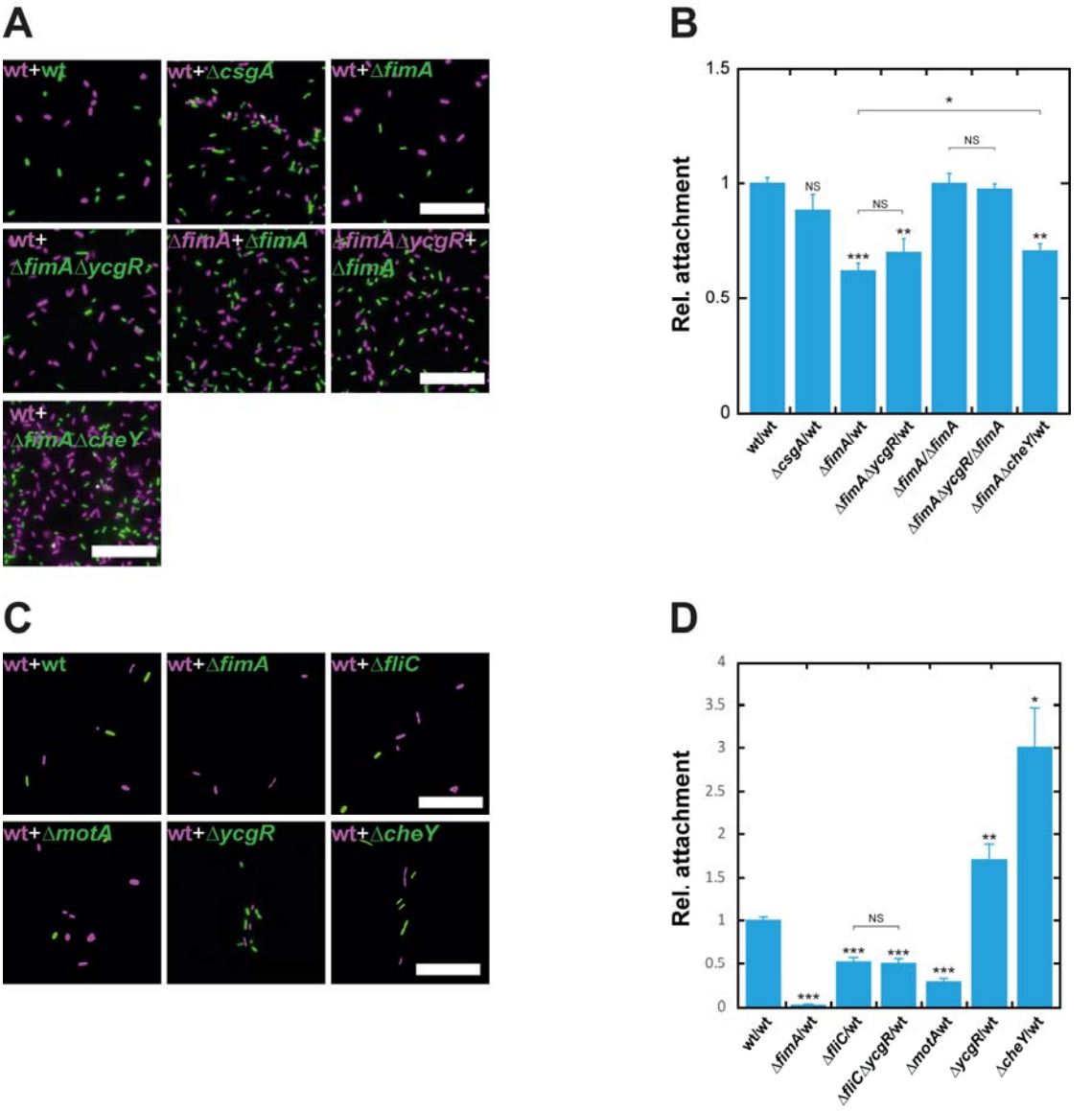

Figure 19. Fimbriae enable increased attachment of faster swimming bacteria. A, B. Relative attachment of wild-type and indicated mutants to abiotic surface in motility buffer. Wild-type, Δ*csgA, ΔfimA, ΔfimAΔycgR* or *ΔfimAΔcheY* cells labeled with mCherry were mixed 1:1 with wild-type or *ΔfimA* cells labeled with GFP and incubated on ibidi uncoated imaging plates for 1 h. **A**. Exemplary images of mixed cultures. Scale bar: 25 µm. **B**. Relative numbers of attached cells were quantified and normalized as Fig. 9C. Shown are mean and standard error of three to five replicates. **C, D**. Relative attachment of wild-type and indicated mutants to mannosylated surface in motility buffer. Experiments were performed and analyzed as in **(A, B)**, except that ibidi uncoated imaging plates were mannosylated as described in Experimental procedures. Statistical analyses were performed here and throughout using a two-sample t-test with unequal sample size and unequal variance, with $P < 0.05$ (*), $P < 0.005$ (**), $P < 0.0005$ (***), NS, not significant.

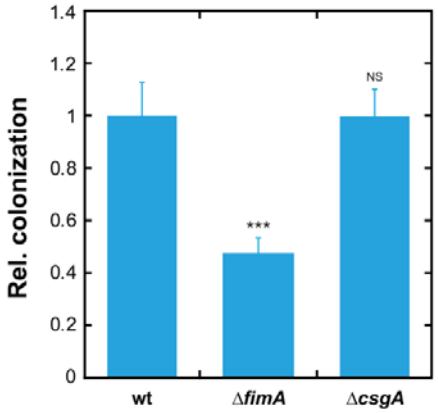

Figure 20. Type 1 fimbriae are important for surface colonization. Relative surface colonization by wild-type, Δ*fimA* and Δ*csgA* cells. Experiments were performed and analyzed as in Fig. 9A. Shown are mean and standard error of four to eight replicates. Statistical analysis was performed using a two-sample t-test with unequal sample size and unequal variance, with P < 0.0005 (***), NS, not significant.

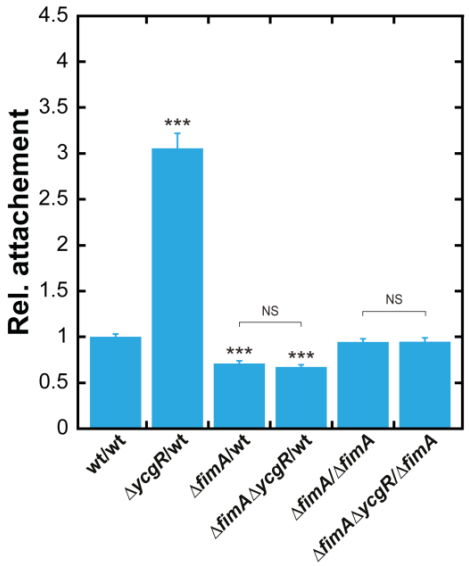

Figure 21. Fimbriae mediates attachment of faster swimming bacteria at 30°C. Relative attachment of the wild-type and indicated mutants in motility buffer to the surface of ibidi uncoated imaging plates at 30°C after 1 h incubation. Attached cells were quantified and normalized as in Fig. 9C. Shown are mean and standard error of three to five replicates. Statistical analysis was performed using a two-sample t-test with unequal sample size and unequal variance, with P < 0.0005 (***), NS, not significant.

Strikingly, lack of fimbriae also abolished the effect of the YcgR deletion, with attachment of Δ*fimA* and Δ*fimA*Δ*ycgR* being identical (Figure 19B). This indicates that fimbriae are responsible for the increased number of attached cells seen for the Δ*ycgR* mutant, which was confirmed by similar attachment of fimbria-less strains with and without *ycgR*. In contrast, Δ*cheY* cells attached better even in absence of fimbriae (Figure 19B), although

this enhancement was weaker than in the wild-type background. This suggests that prolonged swimming enhances attachment independently of the adhesin involved. Comparable results were obtained when the experiment was performed at higher temperature, 30°C (Figure 21).

Specificity of Δ*fimA* effects on attachment could be confirmed by complementation with FimA expression from a plasmid (Figure 22). Moreover, the activity of type 1 fimbriae *fimD* promoter was not affected by *ycgR* deletion (Figure S1A), favoring the hypothesis that attachment mediated by type 1 fimbriae is directly promoted by cell swimming speed. Similarly, no differences in *fimD* promoter activity were observed in Δ*dgcE* cells (Figure S1B). In contrast, *fimD* promoter activity was decreased in Δ*pdeH* and elevated in Δ*cheY* cells. Nevertheless, these modest changes were opposite to the observed adhesiveness of Δ*pdeH* and Δ*cheY* strains in centrifugation experiments (Figure 11C and Figure 14) and are thus unlikely to explain differences in their attachment.

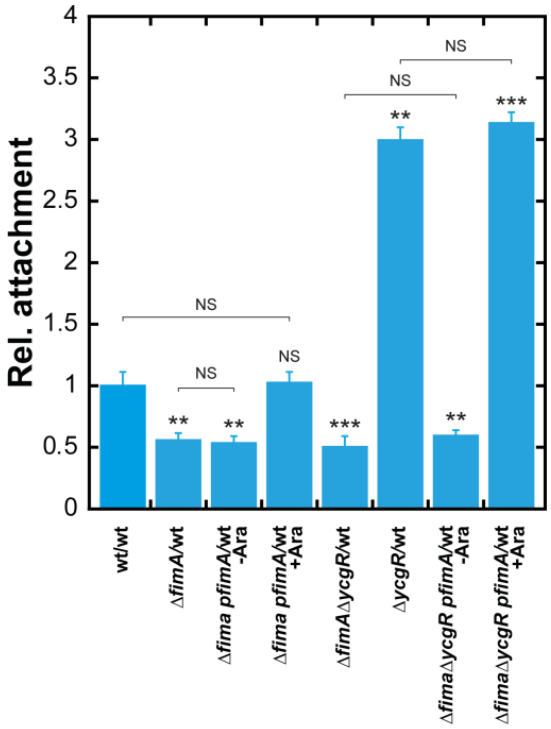

Figure 22. Complementation restores attachment of Δ*fimA* cells. Relative attachment of wild-type, Δ*fimA* and Δ*fimA*Δ*ycgR* cells transformed with an inducible plasmid encoding FimA. Experiments were performed in motility buffer and with ibidi uncoated imaging plates with 1 h incubation. Cells were grown with or without induction with arabinose in the medium, as indicated. Attached cells were quantified and normalized as in Fig. 4B. Shown are mean and standard error of four to six replicates. Statistical analysis was performed using a two-sample t-test with unequal sample size and unequal variance, with $P < 0.0005$ (***), $P < 0.005$ (**), NS, not significant.

The effect of c-di-GMP was also observed for the specific attachment on mannosylated surface, which is strictly dependent on type 1 fimbriae (Figure 19C, D and Figure 23). For a relatively brief (20 min) incubation, the attachment to this surface was strongly promoted by motility (Figure 19C, D), although flagella-less Δ*fliC* cells attached somewhat better than Δ*motA* cells, possibly because immobile flagella partially hinder the attachment. Importantly, the attachment of Δ*ycgR* cells under these conditions was almost twice of that observed for the wild-type. In contrast, attachment of Δ*ycgR*Δ*fliC* and Δ*fliC* cells was indistinguishable, confirming that the effect of YcgR on attachment is motility-dependent. Strongly increased attachment was also observed for the smooth-swimming Δ*cheY* cells. However, motility became less important for attachment at later time points, with attachment of Δ*motA* and Δ*ycgR* cells becoming similar to that of the wild-type after 1 h, and the advantage of Δ*cheY* cells being reduced (Figure 23). At this later time point the lack of flagella reduces the number of attached cells, as Δ*fliC* cells attached less efficiently than Δ*motA* cells, pointing to a possible role of flagella as (non-specific) secondary adhesins that can stabilize the fimbriae-mediated primary adhesion.

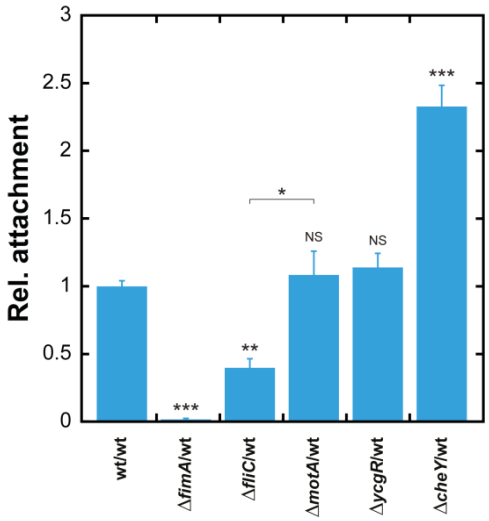

Figure 23. Effects of motility on attachment to mannosylated surfaces after 1 h. Relative attachment of the wild-type and indicated knockout strains in motility buffer to mannosylated surfaces is shown after 1 h incubation. Attached cells were quantified and normalized as in Fig. 9C. Shown are mean and standard error of three to five replicates. Statistical analysis was performed using a two-sample t-test with unequal sample size and unequal variance, with $P < 0.005$ (**), $P < 0.05$ (*), NS, not significant.

2.3. Bacterial attachment under flow

Bacteria in their natural environment often live attached to a surface and are exposed to shear flow. Therefore, the behavior of *E. coli* W3110 *rpoS*$^+$ cells under flow was of interest for this study. For this purpose, cells were grown until exponential phase and then fed into microfluidic channels. Firstly, the influence of different flows on attachment and surface colonization was tested. Three flow rates were applied: 0.2 dyne/cm^2, 0.5 dyne/cm^2 and 1 dyne/cm^2 corresponding to lower, double and four times higher than the swimming speed of *E. coli,* respectively. Bacterial surface colonization of the surface was quantified over time.

After exposing *E. coli* for 11 hours to the different flow rates, the cells managed to attach and grow on the surface in different ways depending on the flow rate studied. The highest and fastest colonization was observed at 0.5 dyne/cm^2. Thus, it seems that there is an optimal swimming speed for attachment. Cells attached and colonized a bigger surface at the lowest flow rate. Finally, at the highest flow rate cells managed to cover around 20 percent of area after 11 hours (Figure 24).

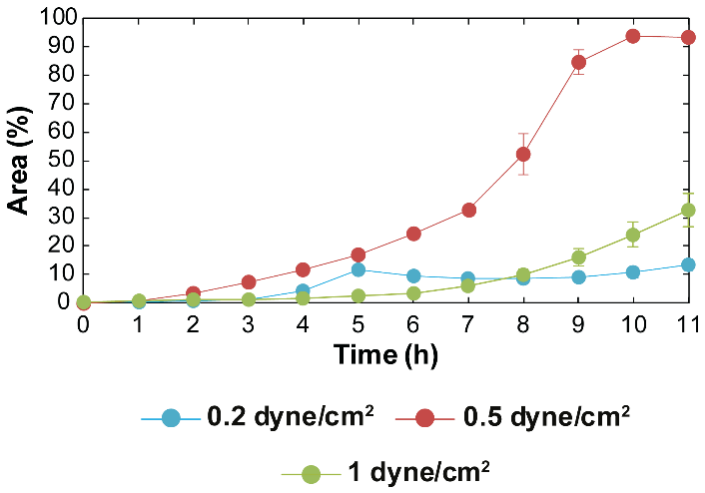

Figure 24. Quantification of the attachment of wild-type W3110 *rpoS*+ cells under 0.2, 0.5 and 1 dyne/cm². Cells were grown until OD_{600} 0.5, harvested and diluted in fresh media until OD_{600} 0.05. Cells were flushed for 2 minutes at 1 dyne/cm^2 and fresh media was flushed at a constant 0.2, 0.5 or 1 dyne/cm^2 flow for 11 hours. Images were taken every hour and the percentage of area covered by cells was quantified.

In addition, the role of the major adhesins and bacterial motility in attachment, under low and high flow rates, was investigated. For these experiments, besides exposing the cells to different flow rates, new cells were constantly being introduced into the channels for 9-15 hours. Attachment of wild-type cells was tested first (Figure 25). Wild-type cells

managed to attach and grow on the surface leading to the whole colonization of the channels surface after 15 hours, at both flow rates tested. Furthermore, the formation of 3D structures especially at a high flow rate could be seen (Figure 25B).

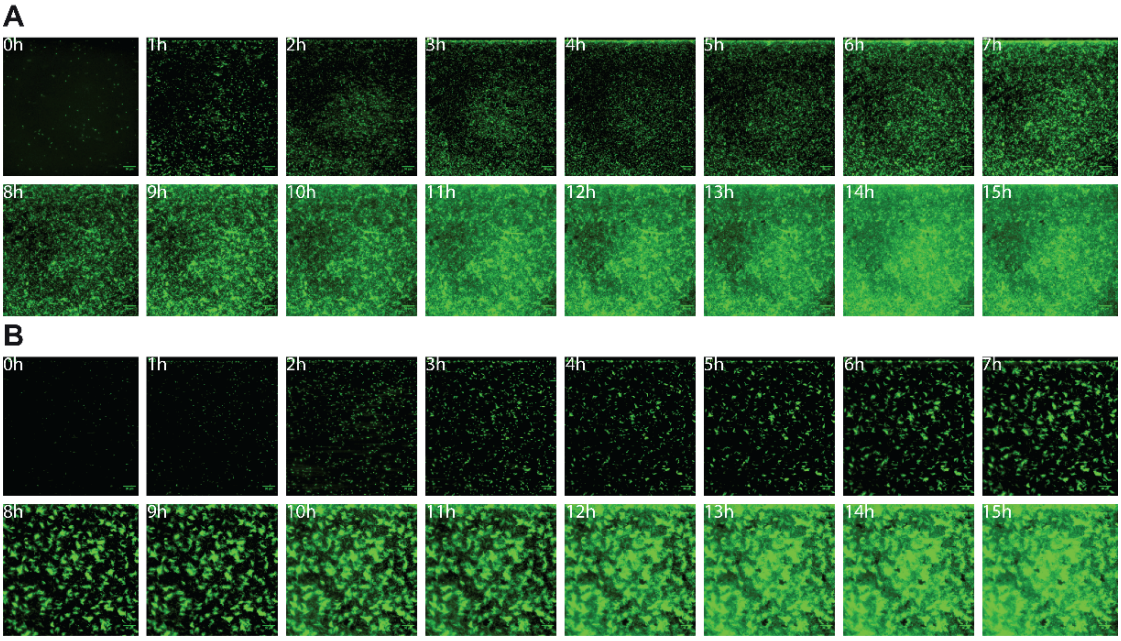

Figure 25. Attachment of wild-type W3110 *rpoS*$^{+}$ cells under 0.2 dyne/cm^2 (A) and 1 dyne/cm^2 (B). Attachment was assessed for 15 hours at a constant flow with no incubation time. Images were taken every hour.

In order to investigate the role of curli fibers on attachment under flow, *ΔcsgA* was used. These curli deficient cells did attach similarly to wild-type cells at both flow rates (Figure 26). This agrees with our results under static conditions where curli fibers were not involved in surface attachment when cells were growing exponentially (Figure 7C, Figure 8C).

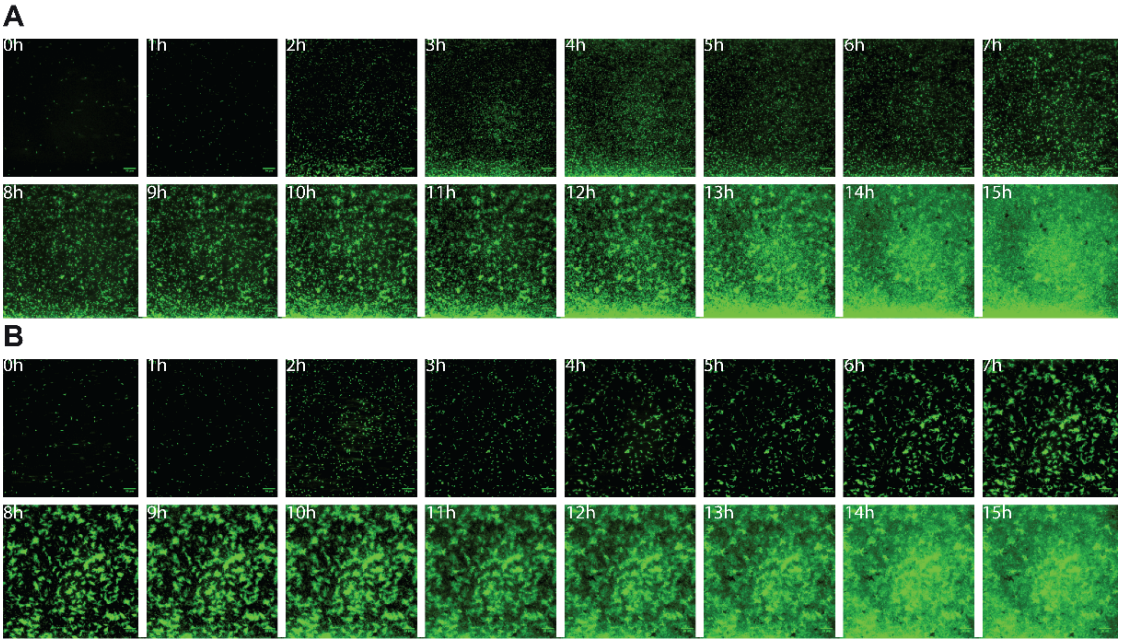

Figure 26. Attachment of *ΔcsgA* W3110 *rpoS*$^{+}$ cells under 0.2 dyne/cm^2 (A) and 1 dyne/cm^2 (B). Attachment was assessed for 15 hours at a constant flow with no incubation time. Images were taken every hour.

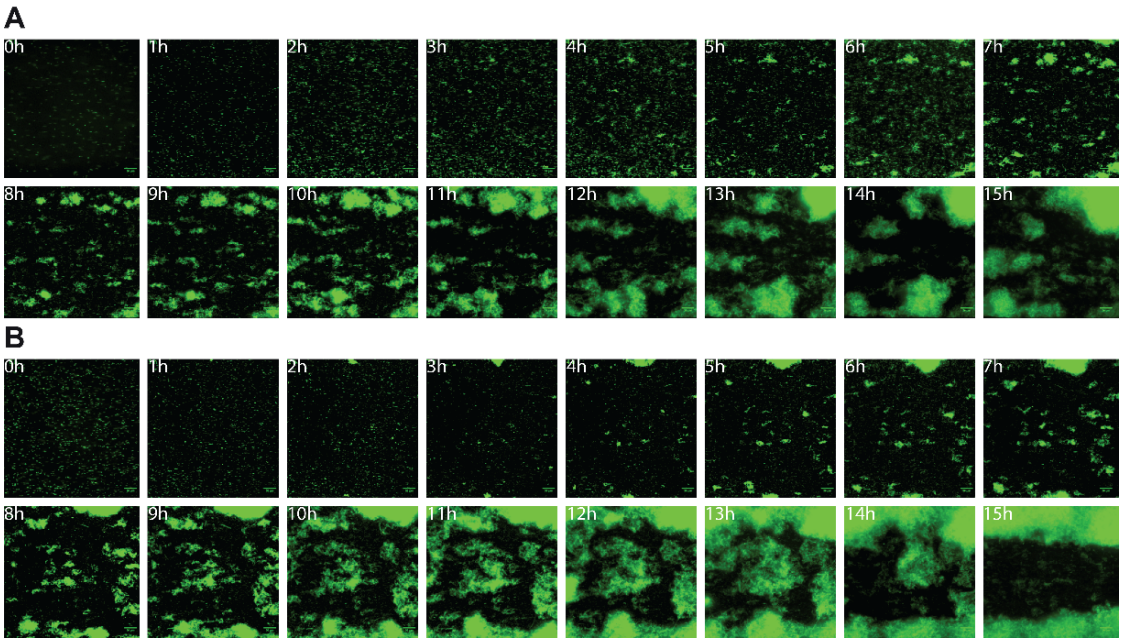

Figure 27. Attachment of *ΔfliC* W3110 *rpoS*$^{+}$ cells under 0.2 dyne/cm^2 (A) and 1 dyne/cm^2 (B). Attachment was assessed for 15 hours at a constant flow with no incubation time. Images were taken every hour.

Furthermore, motility deficient strains *ΔfliC* and *ΔmotA* were tested. Opposite to wild-type, non-flagellated cells did not form monolayers. Instead, cells clumped forming cloud-like structures (Figure 27). These structures were observed at all the flow rates studied and were bigger at higher flow rates (Figure 27B). In addition, cell clumps did not seem

to be attached to the surface of the channel and instead, moved following the liquid flow. When comparing the two strains, *ΔmotA* cells attach more efficiently than *ΔfliC* ones. *ΔmotA* cells did manage to form colonies on the surface of the channel but, unlike the wild-type, formed tree-like structures (Figure 28). This could be due to unorganized flagella surrounding bacteria and interacting with other cells, leading to a mesh structure. Both these results indicate that, in these experimental setups, flagella might play a role as an adhesin.

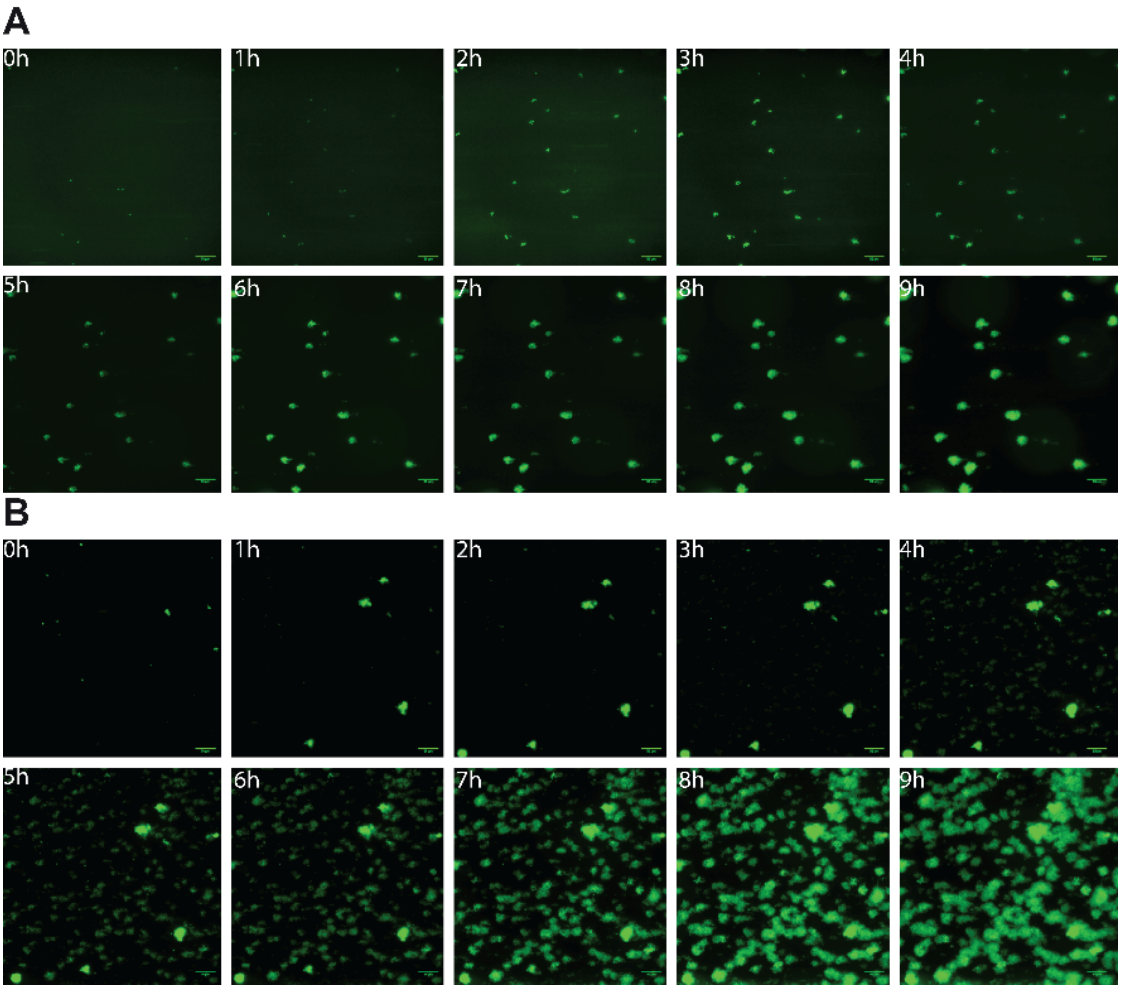

Figure 28. Attachment of *ΔmotA* W3110 rpoS+ cells under 0.2 dyne/cm^2 (A) and 1 dyne/cm^2 (B). Attachment was assessed for 9 hours at a constant flow with no incubation time. Images were taken every hour.

Finally, attachment of cells lacking type 1 fimbriae was assessed. An interesting phenotype was observed for this strain. At a high flow rate (1 dyne/cm^2), *ΔfimA* cells could attach as well as wild-type cells during the first 3 hours of the experiment when cells were fed into the channel at a high rate (1 dyne/cm^2). However, after this period, *ΔfimA* cells did not manage to grow on the surface and failed to remain attached to the

surface (Figure 29B). On the other hand, when a lower flow rate was applied, fimbrialess cells remained attached for longer periods of time (Figure 29A). At medium flow rates (0.5 dyne/cm^2) an intermediate result was obtained, with significant more and faster detachment than at 0.2 but not as dramatic as the observed for the highest flow rate studied (Figure S2).

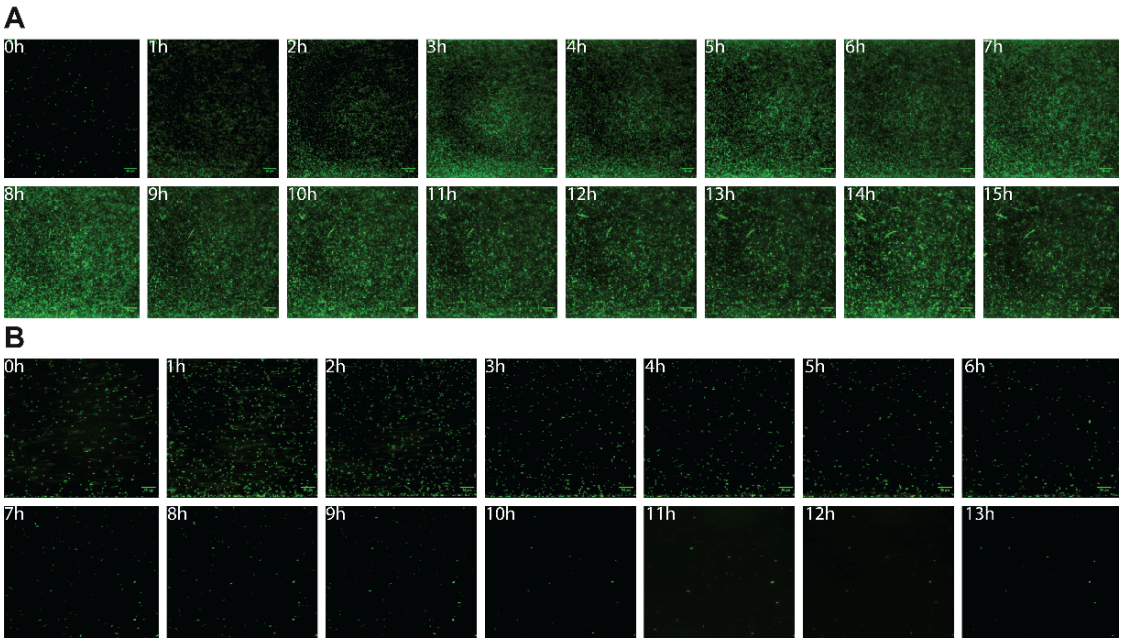

Figure 29. Attachment of *ΔfimA* W3110 *rpoS*$^+$ cells under 0.2 dyne/cm^2 (A) and 1 dyne/cm^2 (B). Attachment was assessed for 15 or 13 hours at a constant flow with no incubation time. Images were taken every hour.

In this microfluidic setup our results indicate that the presence of flagella and not type 1 fimbriae, are important for initial surface attachment. However, it seems that fimbriae are critical for keeping the cells attached to the surface for longer times periods.

2.4. Importance of type 1 fimbriae in surface attachment

During the screening of the different adhesins under flow, it was observed that cells lacking type 1 fimbriae are capable of initially attaching to the surface similarly to the wild-type cells but are not capable of growing or remaining attached to the surface (Figure 30).

Furthermore, the role of the fimbrial tip in this detachment was assessed. For this purpose, *ΔfimH,* which possesses type 1 fimbriae but lacks the last protein of the tip (Figure 4), responsible for specific mannose attachment, was introduced in a microfluidic

channel and exposed to a flow rate of 1 dyne/cm^2. Results showed that the fimbrial tip is not required for attachment or growth on the surface (Figure 31). Therefore, the effect of the absence of the whole fimbrial structure was investigated.

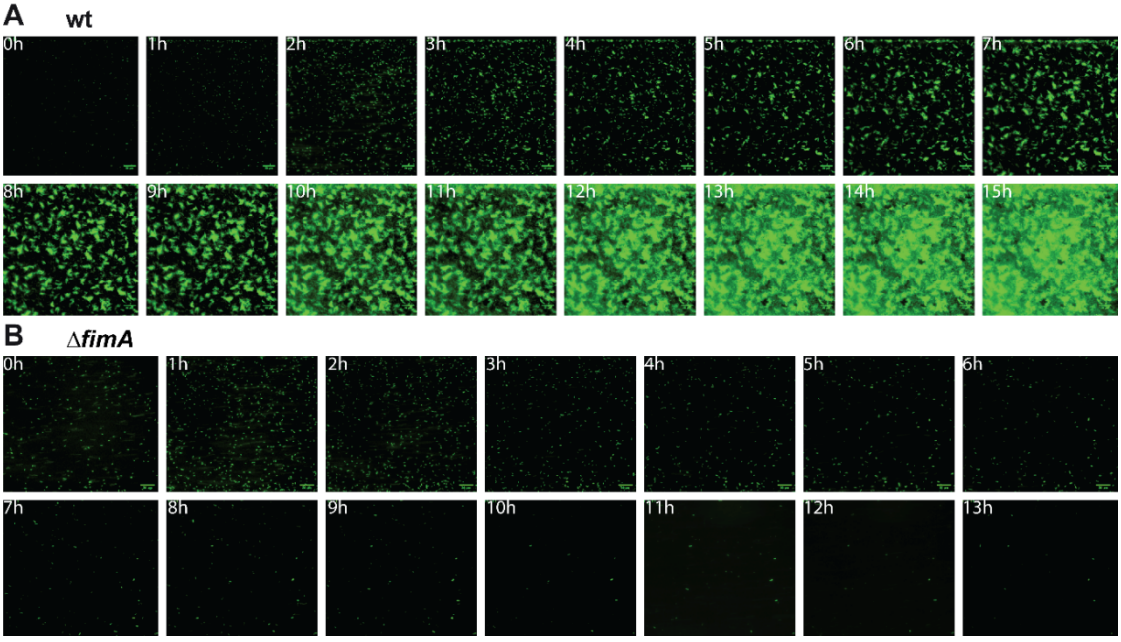

Figure 30. Attachment of wild-type (A) and *ΔfimA* (B) cells under 1 dyne/cm^2. Attachment was assessed for 13 or 15 hours at a constant flow with no incubation time. Images were taken every hour.

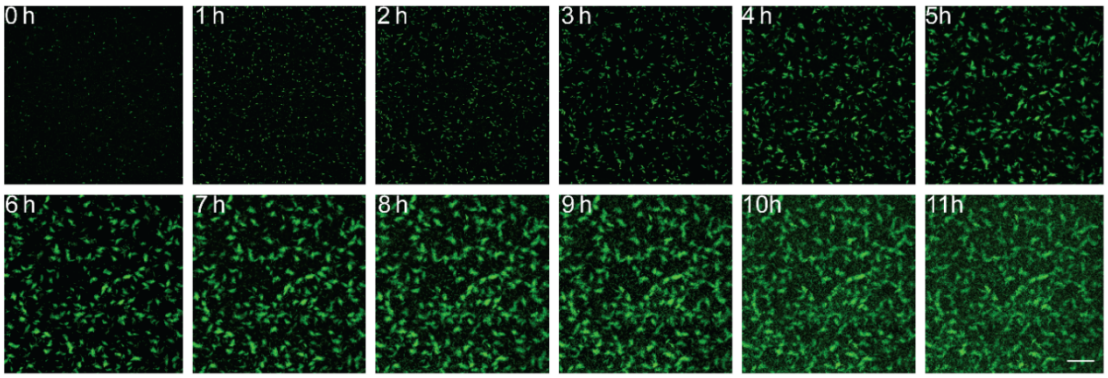

Figure 31. Attachment of *ΔfimH* W3110 *rpoS*$^+$ cells under 1 dyne/cm^2 flow. Cells were introduced in the channels for 2 minutes at 1 dyne/cm^2 and fresh media was flushed at a constant 1 dyne/cm^2 flow for 11 hours.

2.4.1. Inhibition of protein synthesis circumvents the need of type 1 fimbriae for lasting attachment

In the original experimental setup (part 2.3), new cells were introduced in the microfluidics channels throughout the experiment and were also able to divide and grow

on the surface. Therefore, in order to decouple the effect of the attachment of new cells and the division of the ones already in the channels, the attachment of non-dividing cells was investigated. This not only allows to focus on the contribution of the arriving cells, but also to detect the physical effect of the presence of fimbriae. Therefore, cells were harvested, washed once in tethering buffer supplemented with chloramphenicol and kept at 4°C for 20 minutes to avoid cell division. Cells were then flushed constantly for 12 hours at 0.2 or 1 dyne/cm^2 (Figure 32). In addition, the number of cells attached at each time point was quantified (Figure 33).

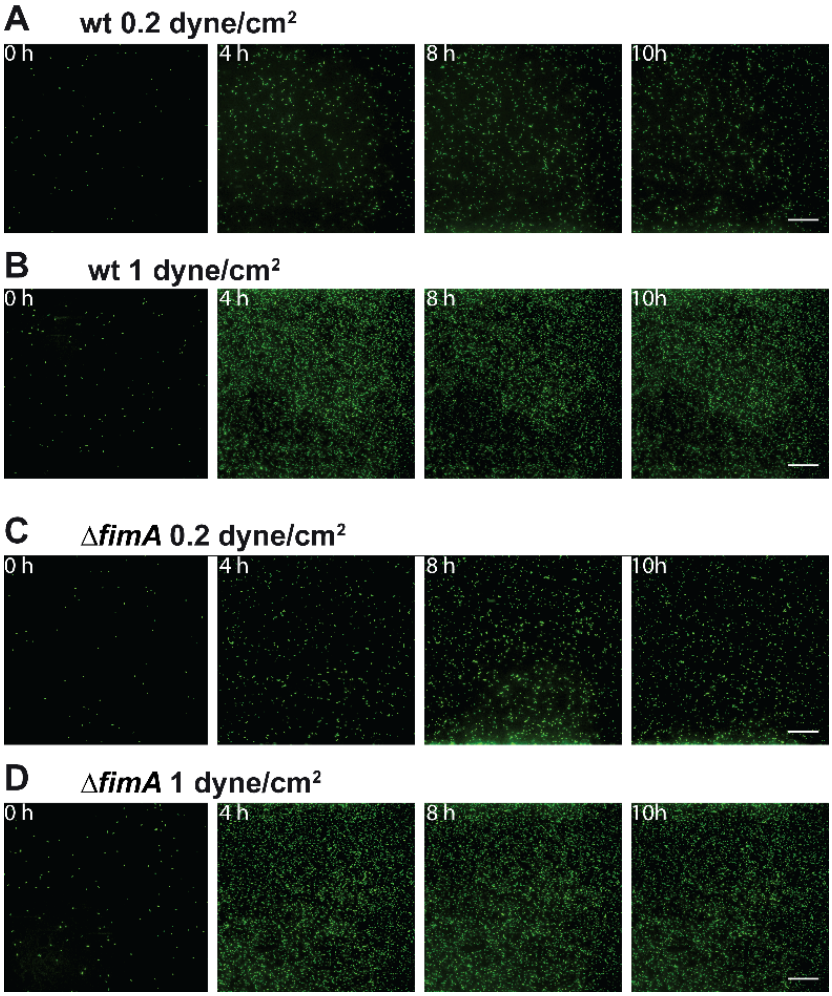

Figure 32. Attachment of non-dividing wild-type (A) and *ΔfimA* (B) W3110 *rpoS*$^+$ cells under flow. Cells were harvested and washed twice on tethering buffer supplemented with chloramphenicol and kept at 4°C for 20 minutes before being flushed constantly at 0.2 or 1 dyne/cm^2. Images were taken every 20 minutes.

Firstly, it was observed that, unlike what was seen previously, fimbriae deficient (*ΔfimA*) cells remained attached to the channel throughout the experiment and no major detachment could be detected at any of the flow rates studied (Figure 32C, D). After the number of attached cells was quantified, the results showed that, when exposed to the

lower flow rate, *ΔfimA* cells attached slightly better than wild-type cells at every time point analyzed. This attachment advantage was absent when cells were flushed at a higher flow rate, with both wild-type and *ΔfimA* cells attaching similarly (Figure 19B, D, Figure 33).

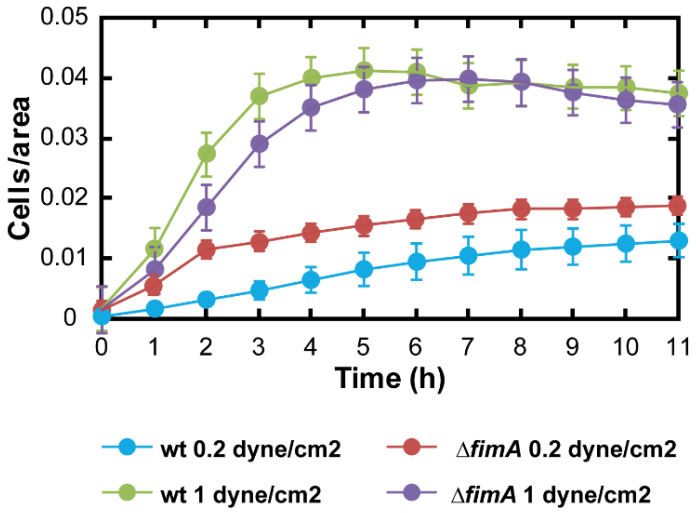

Figure 33. Quantification of attached non-dividing wild-type and *ΔfimA* cells under flow. Cells were harvested and washed twice on tethering buffer supplemented with chloramphenicol and kept at 4°C for 20 minutes before being flushed constantly at 0.2 and 1 dyne/cm^2. Shown are mean and standard error of two to three replicates. Statistical analysis was performed using a two-sample t-test with unequal sample size and unequal variance. Statistically significant differences were found between wild-type and *ΔfimA* cells when flushed at 0.2 dyne/cm^2 from the second time point on (t=1). No statistical significance was found when cells were flushed at 1 dyne/cm^2.

This higher number of *ΔfimA* cells at 0.2 dyne/cm^2 could be the result of an increased number of arriving cells or a higher residence time of cells in the channel. To clarify which was responsible for this increase in attachment, the number of cells arriving at each point as well as the fraction of leaving cells, defined as the cells that leaved from one hour to the next out of all the possible cells that could have left, was analyzed (Figure 34). The fraction of leaving cells seen for *ΔfimA* cells was similar to wild-type cells. However, a higher number of *ΔfimA* cells arriving was detected (Figure 34A, B). This indicates that *ΔfimA* cells are more “sticky” and thus are able to attach more frequently to the surface than wild-type cells.

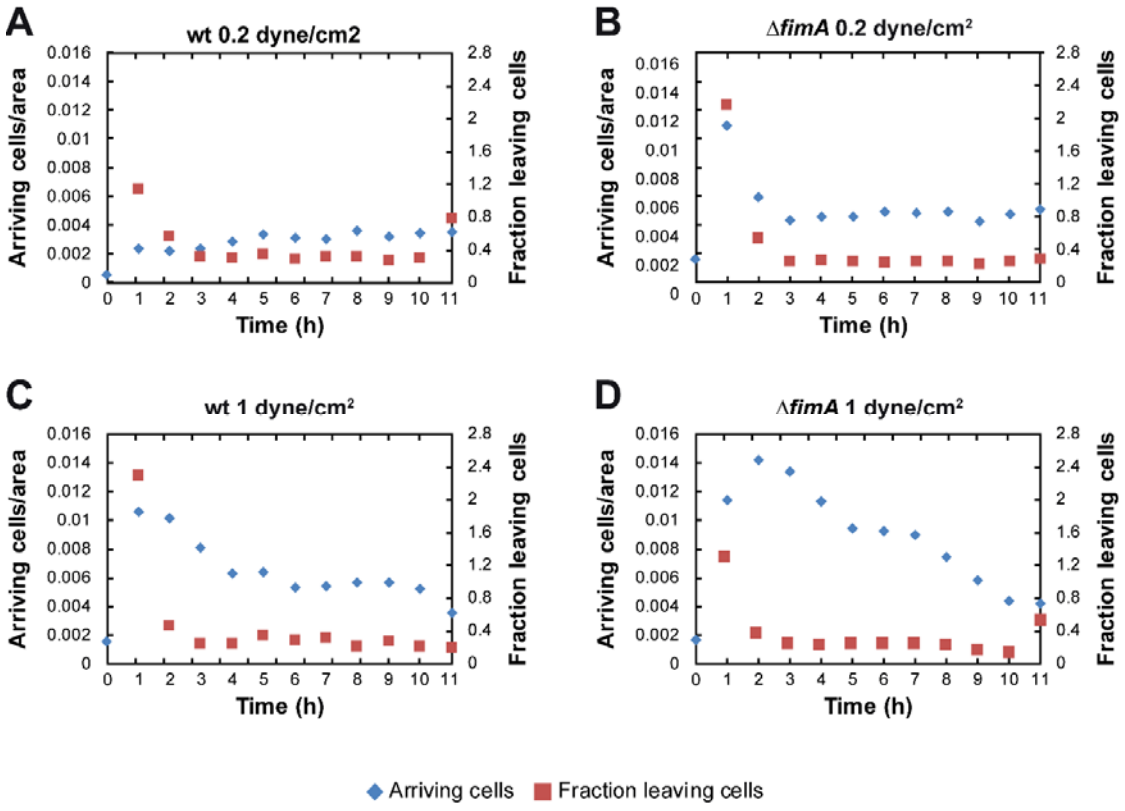

Figure 34. Attachment and detachment of non-dividing wild-type (A, C) and *ΔfimA* (B, D) cells at 0.2 (A, B) and 1 dyne/cm² (C, D). Cells were harvested and washed twice on tethering buffer supplemented with chloramphenicol and kept at 4°C for 20 minutes before constantly being fed into the channels at the indicated flow rates. Fraction of leaving cells was calculated relative to the total number of cells detected in the hour before.

These results indicate that, when translation is inhibited, fimbrialess cells have an attachment advantage at a low flow rate. One possible explanation could be that fimbrialess cells are faster swimmers than wild-type cells. Because the flow rate used was lower than the swimming speed of wild-type cells, differences in their swimming speed could translate into differences in their surface attachment, as seen in part 2.2. For the higher flow rate studied, swimming speed would not be relevant. For that reason, the swimming speed of both wild-type and *ΔfimA* cells was measured. However, contrary to the hypothesis presented here, fimbrialess cells swam slower than wild-type cells (Figure 35). Therefore, it seems that swimming speed does not affect the differential attachment of these strains. Another possibility could be that in a *ΔfimA* background the expression of other adhesin is compensating for the loss of type 1 fimbriae.

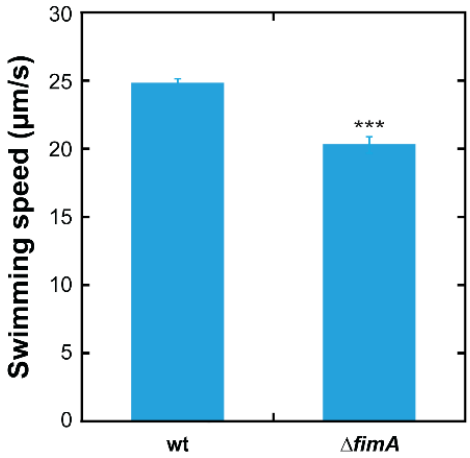

Figure 35. Swimming speed of wilt type and *ΔfimA* cells. Planktonic cultures were grown to OD_{600} 0.5, and swimming speed of cells swimming at the surface were quantified. Shown are mean and standard error of three replicates. Statistical analyses were performed here and throughout using a two-sample t-test with unequal sample size and unequal variance, with $P < 0.0005$ (***).

Furthermore, to ensure that differences in the composition of the TB medium used for the original experiments and the tethering buffer are not affecting the results, the attachment of cells in medium or buffer supplemented with chloramphenicol was tested, this time in static conditions. In agreement with our previous results (Figure 33), no major detachment was observed for wild-type or *ΔfimA* cells when resuspended in buffer supplemented with chloramphenicol (Figure 36). In static conditions, unlike what was observed under flow, wild-type surface colonization was faster than *ΔfimA* cells. It is possible that in this setup the higher swimming speed observed for wild-type cells (Figure 35) gives an advantage in colonization. A slight detachment of fimbrialess cells in TB medium was detected (Figure 36). However, this detachment was not sufficient to explain the results seen when protein synthesis was not inhibited. Therefore, the physical absence of fimbriae is not enough to explain differences in attachment between wild-type and fimbrialess cells.

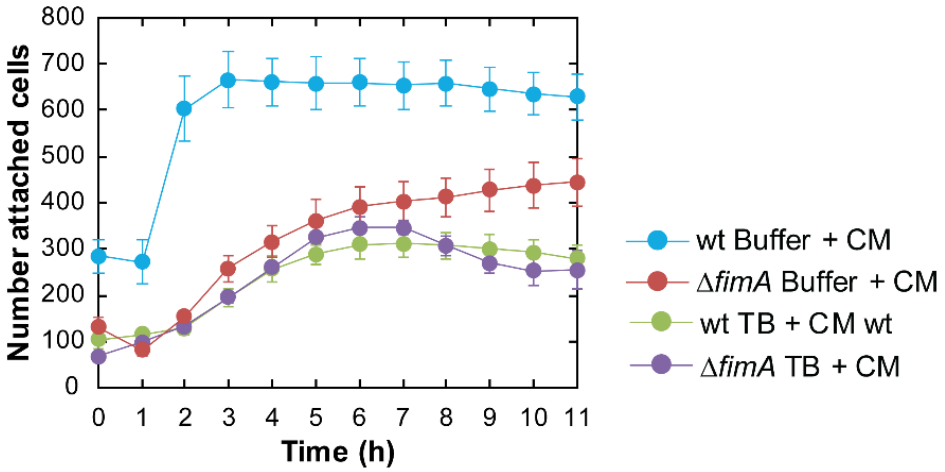

Figure 36. Quantification of attached wild-type and *ΔfimA* cells on buffer or TB medium supplemented with chloramphenicol in static conditions. Cells were harvested and washed and resuspended either on tethering buffer or TB medium supplemented with chloramphenicol and kept at 4°C for 20 minutes before being seeded for 5 minutes on ibidi uncoated plates. Shown are mean and standard error of three replicates.

2.4.2. Flagella expression does not compensate for the loss of fimbriae

Attachment to the surfaces is not a mere physical phenomenon. Once cells are attached their gene expression changes allowing them to adapt to a sessile life style. In the previous part, the attachment contribution of new cells entering the channel was assessed, the results showed that division and protein synthesis are responsible for the loss of adhesiveness of fimbrialess cells. Therefore, the fate of the cells once attached and dividing on the surface was studied next. For this purpose, a series of experiments where cells were seeded in the microfluidic channels were performed. These cells were followed over time with only fresh media being flushed through the system. This way the contribution of new cells entering the channel was abolished.

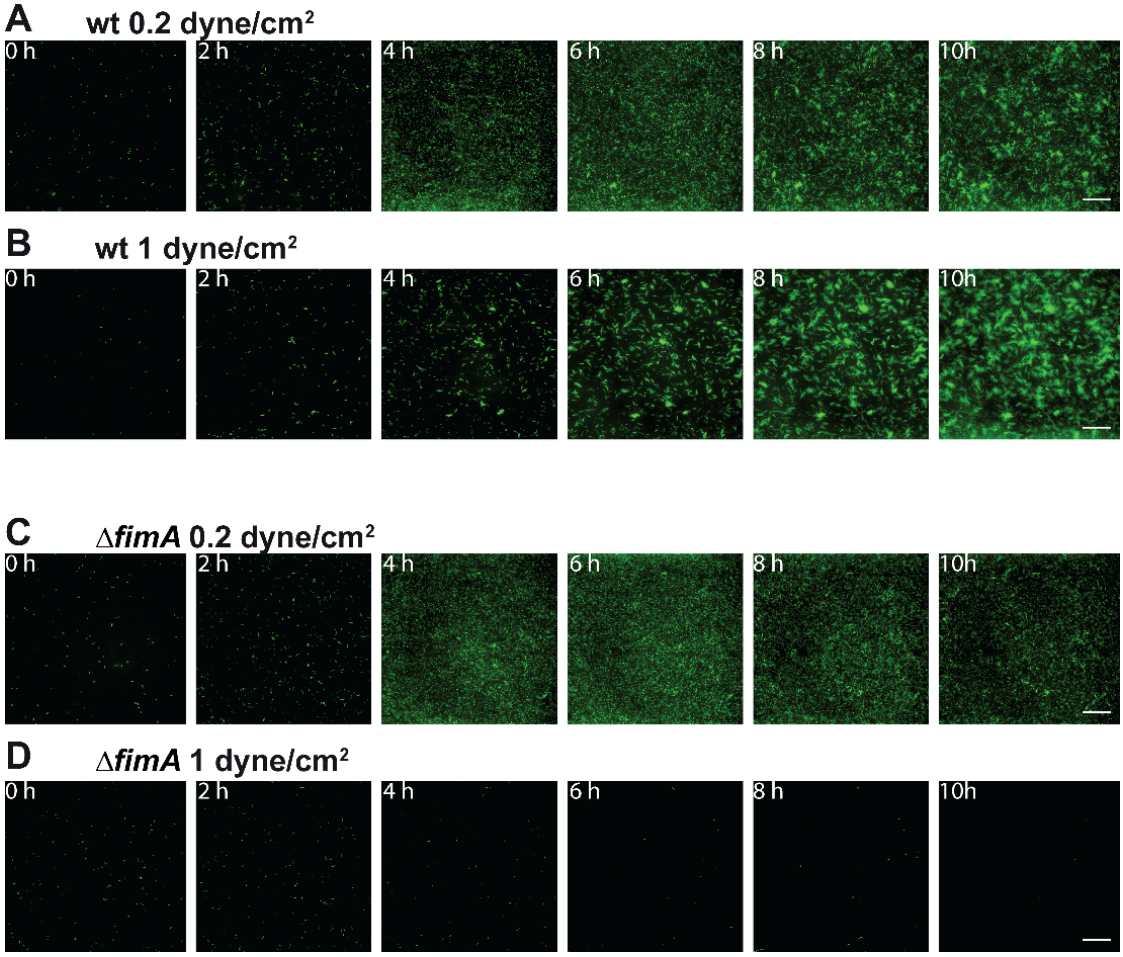

Figure 37. Attachment of wild-type (A, B) and *ΔfimA* (C, D) W3110 *rpoS*$^+$ cells under flow. Cells were introduced in the channels for 2 minutes at 1 dyne/cm^2 and fresh media was flushed at a constant 0.2 **(A, C)** or 1 dyne/cm^2 flow **(B, D)** for 10 hours.

Similarly to the first experiments (Figure 25, Figure 29), wild-type cells were able to colonize and grow on the surface at both flow rates while fimbrialess cells (*ΔfimA*) were not able to remain attached or grow in colonies on the surface (Figure 37). After quantifying the colonization of the surface at each hour, it was observed that fimbrialess cells and wild-type ones attached similarly during the first three hours at both flow rates studied (Figure 38). Peak colonization of fimbrialess cells was observed after 6 and 3 hours when exposed to low and high flow rates, respectively (Figure 38A B).

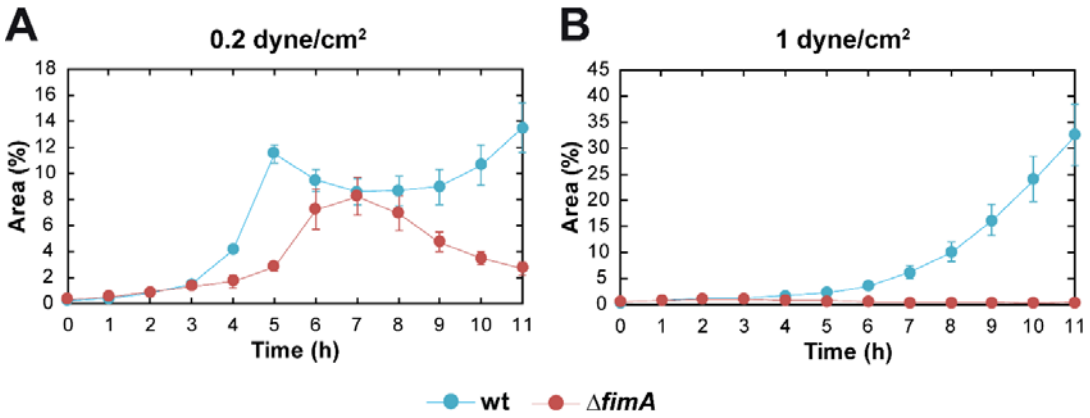

Figure 38. Attachment of wild-type and *ΔfimA* cells under flow. Cells were introduced in the channels for 2 minutes at 1 dyne/cm^2 and fresh media was flushed at a constant 0.2 **(A)** or 1 dyne/cm^2 flow **(B)** for 11 hours. The percentage of area occupied by cells was quantified every hour. Shown are mean and standard error of two to three replicates.

The results in part 2.3 showed that the presence of flagella is important for initial attachment. Furthermore, as it was mentioned previously, wild-type cells, when attached to the surface, actively produced flagella. Thus, it was hypothesized that type 1 fimbriae might play a role in mechanosensing. Therefore, cells lacking fimbriae would be unable to produce flagella upon contact with the surface. This way, these cells might attach first via flagella to the surface but, after some time, the number of flagella per cell in a fimbrialess background would decrease because of cell division. Thus, at some point, flagella alone might not be sufficient to keep the cells attached to the surface.

In order to test this hypothesis, a promoter reporter plasmid for *fliC,* a class III gene regulating flagella expression and encoding the main flagellin, was used. The results obtained for the percentage of occupied area was similar to the growth experiment (Figure 38): wild-type cells grew on the surface while *ΔfimA* cells did not manage to stay attached and colonize it (Figure 39A). As for the *fliC* intensity, while an increase in flagellin production was seen over time for wild-type cells, *ΔfimA* cells kept its production low throughout the experiment (Figure 39A). However, the expression was similar for both strains during the time when detachment of fimbrialess cells was observed. To corroborate the data obtained by microscopy, *fliC* expression of wild-type and fimbrialess cells was studied using flow cytometry. *fliC* expression of attached cells was assessed after 3 and 5 hours of attachment and compared to the levels of planktonic cells. No upregulation of flagellar genes for wild-type or fimbrialess cells could be detected (Figure 39B).

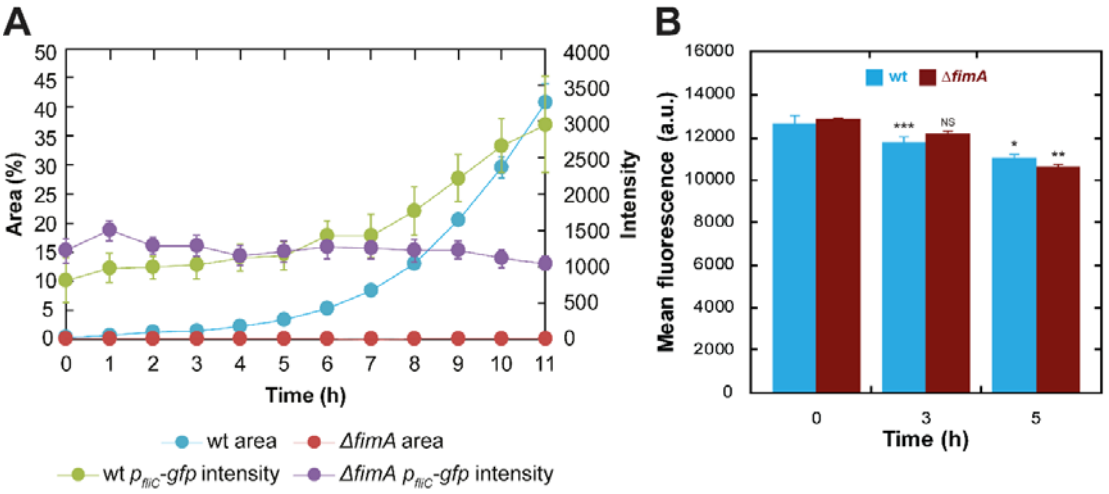

Figure 39. Attachment and flagellin expression of wild-type and *ΔfimA* p_{fliC}*-gfp* cells. A. Cells were grown until OD_{600} 0.5 and introduced in the channels for 2 minutes at 1 dyne/cm^2. Fresh media was flushed at a constant 1 dyne/cm^2 flow for 11 hours. Percentage of area occupied by cells and intensity of the reporter p_{fliC}*-gfp* were quantified every hour. **B**. Cells were grown as for microfluidic experiments and *fliC* expression was measured (t=0). These cells were seeded on ibidi uncoated plates for 5 minutes and media containing cells changed for fresh TB. Plates were incubated for 3 or 5 hours, cells were scratched out of the surface and *fliC* expression was measured. Shown are mean and standard error of two to three replicates. Statistical analysis was performed using a two-sample t-test with unequal sample size and unequal variance, with P < 0.05 (*), P < 0.005 (**), P < 0.0005 (***), NS, not significant.

In order to test if the presence of flagella could compensate the lack of fimbriae, *fliC* and *fliA* (class II gene in the flagella regulation cascade) were induced from expression plasmids. However, none of the genes induced an increasement in the area occupied by fimbrialess cells and cell detachment could be detected (Figure 40). Furthermore, a direct comparison of *fliC* and *fliA* induction showed, contrary to what was expected, that induction of these genes led to a lower surface colonization (Figure 41A, B), even though results indicate that the production of flagellin increased when *fliA* was induced (Figure 41C, D). This was observed for both wild-type and fimbrialess cells.

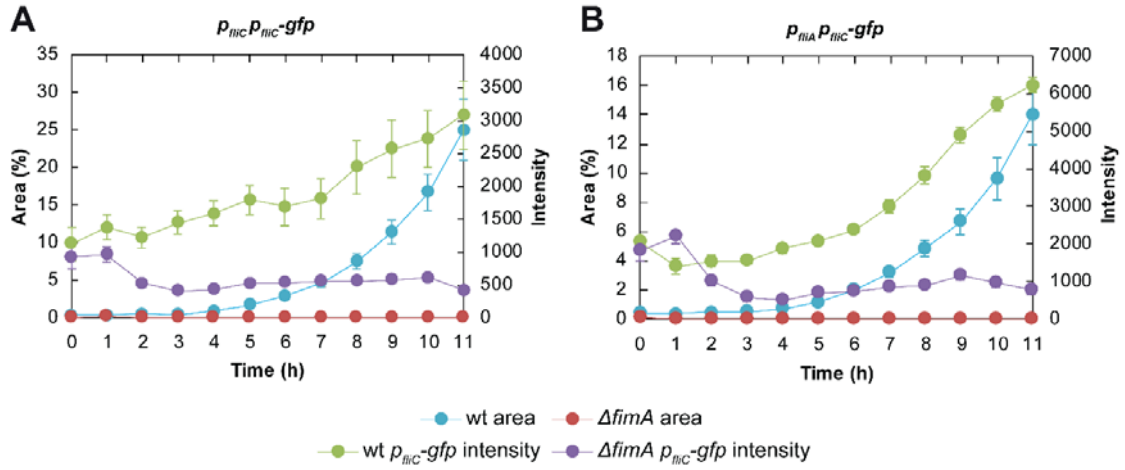

Figure 40. Attachment of wild-type and *ΔfimA* P_{lacI}-*fliC* P_{fliC}-*gfp* (A) P_{lacI}-*fliA* P_{fliC}-*gfp* (B) cells under flow. Cells were introduced in the channels for 2 minutes at 1 dyne/cm^2 and fresh media was flushed at a constant 1 dyne/cm^2 flow for 11 hours. Percentage of area occupied by cells and intensity of the *reporters* P_{lacI}-*fliC* P_{fliC}-*gfp* **(A)** P_{lacI}-*fliA* P_{fliC}-*gfp* **(B)** were quantified every hour. Shown are mean and standard error of two to three replicates.

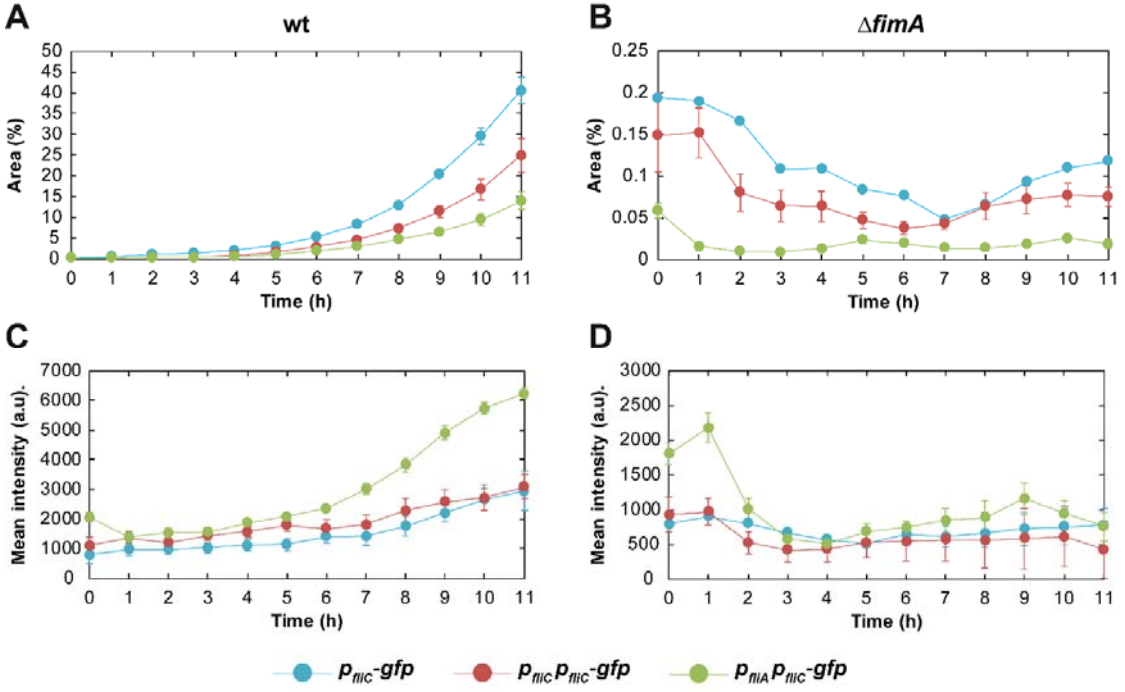

Figure 41. Area occupied by wild-type (A) and *ΔfimA* (B) after induction of flagellar genes. Cells carrying P_{fliC}-*gfp, P_{lacI}-fliC P_{fliC}-gfp or P_{lacI}-fliA P_{fliC}-gfp* introduced in the channels for 2 minutes at 1 dyne/cm^2 and fresh media was flushed at a constant 1 dyne/cm^2 flow for 11 hours. Percentage of area occupied by cells **(A, B)** and intensity of the reporter P_{fliC}-*gfp* **(C, D)** were quantified every hour. Shown are mean and standard error of two to three replicates.

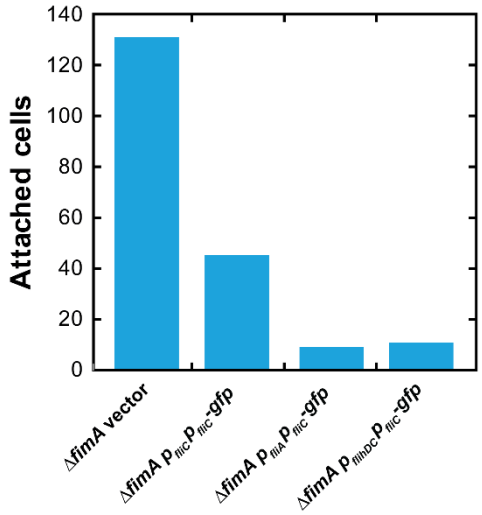

Figure 42. Number of *ΔfimA* cells attached after incubation with the surface for 5 hours in static conditions. Cells carrying *P_{fliC}-gfp, P_{lacI}-fliC P_{fliC}-gfp, P_{lacI}-fliA P_{fliC}-gfp* or *P_{lacI}-fliA P_{fliC}-gfp* were seeded for 2 minutes on ibidi uncoated plates Media was then changed for fresh one and cells were incubated on the surface for 5 hours. Wells were washed and imaged in fresh media and number of cells attached to the surface was calculated.

Nevertheless, expressing class II and class I flagellar genes does not affect the number of flagella present in the cells. In fact, the reduction on the number of cells attached in the *P_{lacI}-fliA P_{fliC}-gfp* strain could be due to the cells having longer flagella and therefore having their cell body more exposed to the flow. Therefore, the expression of class I genes *flhDC* on a plasmid was tested. However, preliminary data under static conditions showed, in agreement with the results under flow (Figure 41A, B), that the induction of flagellar genes did not increase surface colonization of fimbrialess cells (Figure 42). In addition, *fliC* levels in these strains were assessed using flow cytometry, confirming that the expression plasmids used are capable of inducing downstream flagellar genes (Figure 43).

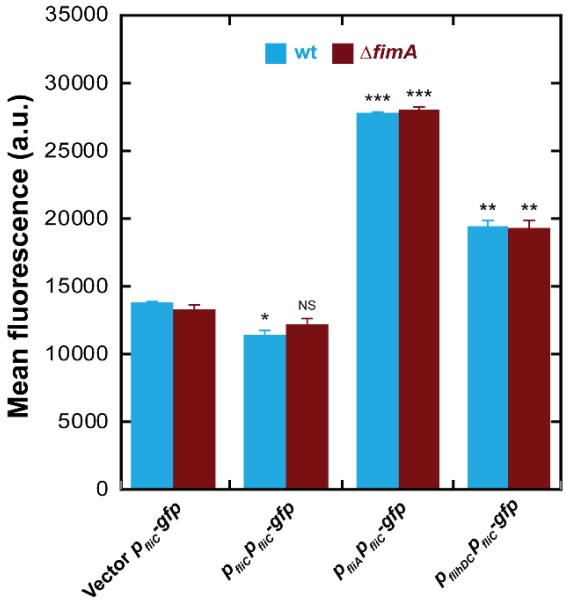

Figure 43. Flagellin expression of planktonic cultures of wild-type and *ΔfimA* cells. Cells were grown as for the microfluidics experiments and intensity of the promoter reporter *P_{fliC}-gfp* was then measured for the planktonic cultures. Shown are mean and standard error of three to four replicates. Statistical analysis was performed using a two-sample t-test with unequal sample size and unequal variance, with P < 0.05 (*), P < 0.005 (**), P < 0.0005 (***), NS, not significant.

Furthermore, in order to test if cells were capable of upregulating flagella production upon surface contact, *fliC* expression between cells that were grown under centrifugation, and therefore forced to the surface, and swimming cells was compared. No major change of *fliC* expression could be detected for wild-type or *ΔfimA* cells (Figure 44).

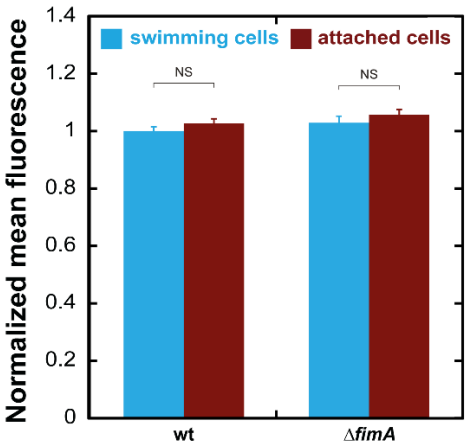

Figure 44. Flagellin expression of swimming and enforced attached wild-type and *ΔfimA* cells. Exponentially growing cells were plated into ibidi uncoated plates and grown or 2 hours either under static (swimming) or under centrifugation (attached) at 4000 rpm at 30°C. Cells present in the supernatant and cells scrapped off the surface of the plates respectively were taken and *fliC* intensity measured. Statistical analysis was performed using a two-sample t-test with unequal sample size and unequal variance, with NS, not significant.

2.4.3. Fimbriae are essential for long term attachment of motile cells

In order to see if the loss of other adhesins or motility related proteins could compensate for the lack of fimbriae, the attachment of double knockout strains lacking type 1 fimbriae was assessed. The same experimental setup as in 2.3 was used and cells were exposed to a 1 dyne/cm^2 flow.

Firstly, *ΔfimAΔcsgA,* which lacks both curli and fimbriae, showed the same phenotype as seen for *ΔfimA* cells and, after 3 h, no attachment could be seen (Figure 45A). The lack of flagella in a fimbrialess background (*ΔfliCΔfimA*) showed a strong reduction in attachment when compared to the wild-type (Figure 45B) and did not manage to grow on the surface. However, the few cells that managed to attach did not detach over time (Figure 45B). This indicates that the lack of motility or flagella is important for the cells to keep attached to the surface after relatively long periods of time. Finally, the flagellated but non-motile strain *ΔmotAΔfimA* was capable of remaining attached to the surface and, most importantly, growing on it (Figure 45C), showing a similar phenotype than *ΔmotA* cells (Figure 28).

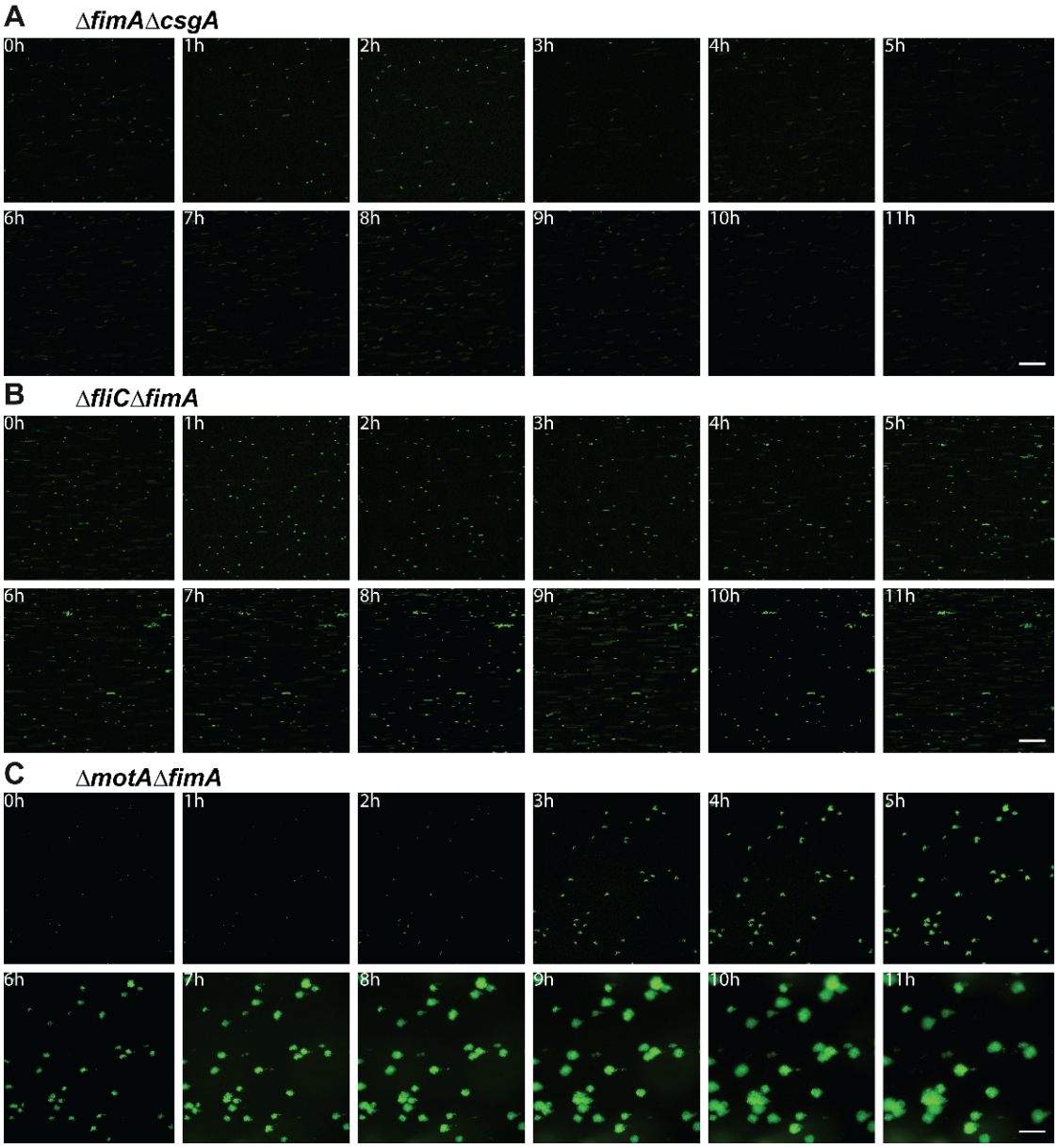

Figure 45. Attachment of *ΔfimAΔcsgA* (A) *ΔfliCΔfimA* (B) and *ΔmotAΔfimA* W3110 *rpoS*$^{+}$ cells under flow. Cells were introduced in the channels for 2 minutes at 1 dyne/cm^2 and fresh media was flushed at a constant 1 dyne/cm^2 flow for 11 hours.

When the attachment of these strains was quantified, it was observed that the area covered by *ΔmotA*, *ΔmotAΔfimA* and wild-type cells was similar during the first 7 hours of exposure to flow (Figure 46). These results point to fimbrialess cells being unable to detach in the absence of motility. Therefore, the detachment observed for these cells seems to not be caused by cells not being able to keep attached but rather because cells actively detach.

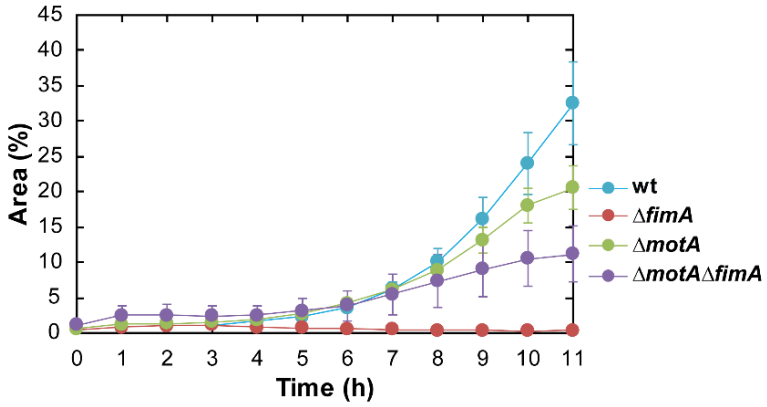

Figure 46. Attachment of wild-type, *ΔfimA, ΔmotA and ΔmotAΔfimA* cells under flow. Cells were flushed for 2 minutes at 1 dyne/cm^2 and fresh media was flushed at a constant 1 dyne/cm^2 flow for 11 hours. Percentage of area occupied by cells were quantified every hour.

Flagellin expression was measured for these non-motile strains using a promoter reporter for flagellin expression. *ΔmotA* and *ΔmotAΔfimA* strains showed a higher flagellin expression than wild-type and *ΔfimA* cells (Figure 47). It is therefore possible that the lack of detachment of *ΔmotAΔfimA* cells is due to the inability of these to detach in the absence of motility and their ability to grow on the surface, due to the higher number of flagella present in these cells.

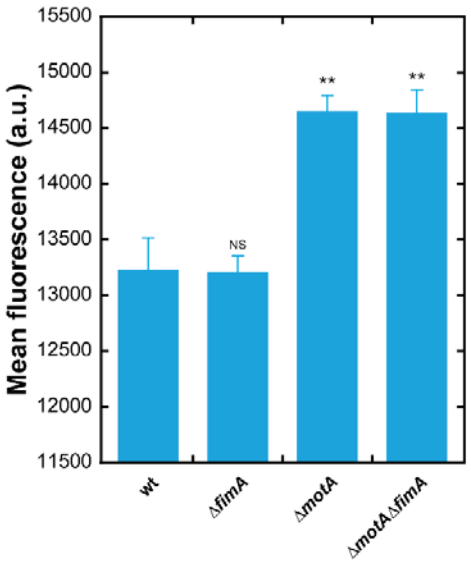

Figure 47. Flagellin expression of wild-type, *ΔfimA, ΔmotA and ΔmotAΔfimA* cells. Cells were grown as for the microfluidics experiments and *fliC* expression was then measured.

Differences between *ΔmotA* and wild-type cells, could be responsible for the different effect of the deletion of fimbriae in these strains. Whole proteome analysis of this strains was therefore performed. Samples of wild-type and *ΔmotA* cells were taken in planktonic

conditions and after attachment to abiotic surfaces for 5 hours. In addition, *ΔfimA* and *ΔmotAΔfimA* samples were taken only in planktonic conditions (Figure 48).

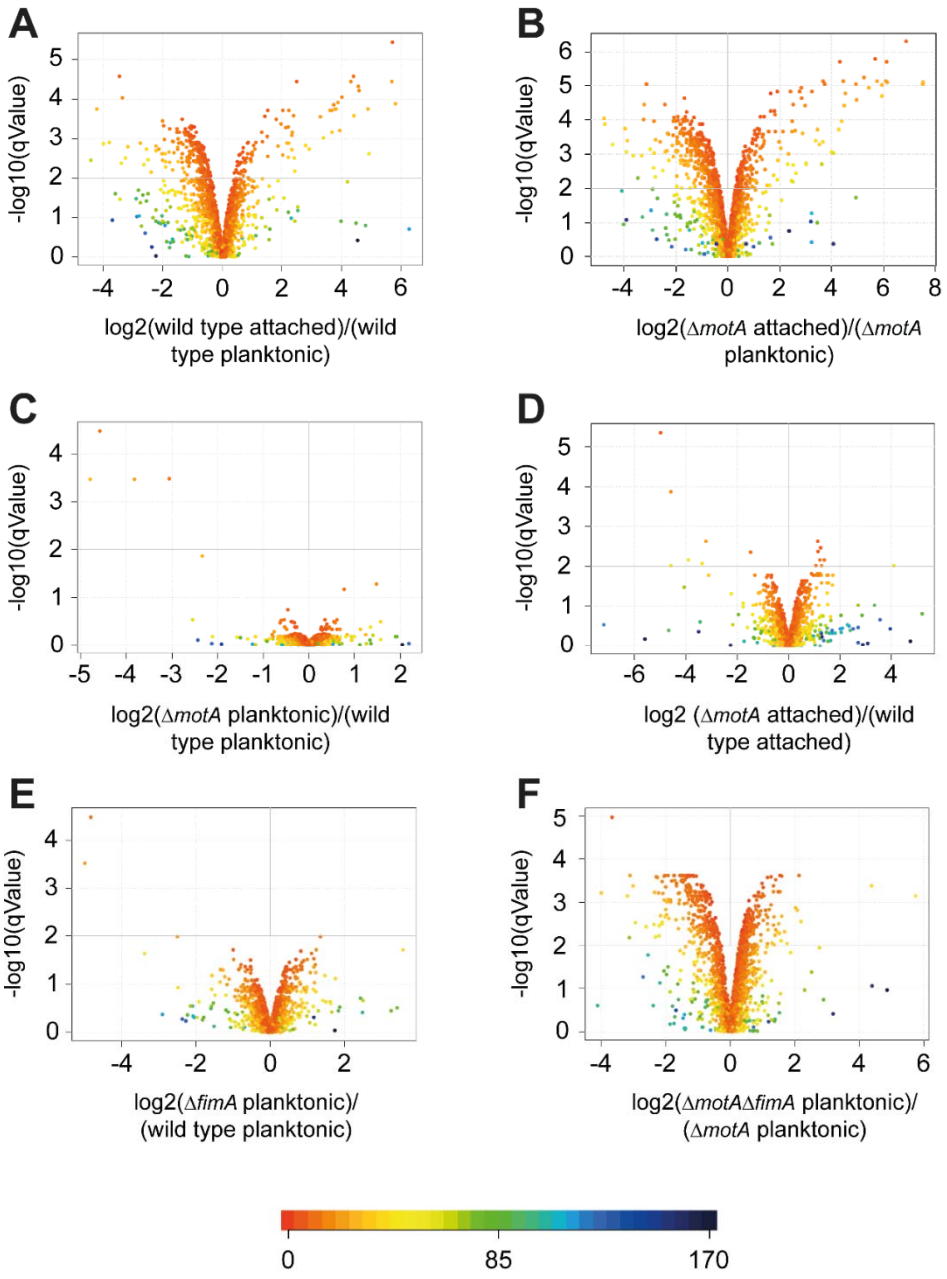

Figure 48. Variation in protein expression after whole proteome analysis. Cultures were grown until OD_{600} 0.5 and harvested for proteomic analysis or seeded on the surface and grown for 5 h in static conditions. Three individual replicates were tested. Comparisons were made between wild-type after 5 hours attachment versus wild-type planktonic culture **(A),** *ΔmotA* after 5 hours attachment versus *ΔmotA* planktonic culture (**B),** *ΔmotA* planktonic culture versus wild-type planktonic culture (**C),** *ΔmotA* after 5 hours attachment versus wild-type after 5 hours attachment **(D),** *ΔfimA* planktonic culture versus wild-type planktonic culture **(E)** and *ΔmotAΔfimA* planktonic culture and *ΔmotA* planktonic culture **(F).**

In general, after attachment of both wild-type and *ΔmotA,* proteins involved in different metabolic routes, stress related proteins and proteins related to the entrance in stationary phase we upregulated (Table S1, Table S2). As an example of the last group, the ribosome-associated inhibitor A, RaiA was found. On the other hand, other metabolism related proteins such as putrescine and GABA metabolism were downregulated. These genes are part of the same regulon and are metabolically related which might explain why they both appear to be affected after attachment. Furthermore, also downregulated upon attachment for both wild-type and non-motile cells are proteins involved in quorum sensing via the autoinducer 2 (AI-2) (Table S1, Table S2).

When comparing directly wild-type and *ΔmotA* planktonic cultures, not many differences were found (Table 1). However, some proteins directly involved in attachment were found to be lower expressed in non-motile cells. Curli fiber proteins were significantly lower expressed in *ΔmotA* when compared to wild-type both before and after attachment though they were not significantly altered after attachment for either strain and no differences were either found between fimbrialess and wild-type cells (Table 1, Table S1, Table S2, Table S7). This lower expression of curli proteins might be an effect of the disruption of motility since they were also downregulated in *ΔmotAΔfimA* when compared to *ΔfimA* cells (Table S7). In addition, levels of Ag43 were also lower in *ΔmotA* when compared to wild-type, both before and after attachment (Table 1, Table 2, Table S3). In this case, disruption of both motility or type 1 fimbriae separately lead to a striking lower expression of this protein when compared to wild-type whereas double knockout *ΔmotAΔfimA* increased dramatically these levels compared to the single knockouts (Table S3).

Attached *ΔmotA* cells differed further from wild-type cells than the planktonic cultures showing that lack of flagella rotation does impact regulation upon attachment (Table 2). However most of these proteins are uncharacterized or not much is known about them while others are related to metabolic routes that have not been described to impact surface colonization. It is therefore difficult to establish a link between them and a possible attachment effect (Table 2).

Interestingly, fimbrial proteins were found in higher numbers in wild-type cells when compared to non-motile ones only after attachment (Table 2). Indeed, levels of fimbrial proteins increased upon attachment to the surface. However, this was not observed for *ΔmotA* cells (Table 3, Table S1, Table S2, Table S8). Since, as it was previously

mentioned, mechanosensing via flagella requires of their rotation, it is possible that the upregulation of fimbriae is downstream effect of flagella surface sensing. This might contribute tokeep the cells attached to the surface. Unfortunately, it was not possible to detect all the fimbrial proteins, such as FimA, with this approach and further experiments might be needed to corroborate this.

Table 1. Significantly differentially expressed proteins in planktonic *ΔmotA* cells versus planktonic wild-type ones. Shown are proteins that showed a 2-fold or more change.

Name	Description	pValue	qValue	Fold change
CysH	Phosphoadenosine phosphosulfate reductase	2.2E-03	0.31865	2.97
Ves	HutD family protein	1.4E-04	0.05252	2.79
CysN	Sulfate adenylyltransferase subunit 1	4.2E-03	0.42086	2.55
CsgG	Curli production assembly/transport component	3.1E-05	0.01373	0.20
CsgF	Curli production assembly/transport component	1.2E-03	0.29024	0.17
MotB	Motility protein B	3.0E-07	0.00033	0.12
MotA	Motility protein A	6.1E-07	0.00034	0.07
Ag43	Antigen 43	1.5E-08	0.00003	0.04
YeeR	Inner membrane protein	6.2E-07	0.00034	0.04

Table 2. Significantly differentially expressed proteins in *ΔmotA* cells versus wild-type ones after 5 hours attachment. Shown are proteins that showed a 2-fold or more change.

Name	Description	pValue	qValue	Fold change
YjbQ	UPF0047 protein	6.8E-05	0.00964	17.17
YgfT	Putative oxidoreductase	2.0E-04	0.01604	3.31
MbhS	Hydrogenase-1 small chain	7.2E-04	0.02904	3.28
SdhD	D-serine dehydratase	5.1E-04	0.02571	2.95
YcgN	UPF0260 protein	1.8E-04	0.01604	2.91
YdjL	Uncharacterized zinc-type alcohol dehydrogenase-like protein	1.8E-04	0.01604	2.82
YchJ	UPF0225 protein	5.2E-04	0.02571	2.82
GuaD	Guanine deaminase	3.4E-05	0.00685	2.64
SsnA	Putative aminohydrolase	3.0E-05	0.00685	2.63
YgfK	Putative oxidoreductase	7.0E-05	0.00964	2.44
YdjJ	Uncharacterized zinc-type alcohol dehydrogenase-like protein	4.9E-04	0.02571	2.44
FdhF	Formate dehydrogenase H	1.6E-04	0.01604	2.42
YgeY	Putative peptidase	7.6E-06	0.00336	2.37
YgeW	Putative carbamoyltransferase	1.2E-04	0.01470	2.35
XdhC	Xanthine dehydrogenase iron-sulfur-binding subunit	2.9E-05	0.00685	2.33

XdhA	Xanthine dehydrogenase molybdenum-binding subunit	1.6E-04	0.01604	2.26
ArcL	Carbamate kinase-like protein	1.2E-05	0.00422	2.20
XdhB	Xanthine dehydrogenase FAD-binding subunit	4.3E-06	0.00233	2.20
YgfM	Putative oxidoreductase	1.2E-04	0.01470	2.16
PhyDA	D-phenylhydantoinase	2.0E-04	0.01604	2.12
XdhD	Probable hypoxanthine oxidase	1.0E-03	0.03369	2.10
DpaL	Diaminopropionate ammonia-lyase	7.0E-05	0.00964	2.09
Rmf	Ribosome modulation factor	2.8E-03	0.05781	2.04
PaaH	3-hydroxyadipyl-CoA dehydrogenase	1.8E-03	0.04363	0.47
YgbI	Uncharacterized HTH-type transcriptional regulator	1.9E-03	0.04483	0.44
PaaG	1,2-epoxyphenylacetyl-CoA isomerase	2.1E-04	0.01625	0.40
DdpX	D-alanyl-D-alanine dipeptidase	1.4E-05	0.00427	0.36
PaaC	1,2-phenylacetyl-CoA epoxidase, subunit C	4.8E-03	0.08076	0.29
MotB	Motility protein B	2.2E-03	0.04736	0.21
PaaI	Acyl-coenzyme A thioesterase	2.3E-04	0.01647	0.12
FimC	Chaperone protein FimC	3.4E-06	0.00233	0.11
CsgG	Curli production assembly/transport component	4.6E-05	0.00844	0.10
MotA	Motility protein A	3.1E-05	0.00685	0.07
CsgF	Curli production assembly/transport component C	9.2E-04	0.03291	0.06
FimG	Protein FimG	6.5E-05	0.00964	0.04
YeeR	Inner membrane protein	1.2E-07	0.00013	0.04
Ag43	Antigen 43	2.0E-09	0.00000	0.03

Table 3. Significantly differentially expressed type 1 fimbriae proteins in *ΔmotA* cells versus wild-type.

	Wild-type attached vs wild-type planktonic			
Name	**Description**	**pValue**	**qValue**	**Fold change**
FimG	Type 1 fimbriae minor subunit	0.00016	0.00243	30.48
FimC	Chaperone protein	3.60E-07	8.79E-05	16.26
	***ΔmotA* attached vs *ΔmotA* attached**			
Name	**Description**	**pValue**	**qValue**	**Fold change**
FimC	Chaperone protein	3.42E-06	0.00233	0.11
FimG	Type 1 fimbriae minor subunit	6.53E-05	0.00964	0.04

Flagellar proteins were looked at in more detail. Comparing attached versus planktonic cells, some of the proteins were observed to be highly expressed when attached for both wild-type and *ΔmotA* cells (Table 4, Table 5). In both cases the levels of flagellar hook associated proteins like FlgK and FlgL which connect the hook and the filament synthesis were higher when cells were attached, as well as the sigma factor FliA (Table 4, Table 5). However, in both cases FlhD levels were lower in attached cells (Table S4). In addition, in *ΔmotA* cells some proteins found at the basal body were upregulated, like FliG (Table 5). In the case of *ΔfimA* cells, some proteins of both the flagellar hook and basal body appeared to be higher expressed in planktonic cells, as FlgK or FlgL (Table 6). Though, in agreement with the reporter experiments, FliC was not significantly altered (Table S4). When looking at proteins in the flagellar stator, for wild-type cells both MotA and MotB were lower expressed in the attached state (Table 4 and Table S4). No differences were found for either MotA or MotB between wild-type and *ΔfimA* cells in their planktonic state (Table 6).

Table 4. Significantly differentially expressed flagellar proteins in wild-type cells after 5 hours attached versus planktonic cells.

Name	Description	pValue	qValue	Fold change
FliD	Flagellar filament capping protein	0.00024	0.00307	5.34
FlgK	Flagellar hook-filament junction protein 1	0.00023	0.00298	4.64
FlgL	Flagellar hook-filament junction protein 2	0.00007	0.00153	3.66
FliA	RNA polymerase sigma 28 factor	0.00184	0.01214	1.34
MotB	Motility protein B	0.004391	0.02190	0.29
FlgA	Flagella basal body P-ring formation protein	0.00030	0.00348	0.18

Table 5. Significantly differentially expressed flagellar proteins in *ΔmotA* cells after 5 hours attached versus planktonic cells.

Name	Description	pValue	qValue	Fold change
FlgK	Flagellar hook-filament junction protein 1	0.00021	0.00166	2.17
FlgL	Flagellar hook-filament junction protein 2	0.00289	0.01161	2.08
FlhE	Type 3 flagellar export proteins	0.00564	0.01959	1.43
FliO	Flagellar biosynthesis protein	0.00257	0.01064	1.39
FliG	Flagellar motor switch protein	0.00392	0.01479	1.33
FliA	RNA polymerase sigma 28 factor	0.00491	0.01760	1.25
FliS	Flagellar biosynthesis protein	0.00286	0.01156	0.60
FliK	Flagellar hook-length control protein	0.00080	0.00449	0.26
FlgA	Flagella basal body P-ring formation protein	9.20E-05	0.00092	0.14
FlhD	Flagellar transcriptional regulator	0.00256	0.01062	0.13

Table 6. Significantly differentially expressed flagellar proteins in planktonic *ΔfimA* cells versus planktonic wild-type cells.

Name	Description	pValue	qValue	Fold change
FliD	Flagellar filament capping protein	0.007683	0.129229	1.97
FliK	Flagellar hook-length control protein	0.009014	0.131727	1.93
FlgC	Flagellar basal-body rod protein	0.000183	0.030077	1.63
FlgK	Flagellar hook-filament junction protein 1	0.002409	0.076496	1.62
FlgI	Flagellar P-ring protein	0.006185	0.115252	1.42
FlgE	Flagellar hook protein	0.000828	0.049318	1.39
FlgL	Flagellar hook-filament junction protein 2	0.00482	0.107382	1.32
FlgB	Flagellar basal body rod protein	0.001933	0.069877	1.32
FlhB	Flagellar biosynthetic protein	0.001308	0.056186	1.30

Though chemotaxis and c-di-GMP related proteins were also looked at for their importance in motility regulation and therefore, in attachment only mild changes were observed (Table S5, Table S6). In the case of c-di-GMP, both diguanylate cyclases and phosphodiesterases were either up or downregulated together and it is therefore difficult to establish the importance of c-di-GMP regulation at the protein level (Table S6).

It could be concluded that, though differences were found between wild-type and non-motile cells at the proteome level, both in planktonic cultures and after attachment, it is

difficult to directly link these changes to the phenotypes observed after the deletion of type 1 fimbriae. It is therefore possible that the absence of motility itself is the main responsible for the lack of detachment of *ΔmotAΔfimA.*

3. Discussion

Bacteria in their natural environment, live often as part of communities called biofilms. In order to form biofilms, bacteria have to typically reach a surface and attach to it (O'Toole *et al.*, 2000). Attachment is not only important for biofilm formation, but also for the establishment of infections. To aid this attachment, *E. coli* possesses a number of cell surface appendages, referred to as adhesins (Abdallah *et al.*, 2014, Monroe, 2007). Though attachment and biofilm formation has been object of study for many years, there are many questions that remain unclear about how bacteria establish contact with the surfaces and which kind of signals are needed for bacteria to switch to a sessile life style.

In this work, the attachment of *E. coli* cells to different surfaces, from abiotic to biomimetic, under flow and static conditions, as well as the overall role of motility and major adhesins in attachment were studied. More in depth was further assessed the role of type 1 fimbriae in attachment to abiotic surfaces and the interplay of these adhesins and motility.

3.1. Surface and flow influence on attachment

E. coli is capable of attaching to a wide variety of surfaces (Chao & Zhang, 2011; Korea *et al.*, 2010). However, surface chemistry can affect bacterial attachment. In this work, wild-type cells were observed to attach better to hydrophobic surfaces, as previously reported (Boyer *et al.*, 2007; Liu *et al.*, 2004). In the case of hydrophilic surfaces, it is not entirely clear how cells (W3110 *rpoS*$^{+}$) attach to the surface. First, since the attachment was very low, it is possible that the cells attached are interacting with the surface in a non-specific manner, via their cell body (Berne *et al.*, 2018; Kimkes & Heinemann, 2020). Furthermore, even though these adhesins have been reported to be the most important for attachment, *E. coli* cells possess a lot more proteins that have been reported to play a role in attachment to different surfaces. It is possible that these structures are important in this experimental setup (Korea *et al.*, 2010; Wurpel *et al.*, 2013). Another possible explanation is that these adhesins are capable of compensating the absence of another and therefore single knockouts do not show a major effect in attachment.

Flow has been reported to affect attachment and biofilm formation (Sherman *et al.*, 2019; Thomen *et al.*, 2017) and thus, its effect was studied in this work. Cells exposed to increasing flow rates attached differently, with intermediate flows leading to the highest

and most rapid colonization of the surface. Though flow can aid bacterial attachment, too high flows can reduce the size of the boundary layer or the liquid surface interface. In turn, this leads to cells present in the bulk not being able to reach the surface and cells already attached being more exposed to shear forces (Berne *et al.*, 2018; Tuson & Weibel, 2013).

In addition, the involvement of adhesins in attachment was studied. Though curli fibers were looked at, they were only relevant for initial attachment when cells were previously grown until stationary phase before being exposed to the surface. This agrees with curli being only expressed at OD_{600} higher than 0.8 (Hengge, 2009). Furthermore, flow did not affect the surface colonization though they have been reported to be important for the 3D structure of biofilms (Serra *et al.*, 2013). For these reasons this discussion will focus on the roles of motility, flagella and type 1 fimbriae.

3.2. Flagella and motility influence initial attachment

Motility, mediated by flagella rotation, has been reported to be important for attachment since it allows bacteria to get in contact with the surface (Berne *et al.*, 2015; Duan *et al.*, 2013; Friedlander *et al.*, 2015; Tuson & Weibel, 2013). The results presented in this work support these observations and show motility is crucial for attachment to abiotic and mannosylated surfaces. Motility was especially important when cells were in exponential phase and loss of motility reduced or abolished surface attachment. However, when cells attached to mannosylated surfaces, the relevance of motility was time dependent, being only important in the first minutes of contact with the surface, but did not further improve the attachment at later time points. Something similar could explain the results of attachment to hydrophilic surfaces. Thus, motility could still be important for attachment but at earlier time points than the one looked at in this experimental setup.

Under flow, motility does not appear to be crucial for initial attachment. In fact, the presence of non-rotating flagella seems enough to colonize the surface during the first hours of attachment. However, phenotypically, non-motile flagellated cells create tree-like structures when exposed to the surface. These clumps are attached to the surface, though growing in a less organized way than wild-type cells. This might point to the role of flagella as a scaffold during biofilm formation and might explain why cells attached to

the surface, according to reports, keep actively expressing flagella (Besharova *et al.*, 2016; Serra *et al.*, 2013).

Flagella have been proposed as an adhesin and have been reported to contribute to bacterial attachment beyond motility (Friedlander *et al.*, 2013; Friedlander *et al.*, 2015; Haiko & Westerlund-Wikstrom, 2013). However, in this work, the role of flagella as an adhesin was not observed for attachment to abiotic surfaces. Nonetheless, when assessing the attachment to mannosylated surfaces, flagella were found to possibly play a role as a secondary adhesin. This result agrees with studies testing *E. coli* attachment to epithelial cells, in which the presence of flagella seem to improve bacterial attachment (Duan *et al.*, 2013; Zhou *et al.*, 2013). However, non-rotating flagella were also able to interfere with attachment to both surfaces, indicating that flagella may sterically hinder the attachment. On the other hand, under flow flagella seem to play a more important role. In the absence of flagella, cells clump together, forming cloud-like structures which, unlike the ones seen for non-motile flagellated cells, move along the channels. Nonetheless, when non-flagellated fimbrialess cells were studied, a number of cells were seen to attach to surfaces. Though cells did not grow on the surface, experiments showed that a reduced number of cells did not require these adhesins for attachment. This attachment to the surface, similarly to what was observed in static attachment to hydrophilic surfaces, may be a consequence of the interaction of the cell body to the surface or other adhesins not assessed in this study, may play a role in these interactions (Berne *et al.*, 2018; Korea *et al.*, 2010; Wurpel *et al.*, 2013). Nonetheless, the presence of flagella greatly improved the attachment and surface colonization in this experimental setup.

3.2.1. Chemotaxis can improve initial attachment

The chemotaxis machinery of *E. coli* is in control of the cell swimming behavior. It allows cells to bias their swimming and search for favorable environments (Sourjik & Wingreen, 2012; (Vladimirov & Sourjik, 2009). In the experiments presented in this work it was observed that smooth-swimming *cheA* and *cheY* mutants show largely enhanced initial surface attachment though, as previously reported, had no impact in long term colonization (Pratt & Kolter, 1998). This increased attachment was particularly pronounced during the first several hours of incubation and it required was swimming dependent. Tracking experiments showed smooth swimming mutants of the chemotaxis pathway increase their swimming trajectory length. Therefore, cells spend more time

near the surface, increasing the probability of attachment. Indeed, previous studies have suggested that smooth-swimming bacteria become trapped at the surface by the hydrodynamic forces and can only efficiently escape by tumbling (Berke *et al.*, 2008; Drescher *et al.*, 2011; Frymier *et al.*, 1995; Vigeant *et al.*, 2002). Such hydrodynamic entrapment may be a general mechanism promoting bacterial attachment at abiotic and biotic surfaces (Berke *et al.*, 2008; Drescher *et al.*, 2011; Frymier *et al.*, 1995; Misselwitz *et al.*, 2012; Vigeant *et al.*, 2002). Consistent with the effect of genetic inactivation of the chemotaxis pathway, *E. coli* attachment was also promoted by the chemoattractant stimulation that lowers the pathway activity. The chemotaxis could thus control attachment of *E. coli* and other bacteria to surfaces that secrete chemoeffectors, with attractant secretion promoting attachment and repellent secretion inhibiting it. This might affect surface colonization during formation of submerged biofilms, but also attachment to the epithelial cells that are known to secrete chemoeffectors (Keilberg & Ottemann, 2016; Lopes & Sourjik, 2018). Nevertheless, effects of motility and chemotaxis on attachment and biofilm formation are likely to be species-specific. For example, although motility was similarly important for biofilm formation by *Agrobacterium tumefaciens*, in that case deletion of *cheA* had no apparent effect on cell attachment under static conditions and resulted in reduced biofilm formation under flow (Merritt *et al.*, 2007).

3.2.2. C-di-GMP plays a dual role on attachment

C-di-GMP also affects motility helping the cells switch to a sessile life style. C-di-GMP can control motility via YcgR. This protein, often referred to as flagellar brake, can bind c-di-GMP and interact with the flagellar motor (Ryjenkov *et al.*, 2006). The results presented in this work show that, in the absence of the flagellar brake, and thus, in the absence of c-di-GMP regulation of the flagella, the swimming speed of the cells was increased. This change in swimming speed led to an increase in bacterial attachment to abiotic and mannosylated surfaces. However, this higher attachment appears to be abolished in the presence of *rpoS.* One possible explanation could be related to other targets regulated by c-di-GMP. For example, this second messenger can also regulate motility by inducing the expression of CsgD, together with many regulators, which in turn lowers the expression of flagellar genes at the *fliA* level and would favor surface colonization (Z. Liu *et al.*, 2014; Ogasawara *et al.*, 2010; Pesavento & Hengge, 2009).

The higher attachment observed for *ΔycgR* cells in a *rpoS* background, seems to correlate with the cellular levels of c-di-GMP since similar results were obtained when

using knockouts of the main c-di-GMP cyclase. Furthermore, though previous reports showed that YcgR can affect the tumbling rate of the cells (Girgis *et al.*, 2007; K. Paul *et al.*, 2010), this was not observed in this experimental setup. One possible explanation of this discrepancy is that the effect of c-di-GMP on flagellar motor rotation is load dependent, and therefore, a low viscosity medium does not provide enough load to affect the tumbling rate of swimming cells, while tethered cells do. Instead, these results suggest that the most likely cause of better attachment of Δ*ycgR* cells is their faster swimming.

The results obtained on c-di-GMP suggest that, instead of being only a biofilm-promoting second messenger, it might rather have dual function dependent on the stage of the biofilm formation (Romling, 2012), with low levels of c-di-GMP being important for efficient early attachment, while high levels being required for matrix production in mature biofilms (Hengge, 2009; Romling *et al.*, 2013).

3.3. Type 1 fimbriae are essential for late attachment

Type 1 fimbriae are important virulence factors and adhesins present in many commensal and pathogenic strains of *E. coli*. Though their main role as adhesins is in the attachment to epithelial cells, they have also been reported to adhere non-specifically to abiotic surfaces (Beloin *et al.*, 2008; Chao & Zhang, 2011; Pratt & Kolter, 1998), being important at the early stages of biofilm formation (Monteiro *et al.*, 2012; L. Wang *et al.*, 2018).

In this work, the effect of type 1 fimbriae in both initial and later attachment was studied. They were shown to be important for attachment in the absence of *rpoS*. Sigma S has been reported to inhibit *fimB* which in turn is responsible for the OFF to ON switching of the fimbrial expression (Dove *et al.*, 1997). This would lead to less cells expressing fimbriae and therefore, their importance for attachment would be reduced. Furthermore, type 1 fimbriae were partially responsible for the increased attachment of smooth swimming chemotaxis mutants and, in their absence, the advantage of the previously discussed entrapment was reduced. In addition, type 1 fimbriae mediate the increased attachment of the faster swimming bacteria lacking the flagellar brake. At least in the case of mannosylated surface, enhanced attachment of faster bacteria could be explained by the known force-dependence of mannose binding by FimH (Aprikian *et al.*,

2011; Sauer *et al.*, 2016). This catch-bond mechanism is normally assumed to promote attachment under high shear force, e.g., in the urinary tract, but the same effect could also strengthen attachment of faster cells. While the mechanism of type 1 fimbriae interaction with abiotic surfaces has not being established, it is at least possible that the same large force-induced conformational change is also responsible for better attachment of faster cells these surfaces.

In the case of cells having sigma S, fimbriae do not seem to affect initial attachment to abiotic surfaces, both under flow or static conditions. However, at later time points the presence of fimbriae becomes crucial for attachment. Thus, fimbrialess cells, do not manage to grow on the surface and cells that are already attach and, start detaching. Fimbriae were also essential in the absence of flow and both our results and other studies showed that the detachment of fimbrialess cells also occur under static conditions (H. Wang *et al.*, 2017). In addition, deletion of the fimbrial tip protein, FimH, did not have an effect on attachment and surface colonization. Therefore, it seems that the rest of the structure is enough to maintain cells attached unspecifically growing on the surface.

When protein synthesis and division were inhibited in type 1 fimbriae deficient cells, the detachment of these cells was abolished and attachment became comparable to the wild-type. Previous reports claimed that the presence or absence of fimbriae can affect the outer membrane composition (Orndorff *et al.*, 2004; Otto *et al.*, 2001), and therefore, could affect bacterial attachment. However, the results presented in this study, point to the role of fimbriae not being merely physical. Therefore, it is apparent that changes in protein synthesis are responsible for the need of fimbriae for the cells to remain attached to the surface.

The results of the initial screening under flow where flagella appeared to be essential for initial attachment, together with previous reports of flagella being expressed even in cells growing at the surface of biofilms (Besharova *et al.*, 2016; Serra *et al.*, 2013), lead to a hypothesis on how protein synthesis might influence the need for fimbriae. It was hypothesized that cells might attach first via flagella, due to their length, and fimbriae would interact with the surface later, strengthening the attachment. If fimbriae would be involved in the surface sensing that leads to an increased flagella expression of attached cells, in their absence flagella would be diluted by division, reaching a point when they cannot keep the cell attached. However, promoter reporter experiments did not show changes in flagellin expression during the course of attachment for fimbrialess cells or

between these and wild-type ones. Furthermore, attempts to keep attached fimbrialess cells to the surface by expressing flagellar genes, did not succeed. Additionally, expression of class III and II led to reduced surface colonization for both fimbrialess and wild-type cells. A possible explanation is that by expressing these gene classes in the flagellar cascade of regulation, the number of flagella is not likely to change. In fact, in the case of *fliA*, its increased expression leads to longer flagella (Claret *et al.*, 2007). This would result in the cell body being more exposed to the bulk and thus, more likely to detach. However, even the induction of *flhDC*, master regulator of flagella expression, did not result in increase of attachment, but almost abolished for fimbrialess cells. In this case, it is possible that flagella expression must be temporally controlled in order to improve attachment. Furthermore, FlhDC has been reported to affect other genes not related to motility and the decrease of attachment could be a side effect of the plasmid induced expression (Pruss *et al.*, 2003; Pruss *et al.*, 2001; Stafford *et al.*, 2005).

3.4. Interplay of motility and type 1 fimbriae

Motility, as previously discussed, is important for the cells to reach the surface but can also favor bacterial detachment (Mewborn *et al.*, 2017). Double knockout assays showed that, in non-motile flagellated cells, type 1 fimbriae are not required to remain attached. In fact, cells looked phenotypically similar to *ΔmotA,* and therefore, as was discussed before, surface colonization was comparable to wild-type cells. The different effect of the absence of fimbriae in a motile and non-motile background could be caused by differences in the expression of other proteins that compensate for the lack of fimbriae in a non-motile, flagellated background.

Whole proteome analysis of differences between the wild-type and *ΔmotA* strains in planktonic culture and upon attachment produced some interesting general results. For example, upon attachment proteins involved in the degradation of putrescine were downregulated. Putrescine catabolism has been hypothesized to be a response to several stresses but and it might also enhance biofilm formation via CpxR (Karatan & Michael, 2013; Sakamoto *et al.*, 2012; Schneider *et al.*, 2013). It is possible that lack of degradation leads to the accumulation of this polyamine and therefore, to stimulate biofilm formation. Proteins involved in quorum sensing via AI-2 were also downregulated. Quorum sensing has been reported to influence biofilm formation and attachment (Gonzalez Barrios *et al.*, 2006; Parsek & Greenberg, 2005). Finally, levels of *E. coli*

autoadhesin Ag43 and curli fibers proteins were found to be differentially expressed between non-motile and wild-type cells, although this difference was equally observed in planktonic cultures and in attached cells. Reports have showed that Ag43 can interfere with motility (Ulett *et al.*, 2006), but that the disruption of motility can affect Ag43 expression was not known.In the case of curli, flagella and curli fibers production are known to be inversely regulated (Besharova *et al.*, 2016; Pesavento & Hengge, 2009). However, since reduced levels of Ag43 and curli should rather decrease adhesiveness of *ΔmotA*, these changes are unlikely to explain their more persistent attachment.

Some flagellar proteins were found to be differentially upregulated in attached non-motile cells when compared to wild-type cells. However, many other proteins, including the global regulator FlhD, were not changed between wild-type and motility deficient cells, making it difficult to establish a connection between these differences and their surface attachment. Comparisons between fimbrialess and wild-type cells in planktonic cultures were also performed. Some flagellar proteins were higher expressed in fimbrialess cells compared to wild-type, which might explain the increased attachment seeing under static conditions during the initial screening.

In both motility deficient cells and wild-type ones, chemotaxis and c-di-GMP related proteins were either not affected or downregulated after attachment. In the second group both cyclases and phosphodiesterases were generally downregulated. Therefore c-di-GMP regulation, at least at a protein level, does not seem to be responsible for the attachment phenotype of fimbrialess cells in these backgrounds.

Additionally, in this proteomic analysis, one possible new consequence of surface sensing was discovered. Type 1 fimbriae proteins were highly upregulated after attachment of wild-type cells but this was not observed for motility deficient cells. This could point to this upregulation being mediated by flagella surface sensing since it has been reported to require flagella rotation (Schniederberend *et al.*, 2019; Suchanek *et al.*, 2019). Type 1 fimbriae has not been previously linked to surface sensing though their presence was reported to affect cells at the RNA level after attachment (Bhomkar *et al.*, 2010; Otto *et al.*, 2001).

Overall, the whole proteome analysis of wild-type and non-motile flagellated cells did not present a clear candidate that could explain why fimbrialess cells do not detach in the absence of motility. This leaves the lack of motility as the more plausible explanation why no detachment was observed. Therefore, it is possible that type 1 fimbriae are directly

involved in surface sensing. Thus, changes between the bulk and the surface and the sensing mediated by flagella and fimbriae, would give the necessary cues to the bacteria to remain attached to the surface and grow on it, transitioning to a sessile lifestyle. However, it is also possible that fimbriae themselves are not involved in mechanosensing but are essential for the cells to remain attached to the surface, giving them time so that all the signaling involved in surface sensing can translate into growth on the surface and the transition to a sessile lifestyle.

3.5. Concluding remarks

Biofilm research has been of increasing interest over the past years. Understanding these communities can give an insight on how bacteria live in their natural environment. In addition, biofilms cause serious health problems and issues in industry. Therefore, understanding how bacteria attach and grow on the surface to form biofilms can be important for their prevention and removal. This work gave a detailed look into the first steps of bacterial attachment and the players involved.

Motility allows bacteria like *E. coli* to reach the surface and overcome the electrostatic repulsive forces that they experience when approaching a surface. Flagella playing a role in attachment beyond motility has been hypothesized. The results presented in this work show that the importance of flagella depends on the surface studied and the stage of initial attachment.

The chemotaxis machinery in control of motility can also influence attachment. Tumbling suppression and increasing smooth swimming, like what happens when bacteria sense attractant compounds, can result in an increased number of bacteria attached, though it does not seem to affect long term colonization.

C-di-GMP is a bacterial second messenger long believed to promote biofilm formation by promoting the synthesis of extracellular matrix components. It also influences motility via the flagellar brake YcgR, helping bacteria transition into a sessile life style. However, this study shows that, when motility regulation via YcgR is abolished, bacterial swimming speed was increased, resulting in an enhanced bacterial attachment. Therefore, it seems that tight control of the levels of c-di-GMP is necessary to optimize biofilm formation since

this second messenger seems to play a dual role. Low levels might be important for initial attachment while high levels are important at a later time point.

Type 1 fimbriae are important adhesins for attachment to epithelial cells and also play a role in attachment to abiotic surfaces. These adhesins partially mediated the increased attachment of smooth swimmers affected in their chemotaxis pathway. Furthermore, they also mediate the attachment of fast swimming bacteria, result of the disruption of c-di-GMP control of motility via YcgR. In addition, the presence of fimbriae was shown to be crucial for late attachment. In their absence, cells were incapable of growing at the surfaces and remaining attached for long periods of time. This could explain why cells increase the expression of fimbriae after attaching to the surface. In fact, this seems to be a result of surface sensing via flagella since in the absence of motility this upregulation was not observed. However, in non-motile flagellated cells, type 1 fimbriae ceased to be essential for late attachment. Therefore, fimbriae might either play a direct role in surface sensing and required signaling needed for transitioning into sessile life style, or be important to keep cells at the surface while the signaling provided by flagella and other surface sensing pathways can change the cells programming to a sessile one. However, more research is needed to determine how *E. coli* senses the surface and whether or not type 1 fimbriae are involved in this process.

4. Material and methods

4.1. Chemicals and consumables

Chemicals used in this work are listed in Table S9

4.2. Reaction kits

Table 7. Reaction kits

Kit	Company
GeneJET Plasmid Miniprep Kit	ThermoFisher Scientific
GeneJET DNA Purification Kit	ThermoFisher Scientific
GeneJET Gel Extraction Kit	ThermoFisher Scientific

4.3. Multiwell plates

Table 8. Multiwell plates

Plate	Order number	Company
24-Well Clear TC-Treated Multiple Well Plates, sterile	Product 3527	Corning Costar (Corning Inc.)
96-Well Clear Flat Bottom TC-Treated Microplate, sterile	Product 3585	Corning Costar (Corning Inc.)
µ-Slide 8 Well, Uncoated, 1.5 polymer coverslip, hydrophobic, sterilized	Product 80821	ibidi (ibidi GmbH)
µ-Plate 96 Well Uncoated, 1.5 polymer coverslip, hydrophobic, sterilized	Product 89621	ibidi (ibidi GmbH)
96-Well Tissue Culture Black/Clear Flat-bottom Plates	Product 353219	BD Falcon (Becton, Dickinson and Co.)
Glass-bottom 24 well plate	Product 662892	Greiner Bio-One
BIOFLUX 200 48 well low shear plate	Product 910-0004	Fluxion Biosciences Inc.

4.4. Media

LB (Luria Broth)

10 g/l tryptone

5 g/l yeast extract

5 g/l NaCl

Dissolve in ddH2O and adjusted to pH 7

For LB plates 1.5% agar was added to LB medium and autoclaved.

TB (Luria Broth)

10 g/l tryptone

5 g/l NaCl

Dissolved in ddH2O and adjusted to pH 7

M9 minimal media

47.7 mM Na_2HPO_4x7H2O

22 mM $KH2PO_4$

18.7 mM NH_4Cl

8.55 mM NaCl

2 mM $MgSO_4$

0.1 mM $CaCl_2$

0.4 % ribose

4.5. Buffers

Tethering buffer

10 mM KPO4

0.1 mM EDTA

1 µM methionine

10 mM lactic acid

Dissolved in ddH2O and adjusted to pH 7

Motility buffer

10 mM KPO_4

0.1 mM EDTA

67 mM NaCl

0.5 % glucose

Dissolved in ddH2O and adjusted to pH 7. Sterile filtered.

P1 buffer

10 mM $MgSO_4$

5 mM $CaCl_2$

Sterile filtered

Phosphate buffer

1.742 g K_2HPO_4

1.361 g KH_2PO_4

0.901 g lactic acid

Dissolved in ddH_2O to a total volume of 1 L and adjusted to pH 7

TAE buffer

242 g Tris base

100 ml 0.5 M EDTA (pH 8)

57.1 ml glacial acetic acid

Dissolved in ddH_2O to a total volume of 1 L.

4.6. Antibiotic and inducers

Table 9. Antibiotics and inducers

Compound	Stock concentration
Ampicillin (Amp)	100 mg/ml in H_2O
Chloramphenicol (Cm)	34 mg/ml in ethanol
Kanamycin (Kan)	50 mg/ml in H_2O
Isopropyl-β-D-thiogalactopyranosid (IPTG)	0.1 M IPTG in H_2O
Arabinose	10 % arabinose in H_2O

4.7. Bacterial strains and plasmids

All strains and plasmids used in this study are listed in Table S10 and Table S11 respectively. *E. coli* strains used in this work were derived from W3110 (Hayashi et al., 2006, Serra et al. 2013). Genes were deleted using either the one-step method for inactivation of genes (Datsenko & Wanner, 2000) or by P1 transduction using strains of the Keio collection (Baba et al., 2006) as donors. Kanamycin resistance was excised using FLP recombinase expressed from the plasmid pCP20 (Cherepanov & Wackernagel, 1995). Plasmids pVS130, pVS147 and pVM64 were made by cloning *ecfp, eyfp* and *dgcE* genes into pTrc99a vector with *Sac*I/*Xba*I respectively (Amann et al., 1988). Plasmid pME7 was made by cloning *fimA* gene was cloned into the pBAD33 vector with XbaI/HindIII. Sequences was verified by sequencing at the Eurofins MWG Operon (Ebersberg) company.

4.8. Polymerase chain reaction (PCR)

Table 10. Single colony PCR reaction mixture

Final concentration	Component
25 µl	DreamTaq Green PCR Master Mix (2x)
1 µl	34 mg/ml in ethanol
1 µl	50 mg/ml in H2O
	Colony from plate
Up to 50 µl ddH2O	

Table 11. Single colony PCR thermocycler settings

Time	Temperature	Step	Cycles
5 min	95 °C	Initial denaturation	
30 sec	95 °C	Denaturation	30 cycles
30 sec	55 °C	Annealing	
1 min	72 °C	Extension	
10 min	72 °C	Final extension	

Table 12. PCR with Phusion polymerase reaction mixture

Final concentration	Component
0.5 µl	Phusion polymerase
10 µl	Phusion HF buffer (5x)
1 µl	forward primer
1 µl	reverse primer
8 µl	dNTPs
10 pg - 1 µg	Template DNA
Up to 50 µl ddH_2O	

Table 13. PCR with Phusion polymerase thermocycler settings

Time	Temperature	Step	Cycles
2 min	95 °C	Initial denaturation	
30 sec	95 °C	Denaturation	30 cycles
30 sec	65 °C	Annealing	
30 s/kb	72 °C	Extension	
5 min	72 °C	Final extension	

The PCR reactions were performed in the thermocyclers TPersonal (Biometra) and peqSTAR (PEQLAB). The resulting fragments were analyzed in a 1% TAE-agarose gel and purified with the GeneJET DNA Purification Kit or the GeneJET Gel Extraction Kit. All the primers used are listed in Table S3.

4.9. Restriction digest

Restriction digests were performed using enzymes from New England Biolabs or thermo Scientific. Amounts of buffers and enzymes were used according to manufacturer's recommendations. Restrictions were performed on 10 µl of template DNA and mixtures were incubated for 1 h at 37 °C. Restriction fragments were purified with the GeneJET DNA Purification Kit or GeneJET Gel Extraction Kit

4.10. Ligation

Ligation was performed using a T4 DNA ligase from Thermo Scientific at room temperature for 1 h.

Vector	50 ng
Insert	6x molar ratio vector
10x T4 DNA ligase buffer	2 µl
T4 DNA ligase	0.2 µl
Up to 20 µl ddH_2O	

4.11. Chemical competent cells

E. coli cells were grown at 37 °C until OD_{600} 0.5-0.6, harvested by centrifugation for 5 min at 4000 rpm and washed twice with cold 0.1M $CaCl_2$. Cells were then resuspended in 100 µl of 0.1M $CaCl_2$. Cells were then used directly for transformation.

4.12. Transformation

0.5 µl plasmid DNA or 5µL ligation were added to 100 µl chemical competent cells and kept on ice for 30 min. Sample was heat shocked at 42 °C for 45 s and placed again on ice. 900 µl of LB were added to the cells and they were kept at 37 °C for 1 hour. Cells were then harvested and plated on LB agar plates with selective antibiotics and incubated over night at 37 °C.

4.13. P1 transduction and kanamycin cassette cross-out

Keio collection strains were used as donor to transfer knockout mutations using P1 phage transduction into W3110 *rpoS*$^-$ and W3110 *rpoS*$^+$ (Thomason *et al.*, 2007). Knockouts were tested for the correct insertion of the FRT-site flanked kanamycin cassette by colony PCR. Kanamycin cassettes were then excised using FLP recombinase (Cherepanov & Wackernagel, 1995). Strains were transformed with a pCP20 plasmid encoding a FLP recombinase and tested for the loss of antibiotic resistance after several rounds of growth on LB plates at 42 °C.

4.14. Growth conditions

For attachment experiments in static conditions and under flow, cells were grown in TB medium supplemented with antibiotics, where necessary. Overnight cultures were diluted 1:100 or 1:50 in fresh TB supplemented and grown until OD_{600} 0.5 or 1.2 when specified. Cell cultures were harvested and resuspended in TB medium, tethering buffer or motility buffer until OD_{600} 0.05 or 0.4.

For biofilm growth and surface colonization experiments (Part 2), pre-cultures were grown in Corning Costar® 24-well plates in 1 ml TB medium for 48 h at 30°C. Cells were grown in 96-well polystyrene tissue culture (TC)-treated plates from Corning® Costar® or where indicated polystyrene TC-treated plates from BD Falcon™ in M9 minimal medium supplied with 0.4 % ribose. For growth in M9 medium, cells were first diluted to an OD_{600} of 1.0 in TB and then to 0.1 in M9.

Media were supplied with 100 µg/ml Amp, 50 µg/ml Kan, 34 µg/ml Cm, 0.005% arabinose and/or 50 µM IPTG when applicable.

4.15. Crystal violet staining

Wells were washed three times with 200 µL sterile water and stained with 200 µL 1 % crystal violet (CV) for 20 min. CV was removed and plates were washed with water until no further destaining was visible. Plates were dried overnight and subsequently incubated with 200 µL of 96 % ethanol for 1 h at 150 rpm on a rotary shaker to solubilize CV. CV absorption was then measured in a plate reader at 600 nm. A blank control with an empty medium was included during surface colonization and this control was treated in the same way as the samples. Blank values were subtracted from the raw values of the samples. Values obtained for each strain were further normalized to the wild-type control. For normalization of CV to the OD of the culture, OD_{600} was measured in a plate reader before washing and staining the cells.

4.16. Surface mannosylation

In order to create surfaces containing mannose residues, 1% BSA was added to 96-well imaging uncoated plates from ibidi® and incubated for 30 min at room temperature. Surfaces were then washed to remove the unattached BSA and 0.1 mg/ml 4-Methylumbelliferyl α-D-mannopyranoside was added. Plates were incubated for 15 min

under UV light using an Ebox VX5 system (Vilber Lourmat, France) in order to activate the fluorophore as previously described (Belisle *et al.*, 2008). Wells were then washed and then cells were (Figure 49).

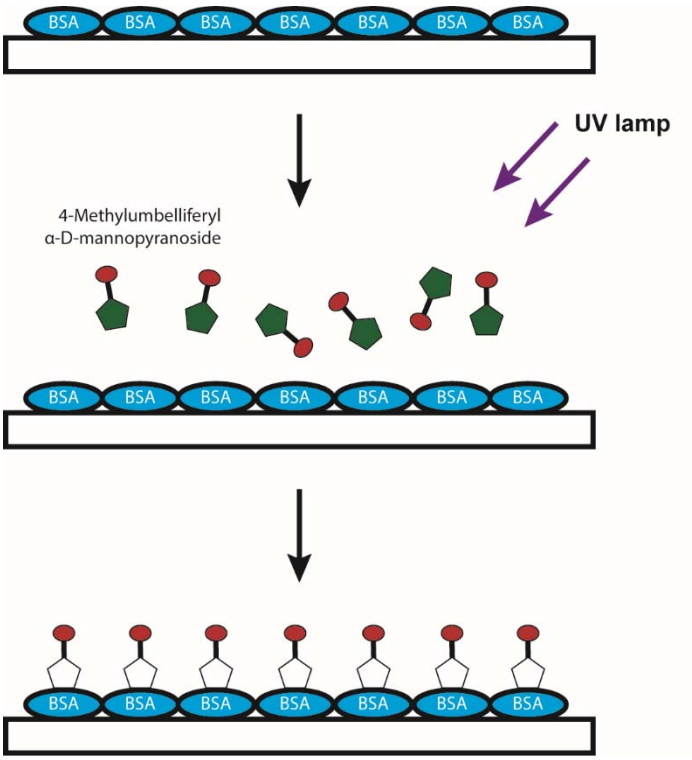

Figure 49. Construction of mannosylated surfaces. Schematic representation of the steps followed for the construction of mannosylated surfaces.

4.17. Microfluidic attachment

Cells were grown as described in 6.14. For adhesin screening, cells were harvested by centrifugation and resuspended in TB medium until OD_{600} 0.05. Cells were then flushed into the channels constantly overnight at 0.2, 0.5 or at 1 dyne/cm^2 as specified.

For the buffer experiments, cells were harvested by centrifugation and resuspended in Motility buffer containing 50µg/ml chloramphenicol and incubated at 4°C for 20 min. Cells were then diluted until OD_{600} of 0.05 and flushed constantly overnight.

For the growth experiments cells were harvested by centrifugation and resuspended in fresh TB until an OD_{600} of 0.05. Cells were then flushed at flow 1 dyne/cm^2 for 2 minutes. Cells were removed from the input well and fresh media was then flushed overnight at 0.2 or 1 dyne/cm^2 as indicated.

Images were taken every 60 min. All the microfluidic assays were performed at 30 °C and using Bioflux 200 system.

4.18. Static attachment

Cells were grown as described in 6.14.

For adhesin screening, cells were harvested by centrifugation and resuspended in fresh motility buffer until OD_{600} of 0.05. 200 µl of cells were then added to ibidi uncoated plates or and Greiner bio-one glass-bottom plates. Glass plates were cleaned using a plasma cleaner for 0.5 min at 75W to remove impurities and to make sure the surface was hydrophilic. After 1 h at 30 °C, wells then washed 3 times with motility buffer and cells were imaged on 200 µl of motility buffer.

For attachment experiments, cells were diluted to an OD_{600} 0.4 in motility buffer and cells expressing different fluorescent proteins were mixed in a 1:1 ratio. 200 µl of cells were seeded in imaging uncoated plates from ibidi® or mannosylated surfaces. After 20 min or 1 h incubation at room temperature as indicated, plates were washed three times with 200 µl motility buffer. Attached cells were covered with 200 µL motility buffer and imaged immediately.

For attachment in the presence of chemoattractants, cells were grown and harvested as described above. After incubation in motility buffer for 20 min at 4°C, cells were diluted to an OD_{600} 0.04 in motility buffer with 10 mM α-metyl-DL-aspartic acid and 10 mM L-serine. 200 µL of cells were seeded in wells of 96-well imaging uncoated plates from ibidi® and imaged without washing after 20 min.

For biofilm growth and surface colonization experiments, cells were diluted until OD 0.1 in M9 minimal medium. Cells expressing different fluorescent proteins were mixed in a 1:1 ratio. 125 µL of cell suspension were seeded into the wells. On plates used for imaging, additional 175 µL medium were added to the wells. Cells were grown at 30°C without shaking for the indicated time. Media was supplemented with antibiotics and inducers when applicable.

4.19. Centrifugation enforced attachment

Cells were grown as described in 6.14. Fluorescent promoter reporter strains or mixed cultures of cells labelled with different fluorophores (1:1 ratio) were added to TC-treated

BD Falcon™ imaging plates or ibidi uncoated imaging plates. Plates were centrifuged for 2 min at 650 g (mild centrifugation) or 2 hours at 4000 rpm (surface attachment enforced growth).

4.20. Fluorescence microscopy

Wide-field fluorescence imaging was performed on a Nikon Eclipse Ti-U fluorescence microscope equipped with an iXon3 897 EMCCD camera using a 40x NA 0.75 objective and using GFP (Ex470/40, Em525/50), mCherry (Ex572/25, Em645/90) filter sets.

For the static attachment experiments on ibidi plates and mannosylated surfaces, 6 positions per well were imaged and at least 4 images of each position were taken without waiting time between them to discard swimming cells

For attachment under flow images from 4 different points of the microfluidic channel every 30 min or 1 h in brightfield and fluorescent channels.

4.21. Quantification of attached cells by microscopy

Images from wide-field microscopy were analyzed using ImageJ (http://imagej.nih.gov/ij/).

For quantification of the area covered by attached cells, a stack of five images acquired within two second time intervals were acquired for each fluorescence channel. Each image in the stack was corrected for background fluorescence with Fiji (https://fiji.sc/) using rolling ball background subtraction (https://imagej.net/plugins/rolling-ball.html). To eliminate swimming cells, the minimal image per stack was calculated. Minimal images were converted to binary images by automated local thresholding using Phansalkar's method. Cells and cell clumps were identified in binary images using segmentation with Fiji. The fraction of the area covered by identified cells and cell clumps in the area of the whole image was calculated (=area fraction). Ratios of area fractions of mutant cells were determined and finally normalized to the ratio of wild-type cells.

For the microfluidics images in non-dividing conditions, a defined area per image was use for quantification. Segmentation of cells was done using MicrobeJ and followed during the experiment allowing us to get the information about each cell throughout the experiment.

For the microfluidics growth experiments and *pfliC*, images were then segmented with Fiji. Masks of segmented cells were then overlaid on fluorescence images and fluorescence intensities of all cells were measured.

4.22. Tracking experiments

Cells were grown to OD_{600} ~ 0.6 or OD_{600} ~ 1.05, as indicated, following the same protocol as for attachment experiments, harvested and washed once by centrifugation at 4,000 rpm (1,300 rcf) for 5 minutes, resuspended in motility buffer, cooled at 4°C for about 20 minutes, and then diluted to the final OD_{600} of ~ 0.02 and ~ 0.005. A small droplet (4 µL) of the suspension was trapped between a slide and a coverslip along with a large volume of air in a grease-sealed compartment. The bacterial motion was observed and recorded at the bottom hydrophilic surface of the sample using phase contrast microscopy at 10x magnification (NA = 0.3) and a Mikrotron Eosens camera (1 px = 0.7 µm) running at 100 frames per seconds (fps) for 30 seconds. The bacteria were tracked using the Mosaic analysis program (Sbalzarini & Koumoutsakos, 2005) running as an ImageJ plugin, and extracted trajectories were analyzed using custom-made algorithms running as ImageJ plugins, to evaluate tumbling rate, run speeds, and trajectory durations and lengths.

The trajectories were analyzed as follows. For trajectories longer than 0.5 s, discrimination between Brownian and stuck particles on the one hand and swimmers on the other hand was performed using a radius of gyration criterion: the measure of diffusivity $\max_{t,t'}(r_t - r_{t'})/t_{traj}$ must be larger than $0.2\,\mathrm{px}^2/\mathrm{fr}$ for the particle to be considered a swimmer, where t_{traj} is the trajectory duration and t and t' are any couple of times within the trajectory. The tumbles were identified using the following criteria. The velocity of the cells is computed as $\vec{v} = 1/\Delta t \sum_{t-\Delta t/2}^{t+\Delta t/2} \Delta\vec{r}$, with $\Delta t = 0.2$ s. The average displacement $d = 1/\Delta t \sum_{t-\Delta t/2}^{t+\Delta t/2} |\Delta\vec{r}|$ is computed over the same duration, and the ratio $r = |\vec{v}|/d$ is then evaluated. This quantity is close to 1 during the runs and low (typically less than 0.6-0.7) during the tumbles. A threshold r_{th} is computed which maximizes Shannon's entropy, following Huang's fuzzy thresholding method (Huang & Wang, 1995), using all the tracks of swimmers in one movie as the sample. This threshold is used to separate each trajectory into putative run and tumble segments. To reduce the noise, the variance v_{run} of r during the run segments is computed, and each putative tumble is accepted as a tumble if $\sum_t (r - r_{th})^2 > 3v_{run}t^2/2$ (*i.e.* if the magnitude of the

tumble excursion is larger than what a random fluctuation would be). The criteria used are thus based on how directed the motion is and not on changes of orientations, because a tumble can happen without a change of direction. The tumbling rate is then the overall number of transitions from run to tumble in all trajectories divided by the sum of the durations of the trajectories. The average swimming speed was determined as the average of the speed during the runs of all swimmers in the film. The average trajectory durations and lengths were computed using only the trajectories identified as swimmers.

4.23. Swimming speed measurements

The same growth and harvesting protocol were used as for tracking experiments, except that the cells were resuspended to a final OD_{600} of 0.5. The sample preparation was the same. It was observed under the same microscope. The motion was then recorded for 100 s at 100 fps. The movie was then analyzed using the Differential Dynamic Microscopy algorithm (Wilson *et al.*, 2011), which evaluates the average swimming speed of the population of cells, as well as the standard deviation of swimming speeds within the population and the fraction of swimming cells. The fraction of swimming cells was above 80% in any case, and the standard deviation about 30% of the mean.

4.24. Flow cytometry

Activity of *fimD* and *fliC* promoter was assessed using a plasmid-based *egfp* reporter from *E. coli* promoter library (Zaslaver *et al.*, 2006). Samples were grown and prepared as described for measurements of planktonic attachment. Cells were diluted to an OD_{600} of 0.4 in motility buffer and their fluorescence was measured. Alternatively, to investigate promoter activity in swimming and attached cells, 500 µL of this cell suspension were seeded in wells of 8-well ibidi® imaging plates. After 1 h incubation at room temperature, supernatants were taken and attached cells were scraped in 200 mL of fresh motility buffer. Fluorescence levels of both fractions were measured with BD LSRFortessa SORP cell analyser (BD Biosciences, Germany).

4.25. Proteomics

Samples were grown as described in 6.14. Planktonic samples were grown until OD600 0.5 and harvested by centrifugation. For attached samples, cells were seeded for 30 mins on ibidi uncoated plates. Media was then changed for fresh TB and samples were

grown on static conditions for 5 hours. Cells were then scrapped out of the surface. Both planktonic and attached cells were washed twice with PBS.

For protein digestion, frozen cell pellets were resuspended in 2% Sodium-lauroyl sarcosinate (SLS) in 100mM Ammoniumbicarbonate, sonicated and incubated for 15min at 90°C. Samples were then centrifuged 5 min at 14000 rpm and 0.2 M TCEP was added to the supernatants and kept for 15 mins at 90°C. 0.4 M Iodoacetamide were added to the samples after they cooled down and kept at 25°C for 30 mins and 500 rpm in the dark. Based on BCA results, 50 µg of protein were used. Trypsin was added in a 1:50 ratio and digest carried out overnight at 30°C after diluting SLS to 0.5% using 100 mM NH4HCO3. Samples were centrifuged at 15000 rpm for 10min at 4°C and supernatants used for solid phase extraction. All samples were desalted using C18 microspin columns (Harvard Apparatus) according to the manufacturer's instructions.

Using the protein digests of the biological triplicate samples, LC-MS/MS analysis was performed on Q-Exactive Plus mass spectrometer connected to an electrospray ion source (Thermo Fisher Scientific). Peptide separation was carried out using Ultimate 3000 nanoLC-system (Thermo Fisher Scientific), equipped with packed in-house C18 resin column (Magic C18 AQ 2.4 µm, Dr. Maisch). The peptides were first loaded onto a C18 precolumn (preconcentration set-up) and then eluted in backflush mode with a gradient from 98 % solvent A (0.15 % formic acid) and 2 % solvent B (99.85 % acetonitrile, 0.15 % formic acid) to 35 % solvent B over 120 min. The flow rate was set to 300 nL/ min. The data acquisition mode for the initial label-free quantification study was set to obtain one high-resolution MS scan at a resolution of 60,000 (m/z 200) with scanning range from 375 to 1500 m/z followed by MS/MS scans of the 10 most intense ions. To increase the efficiency of MS/MS shots, the charged state screening modus was adjusted to exclude unassigned and singly charged ions. The dynamic exclusion duration was set to 30 s. The ion accumulation time was set to 50 ms (both MS and MS/MS). The automatic gain control (AGC) was set to 3 × 106 for MS survey scans and 1 × 105 for MS/MS scans.

For label-free quantification the MS raw data were analyzed with Progenesis QI software (Non-linear Dynamics, version 2.0). MS/MS search of aligned LC-MS runs was performed using MASCOT against a decoy database of the uniprot *Escherichia coli* K12 protein database (UniProt Consortium). The following search parameters were used: full tryptic specificity required (cleavage after lysine or arginine residues); two missed

cleavages allowed; carbamidomethylation (C) set as a fixed modification; deamidation (NQ) and oxidation (M) set as a variable modification. The mass tolerance was set to 10 ppm for precursor ions and 0.02 Da *per* fragment ions for high energy-collision dissociation (HCD). Results from the database search were imported back to Progenesis, mapping peptide identifications to MS1 features. The peak heights of all MS1 features annotated with the same peptide sequence were summed, and protein abundance was calculated per LC-MS run. Next, the data obtained from Progenesis were evaluated using SafeQuant R-package version 2.2.2 (Glatter *et al.*, 2012). Hereby, 1% false discovery rates (FDR) of identification and quantification values were calculated.

Supplementary Figures

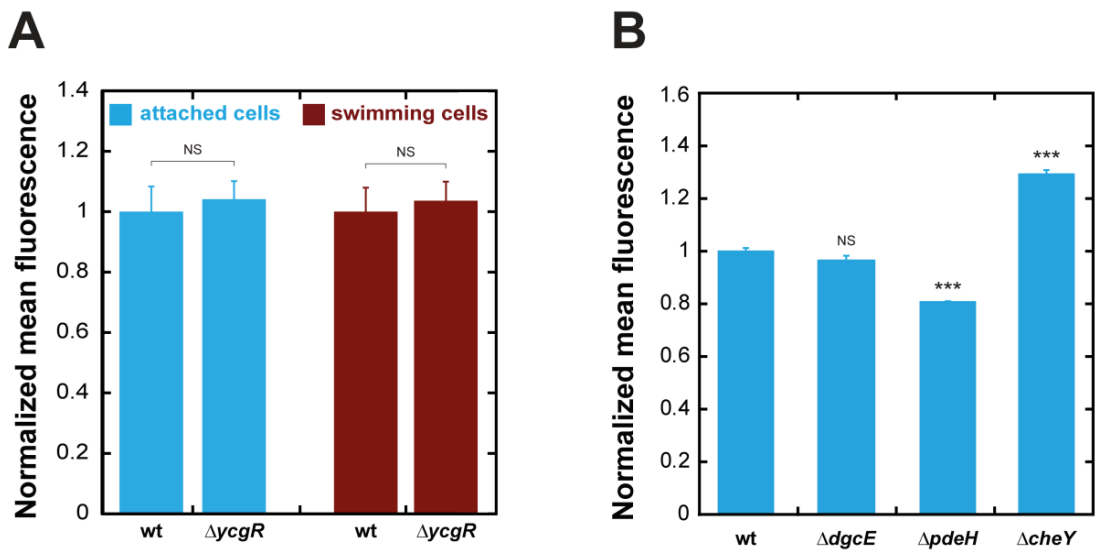

Figure S1. Effects of gene knockouts on type 1 fimbriae expression. A, B. Activity of type 1 fimbriae promoter in wild-type and indicated mutant cells. **A.** Relative promoter activity of type 1 fimbriae usher protein gene *fimD* was studied for swimming and attached wild-type and *ΔycgR* cells on motility buffer to ibidi uncoated imaging plates after 1 h incubation. Values were normalized to promoter activity in wild-type cells. Shown are mean and standard error of three biological replicates. **B.** *fimD* promoter activity in planktonic cultures of the wild-type and indicated mutants. Shown are mean and standard error of six to eight biological replicates. Statistical analysis was performed using a two-sample t-test with unequal sample size and unequal variance, with $P < 0.0005$ (***), NS, not significant.

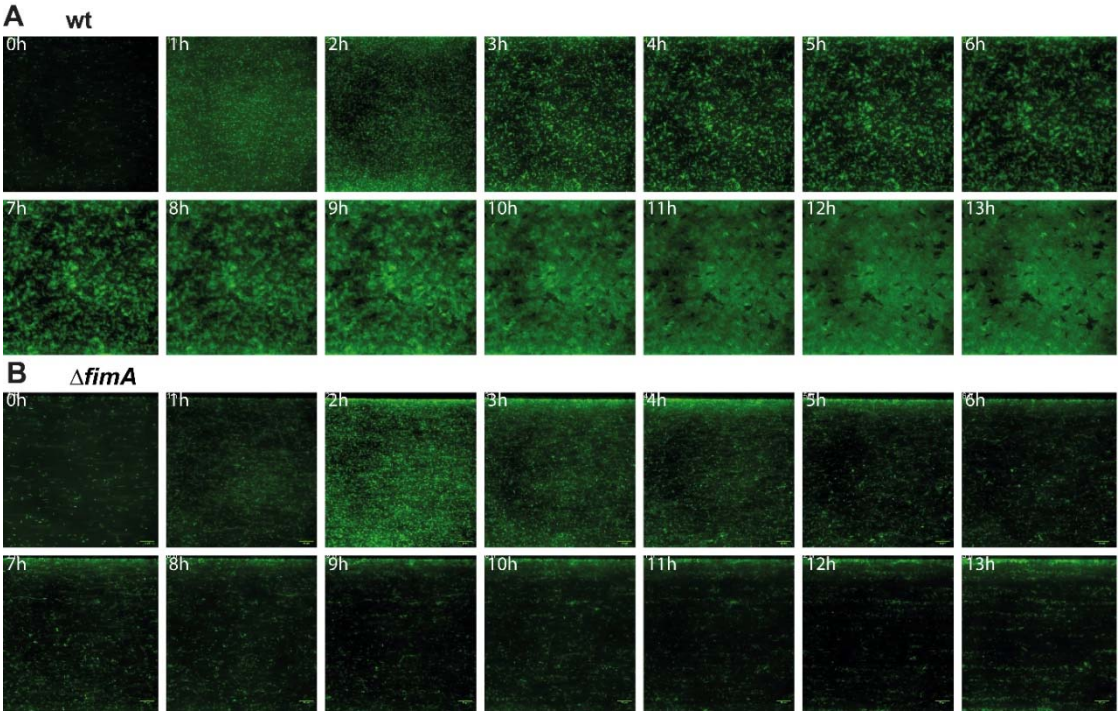

Figure S2. Attachment of wild-type (A) and *ΔfimA* (B) cells under 0.5 dyne/cm². Attachment was assessed for 13 hours at a constant flow with no incubation time. Images were taken every hour.

Supplementary Tables

Table S1. Significantly differentially expressed proteins in wild-type cells after 5 hours attached versus planktonic cells. Shown are proteins that showed a 2-fold or more change.

Name	Description	pValue	qValue	Fold change
YgfT	Putative oxidoreductase	7.2E-07	0.00013	56.58
YgeY	Putative peptidase	1.6E-09	0.00000	52.46
GuaD	Guanine deaminase	8.6E-08	0.00004	52.17
FimG	Type 1 fimbriae minor subunit	1.7E-04	0.00243	30.48
FdhF	Formate dehydrogenase H	1.3E-06	0.00018	29.83
YbfA	DUF2517 domain-containing protein	2.2E-07	0.00006	24.15
YgfM	Putative oxidoreductase	1.5E-07	0.00005	23.77
YgeW	Putative carbamoyltransferase	2.8E-06	0.00026	21.50
SsnA	Putative aminohydrolase	2.6E-08	0.00003	21.38
PhyDA	D-phenylhydantoinase	9.7E-08	0.00004	20.08
FimC	Chaperone protein	3.6E-07	0.00009	16.26
XdhD	Probable hypoxanthine oxidase	1.2E-05	0.00063	15.45
XdhC	Xanthine dehydrogenase iron-sulfur-binding subunit	6.1E-07	0.00012	14.80
GlpC	Anaerobic glycerol-3-phosphate dehydrogenase subunit C	1.4E-06	0.00018	14.28
YgfK	Putative oxidoreductase	1.1E-06	0.00018	14.04
BorD	Lipoprotein bor homolog from lambdoid prophage DLP12	8.3E-07	0.00014	13.43
MbhS	Hydrogenase-1 small chain	1.6E-05	0.00069	12.89
PreT	NAD-dependent dihydropyrimidine dehydrogenase subunit	1.7E-06	0.00019	12.83
ArcL	Carbamate kinase-like protein	1.5E-06	0.00019	12.36
LdcI	Lysine decarboxylase	2.7E-05	0.00095	10.63
XdhA	Xanthine dehydrogenase molybdenum-binding subunit	3.3E-06	0.00028	9.83
GlgS	Surface composition regulator	1.0E-04	0.00185	7.57
MbhL	Hydrogenase-1 large chain	6.7E-05	0.00147	6.99
DpaL	Diaminopropionate ammonia-lyase	8.7E-08	0.00004	5.70
FliD	Flagellar filament capping protein	2.4E-04	0.00307	5.34
YgiQ	Radical SAM superfamily protein	2.8E-06	0.00026	5.27
RaiA	Ribosome-associated inhibitor A	1.6E-05	0.00069	5.12
YtfE	Iron-sulfur cluster repair protein	1.1E-04	0.00188	5.08
HybA	Hydrogenase-2 operon protein	2.0E-05	0.00082	5.08
MbhT	Hydrogenase-2 small chain	5.0E-05	0.00128	4.74
CydB	Cytochrome bd-I ubiquinol oxidase subunit 2	1.9E-06	0.00019	4.73
GatD	Galactitol-1-phosphate 5-dehydrogenase	8.3E-06	0.00051	4.68
FlgK	Flagellar hook-associated protein 1	2.3E-04	0.00298	4.64
YqeB	XdhC-CoxI family protein	5.2E-05	0.00128	4.52
CydA	Cytochrome bd-I ubiquinol oxidase subunit 1	9.2E-06	0.00053	4.39

TdcE	PFL-like enzyme	1.9E-06	0.00019	4.11
FucO	Lactaldehyde reductase	1.9E-04	0.00260	4.09
GlpA	Anaerobic glycerol-3-phosphate dehydrogenase subunit A	5.9E-06	0.00043	3.93
FlgL	Flagellar hook-associated protein 3	7.2E-05	0.00153	3.66
Hmp	Flavohemoprotein	4.2E-06	0.00033	3.51
XdhB	Xanthine dehydrogenase FAD-binding subunit	1.8E-06	0.00019	2.89
GlpB	Anaerobic glycerol-3-phosphate dehydrogenase subunit B	2.1E-04	0.00281	2.89
SrlD	Sorbitol-6-phosphate 2-dehydrogenase	2.4E-05	0.00088	2.85
FtnA	Bacterial non-heme ferritin	3.0E-06	0.00027	2.71
YjiY	Inner membrane protein YjiY	4.0E-05	0.00122	2.54
GatZ	D-tagatose-1,6-bisphosphate aldolase subunit	1.5E-05	0.00069	2.52
PthB	Glucitol/sorbitol-specific phosphotransferase enzyme IIB component	4.4E-05	0.00125	2.20
Cdd	Cytidine deaminase	1.0E-04	0.00185	2.15
ClpB	Chaperone protein ClpB	6.4E-05	0.00147	2.09
YgeV	Uncharacterized sigma-54-dependent transcriptional regulator	1.4E-04	0.00221	2.03
UcpA	Oxidoreductase	1.9E-04	0.00264	2.02
DmlR	HTH-type transcriptional regulator	2.7E-05	0.00095	0.50
GlcE	Glycolate oxidase subunit	1.6E-04	0.00243	0.50
YhjH	Cyclic di-GMP phosphodiesterase	2.3E-05	0.00088	0.49
PdeH	Cyclic di-GMP phosphodiesterase	2.3E-05	0.00088	0.49
AcsA	Acetyl-coenzyme A synthetase	3.0E-05	0.00102	0.49
HisP	Histidine transport ATP-binding protein	6.6E-05	0.00147	0.49
YahO	DUF1471 domain-containing protein	6.7E-06	0.00047	0.49
XylF	D-xylose-binding periplasmic protein	1.3E-04	0.00210	0.49
PotF	Putrescine-binding periplasmic protein	1.1E-05	0.00056	0.49
YebF	Secreted protein	2.0E-05	0.00081	0.48
CycA	D-serine/D-alanine/glycine transporter	1.3E-04	0.00210	0.48
PaaF	2,3-dehydroadipyl-CoA hydratase	1.7E-04	0.00243	0.48
Spy	Spheroplast protein Y	4.6E-05	0.00126	0.47
GlcG	Protein GlcG	3.6E-05	0.00115	0.47
Ggt	Gamma-glutamyltranspeptidase	2.6E-04	0.00314	0.47
LsrG	(4S)-4-hydroxy-5-phosphonooxypentane-2,3-dione isomerase	3.2E-05	0.00106	0.47
FecB	Fe(3+) dicitrate-binding periplasmic protein	4.2E-04	0.00409	0.47
UgpC	sn-glycerol-3-phosphate import ATP-binding protein	2.4E-05	0.00088	0.47
YtfJ	PF09695 family protein	1.9E-04	0.00264	0.47
Crl	Sigma factor-binding protein	1.8E-03	0.01199	0.47
MasY	Malate synthase A	8.9E-06	0.00053	0.47
Pat	Putrescine aminotransferase	1.3E-04	0.00210	0.47
Dpo3E	DNA polymerase III subunit epsilon	5.4E-04	0.00499	0.46
YeeR	Inner membrane protein YeeR	3.5E-04	0.00380	0.46

AceK	Isocitrate dehydrogenase kinase/phosphatase	3.5E-04	0.00380	0.46
LcfA	Long-chain-fatty-acid--CoA ligase	1.6E-05	0.00069	0.45
DlhH	Putative carboxymethylenebutenolidase	2.1E-05	0.00083	0.45
YjdJ	Putative N-acetyltransferase	4.0E-04	0.00399	0.45
YbaA	DUF1428 domain-containing protein	2.9E-04	0.00341	0.45
YgaM	DUF883 domain-containing protein	2.3E-04	0.00299	0.44
LsrK	Autoinducer-2 kinase	3.5E-05	0.00113	0.44
LsrR	Transcriptional regulator LsrR	8.4E-05	0.00166	0.44
FadM	Long-chain acyl-CoA thioesterase	3.3E-04	0.00366	0.44
FeaB	Phenylacetaldehyde dehydrogenase	1.3E-05	0.00066	0.43
LsrF	3-hydroxy-5-phosphonooxypentane-2,4-dione thiolase	2.0E-05	0.00081	0.42
UgpB	sn-glycerol-3-phosphate-binding periplasmic protein	1.1E-05	0.00056	0.42
LsrA	Autoinducer 2 import ATP-binding protein	8.9E-04	0.00727	0.42
CsiD	Protein CsiD	1.5E-05	0.00069	0.41
GadW	HTH-type transcriptional regulator	6.0E-05	0.00139	0.40
PaaK	Phenylacetate-coenzyme A ligase	1.6E-04	0.00243	0.40
LsrB	Autoinducer 2-binding protein	4.1E-06	0.00033	0.39
PrpC	2-methylcitrate synthase	4.1E-04	0.00399	0.39
MscL	Large-conductance mechanosensitive channel	1.7E-03	0.01170	0.39
MtlR	Mannitol operon repressor	2.4E-04	0.00308	0.39
YodC	Uncharacterized protein	4.3E-05	0.00125	0.38
ArgT	Lysine/arginine/ornithine-binding periplasmic protein	1.6E-05	0.00069	0.37
PaaJ	3-oxoadipyl-CoA/3-oxo-5,6-dehydrosuberyl-CoA thiolase	5.4E-05	0.00131	0.37
OppB	Oligopeptide transport system permease protein	3.6E-04	0.00382	0.36
PaaZ	Bifunctional protein	4.6E-03	0.02250	0.36
Cfa	Cyclopropane-fatty-acyl-phospholipid synthase	2.9E-05	0.00101	0.36
GarP	Probable galactarate transporter	1.0E-04	0.00186	0.35
PsiF	Phosphate starvation-inducible protein PsiF	8.0E-05	0.00163	0.35
PaaH	3-hydroxyadipyl-CoA dehydrogenase	1.4E-05	0.00069	0.35
GudP	Probable glucarate transporter	1.0E-05	0.00056	0.35
YeaC	DUF1315 domain-containing protein	1.5E-04	0.00230	0.32
PrpR	Propionate catabolism operon regulatory protein	4.0E-05	0.00122	0.32
CsiR	HTH-type transcriptional repressor CsiR	3.7E-05	0.00115	0.32
LsrC	Autoinducer 2 import system permease protein	9.9E-06	0.00056	0.30
YqeF	Probable acetyl-CoA acetyltransferase	3.9E-04	0.00397	0.29
MotB	Motility protein B	4.4E-03	0.02190	0.29
AriR	Probable two-component-system connector protein	1.4E-04	0.00221	0.29
AmiB	N-acetylmuramoyl-L-alanine amidase	3.6E-04	0.00382	0.27
RavA	ATPase	1.6E-04	0.00243	0.26
PuuR	HTH-type transcriptional regulator	2.6E-03	0.01534	0.26
PuuE	4-aminobutyrate aminotransferase	3.2E-05	0.00106	0.26

PuuD	Gamma-glutamyl-gamma-aminobutyrate hydrolase	6.9E-06	0.00048	0.26
PaaC	1,2-phenylacetyl-CoA epoxidase, subunit C	3.2E-04	0.00361	0.25
PaaG	1,2-epoxyphenylacetyl-CoA isomerase	4.7E-06	0.00036	0.25
MpaA	Murein tripeptide amidase A	1.7E-04	0.00243	0.25
PuuC	Aldehyde dehydrogenase	1.0E-04	0.00185	0.23
PaaI	Acyl-coenzyme A thioesterase	1.2E-04	0.00206	0.22
PaaB	1,2-phenylacetyl-CoA epoxidase, subunit B	7.2E-05	0.00153	0.21
FlgA	Flagella basal body P-ring formation protein	3.0E-04	0.00348	0.18
YibI	DUF3302 domain-containing protein	9.9E-05	0.00185	0.17
PlaP	Low-affinity putrescine importer	4.8E-04	0.00453	0.16
PuuA	Gamma-glutamylputrescine synthetase	5.1E-05	0.00128	0.15
YmiA	Uncharacterized protein	7.8E-05	0.00160	0.11
YfeH	Putative solute:Na+ symporter	2.5E-04	0.00311	0.11
PaaE	1,2-phenylacetyl-CoA epoxidase, subunit E	4.2E-07	0.00009	0.10
FhuF	Ferric iron reductase protein	4.5E-04	0.00427	0.10
YjbQ	UPF0047 protein YjbQ	3.6E-08	0.00003	0.09
McbR	HTH-type transcriptional regulator	4.6E-05	0.00126	0.07
PuuP	Putrescine importer	5.7E-05	0.00135	0.06
KgtP	Alpha-ketoglutarate permease	1.3E-06	0.00018	0.05
PuuB	Gamma-glutamylputrescine oxidoreductase	3.1E-04	0.00353	0.05

Table S2.Significantly differentially expressed proteins in *ΔmotA* cells after 5 hours attached versus planktonic cells. Shown are proteins that showed a 2-fold or more change.

Name	Description	pValue	qValue	Fold change
YgfT	Putative oxidoreductase	4.0E-08	8.08E-06	182.99
GuaD	Guanine deaminase	5.1E-08	8.87E-06	181.23
YgeY	Putative peptidase	2.4E-10	5.18E-07	116.00
GhxQ	Guanine/hypoxanthine permease	4.0E-08	8.08E-06	70.66
YgfM	Putative oxidoreductase	3.6E-09	1.96E-06	69.37
SsnA	Putative aminohydrolase	2.6E-08	7.47E-06	67.92
FdhF	Formate dehydrogenase H	7.2E-08	9.84E-06	60.69
YgeW	Putative carbamoyltransferase	2.4E-07	2.09E-05	60.39
PhyDA	D-phenylhydantoinase	3.1E-08	7.66E-06	53.59
MbhS	Hydrogenase-1 small chain	1.5E-09	1.64E-06	50.87
XdhD	Probable hypoxanthine oxidase	9.9E-08	1.20E-05	43.35
YgfK	Putative oxidoreductase	1.4E-08	5.95E-06	37.64
YbfA	DUF2517 domain-containing protein	3.3E-07	2.58E-05	30.91
XdhC	Xanthine dehydrogenase iron-sulfur-binding subunit	5.3E-08	8.87E-06	30.39
YcjN	Putative ABC transporter periplasmic-binding protein	1.9E-07	1.74E-05	22.81
XdhA	Xanthine dehydrogenase molybdenum-binding subunit	5.5E-07	3.74E-05	22.35

ArcL	Carbamate kinase-like protein	2.7E-08	7.47E-06	21.81
GlpC	Anaerobic glycerol-3-phosphate dehydrogenase subunit C	3.0E-06	0.00011	20.70
PreT	NAD-dependent dihydropyrimidine dehydrogenase subunit	2.9E-09	1.96E-06	19.97
LdcI	Lysine decarboxylase	6.6E-06	0.0002	19.19
MbhL	Hydrogenase-1 large chain	9.6E-05	0.00095	16.83
YtfE	Iron-sulfur cluster repair protein	8.4E-05	0.00088	15.84
YdjL	Uncharacterized zinc-type alcohol dehydrogenase-like protein	6.4E-08	9.34E-06	13.26
DpaL	Diaminopropionate ammonia-lyase	2.7E-08	7.47E-06	12.79
DsdX	Permease	2.8E-05	0.00044	12.54
SbcD	Nuclease SbcCD subunit D	2.6E-04	0.00195	12.29
YqeB	XdhC-CoxI family protein	3.9E-05	0.00052	11.49
BorD	Lipoprotein bor homolog from lambdoid prophage DLP12	6.9E-06	0.0002	11.00
YqeC	Uncharacterized protein	2.6E-05	0.00042	10.48
GatD	Galactitol-1-phosphate 5-dehydrogenase	1.5E-07	1.51E-05	9.47
HybA	Hydrogenase-2 operon protein HybA	2.7E-04	0.00198	8.02
PreA	NAD-dependent dihydropyrimidine dehydrogenase subunit	2.5E-04	0.00186	8.02
GlpA	Anaerobic glycerol-3-phosphate dehydrogenase subunit A	5.6E-07	3.75E-05	7.86
RaiA	Ribosome-associated inhibitor A	1.0E-05	0.00024	7.36
XdhB	Xanthine dehydrogenase FAD-binding subunit	2.7E-07	2.30E-05	7.18
CydA	Cytochrome bd-I ubiquinol oxidase subunit 1	9.8E-08	1.20E-05	7.05
CydB	Cytochrome bd-I ubiquinol oxidase subunit 2	1.3E-07	1.46E-05	6.87
YkgF	Putative amino acid dehydrogenase	6.2E-04	0.00373	6.19
YgiQ	UPF0313 protein	7.1E-06	0.0002	6.04
MbhT	Hydrogenase-2 small chain	3.1E-04	0.00217	5.74
GlpB	Anaerobic glycerol-3-phosphate dehydrogenase subunit B	5.1E-07	3.66E-05	5.73
Hmp	Flavohemoprotein	2.5E-06	0.00011	5.62
SrlD	Sorbitol-6-phosphate 2-dehydrogenase	8.4E-06	0.00022	5.53
YegD	Uncharacterized chaperone protein	1.2E-03	0.00598	5.47
TdcE	PFL-like enzyme TdcE	1.4E-07	1.49E-05	5.30
PthB	Glucitol/sorbitol-specific phosphotransferase enzyme IIB component	1.0E-04	0.00097	5.09
FucO	Lactaldehyde reductase	2.7E-04	0.002	4.92
PthA	Glucitol/sorbitol-specific phosphotransferase enzyme IIA component	8.6E-06	0.00023	4.34
GlpT	Glycerol-3-phosphate transporter	5.7E-05	0.00068	4.07
YdjJ	Uncharacterized zinc-type alcohol dehydrogenase-like protein	2.9E-05	0.00044	3.94
MbhM	Hydrogenase-2 large chain	1.8E-04	0.00152	3.78
YjiY	Inner membrane protein	1.1E-03	0.00578	3.75
FtnA	Bacterial non-heme ferritin	1.3E-07	1.46E-05	3.73
GlpQ	Glycerophosphoryl diester phosphodiesterase	8.2E-06	0.00022	3.57

PtkB	Galactitol-specific phosphotransferase enzyme IIB component	1.2E-06	7.27E-05	3.54
GatZ	D-tagatose-1,6-bisphosphate aldolase subunit	9.0E-07	5.64E-05	3.47
SdhD	D-serine dehydratase	7.2E-04	0.00417	3.38
UspG	Universal stress protein G	1.9E-07	1.74E-05	3.14
PtkA	Galactitol-specific phosphotransferase enzyme IIA component	8.9E-07	5.64E-05	3.14
YcgN	UPF0260 protein	1.8E-03	0.00822	3.02
PtkC	Galactitol permease IIC component	7.8E-06	0.00022	2.94
TreC	Trehalose-6-phosphate hydrolase	1.9E-03	0.00852	2.84
GlgS	Surface composition regulator	3.5E-03	0.01336	2.75
Rmf	Ribosome modulation factor	4.5E-04	0.00294	2.70
Cdd	Cytidine deaminase	1.6E-06	8.31E-05	2.65
Syk2	Lysine--tRNA ligase, heat inducible	2.5E-05	0.00041	2.64
YgeV	Uncharacterized sigma-54-dependent transcriptional regulator	3.6E-05	0.00049	2.60
UlaB	Ascorbate-specific phosphotransferase enzyme IIB component	1.3E-05	0.00027	2.56
RsmF	Ribosomal RNA small subunit methyltransferase F	3.5E-03	0.01368	2.55
SodF	Superoxide dismutase [Fe]	1.8E-05	0.00033	2.52
DhnA	NADH dehydrogenase	4.9E-05	0.00061	2.50
YcbJ	Putative phosphotransferase	1.7E-04	0.00144	2.47
YjbD	DUF3811 domain-containing protein	6.0E-05	0.0007	2.40
AdeC	Adenine deaminase	5.6E-05	0.00068	2.39
ClpB	Chaperone protein ClpB	1.5E-06	8.31E-05	2.39
PtqA	N,N'-diacetylchitobiose-specific phosphotransferase enzyme IIA component	1.4E-04	0.00121	2.36
Edd	Phosphogluconate dehydratase	1.0E-05	0.00024	2.31
CopA	Copper-exporting P-type ATPase A	6.8E-06	0.0002	2.31
TypH	Thymidine phosphorylase	6.0E-06	0.00018	2.22
UcpA	Oxidoreductase UcpA	1.8E-05	0.00033	2.19
FlgK	Flagellar hook-filament junction protein 1	2.1E-04	0.00166	2.17
YacL	UPF0231 protein	5.7E-04	0.0035	2.16
RhlE	ATP-dependent RNA helicase	1.4E-03	0.00686	2.16
YnhG	Probable L,D-transpeptidase	1.2E-05	0.00027	2.16
IadA	Isoaspartyl dipeptidase	4.4E-05	0.00057	2.16
NarP	Nitrate/nitrite response regulator protein NarP	1.2E-03	0.00594	2.12
YjiA	Uncharacterized GTP-binding protein	8.5E-05	0.00088	2.10
Udp	Uridine phosphorylase	2.4E-05	0.0004	2.09
FlgL	Flagellar hook-filament junction protein 2	2.9E-03	0.01161	2.08
YkgG	DUF162 domain-containing lactate utilization protein	2.3E-03	0.00989	2.07
YdjG	Uncharacterized oxidoreductase	1.2E-03	0.00611	2.05
DeoC	Deoxyribose-phosphate aldolase	1.3E-05	0.00027	2.05
PflB	Formate acetyltransferase 1	7.5E-06	0.00021	2.04
CpxP	Periplasmic protein	1.1E-04	0.00105	2.02
AcnA	Aconitate hydratase A	9.0E-05	0.00091	0.50

MsyB	Acidic protein MsyB	1.1E-05	0.00024	0.50
PutP	Sodium/proline symporter	4.9E-04	0.00312	0.50
Alr2	Alanine racemase, catabolic	1.2E-04	0.00114	0.50
YgaM	DUF883 domain-containing protein	2.9E-04	0.0021	0.49
HisJ	Histidine-binding periplasmic protein	1.0E-05	0.00024	0.49
YdhS	Uncharacterized protein	3.0E-05	0.00045	0.49
FadL	Long-chain fatty acid transport protein	4.0E-06	0.00014	0.49
YbaY	Uncharacterized lipoprotein	8.1E-05	0.00086	0.48
YehX	Glycine betaine uptake system ATP-binding protein	3.9E-05	0.00052	0.48
LamB	Maltoporin	2.3E-05	0.00039	0.48
YhbO	Protein	3.9E-04	0.00263	0.48
IlvB	Acetolactate synthase isozyme 1 large subunit	1.5E-03	0.00722	0.48
PhnO	Protein PhnO	3.4E-05	0.00048	0.48
BtuE	Vitamin B12 transport periplasmic protein BtuE	1.4E-04	0.0012	0.48
YdcS	Putative ABC transporter periplasmic-binding protein YdcS	9.2E-06	0.00024	0.48
YicS	Uncharacterized protein	4.1E-04	0.00273	0.48
TreA	Periplasmic trehalase	2.3E-05	0.0004	0.47
YceF	Maf-like protein YceF	7.1E-05	0.0008	0.47
GabP	GABA permease	2.9E-05	0.00045	0.47
YehZ	Glycine betaine-binding protein	3.9E-06	0.00013	0.47
FecE	Fe(3+) dicitrate transport ATP-binding protein FecE	1.3E-05	0.00027	0.47
Spy	Spheroplast protein Y	1.2E-04	0.00111	0.47
YhjG	AsmA family protein	7.8E-05	0.00084	0.46
GlrX2	Glutaredoxin-2	1.0E-04	0.00097	0.46
PliG	Inhibitor of g-type lysozyme	1.9E-04	0.00155	0.46
YodC	Uncharacterized protein	6.0E-04	0.00363	0.46
YbiO	Moderate conductance mechanosensitive channel	3.9E-04	0.00263	0.46
MglA	Galactose/methyl galactoside import ATP-binding protein	4.8E-05	0.0006	0.46
PaaY	Phenylacetic acid degradation protein PaaY	1.4E-05	0.00028	0.46
CstA	Carbon starvation protein A	1.0E-05	0.00024	0.46
YbiU	DUF1479 domain-containing protein	2.7E-04	0.00199	0.45
FadH	2,4-dienoyl-CoA reductase [NADPH]	1.1E-05	0.00024	0.45
KefF	Glutathione-regulated potassium-efflux system ancillary protein	7.9E-04	0.00448	0.45
SodM	Superoxide dismutase [Mn]	2.7E-05	0.00043	0.45
AldB	Aldehyde dehydrogenase B	1.1E-04	0.00105	0.45
ExbB	Biopolymer transport protein	3.5E-05	0.00049	0.45
AceA	Isocitrate lyase	1.3E-05	0.00027	0.45
LsrB	Autoinducer 2-binding protein	2.6E-05	0.00042	0.45
RclA	Probable pyridine nucleotide-disulfide oxidoreductase	3.1E-05	0.00045	0.44
FadI	3-ketoacyl-CoA thiolase	1.2E-05	0.00027	0.44
SthA	Soluble pyridine nucleotide transhydrogenase	1.3E-05	0.00027	0.44

YahO	DUF1471 domain-containing protein	2.0E-05	0.00036	0.44
FumC	Fumarate hydratase class II	5.8E-05	0.00069	0.44
YcaC	Putative hydrolase	7.3E-05	0.00081	0.44
XylF	D-xylose-binding periplasmic protein	9.7E-05	0.00096	0.44
CatE	Catalase HPII	8.8E-05	0.0009	0.43
Amy2	Cytoplasmic alpha-amylase	3.5E-05	0.00049	0.42
GlcG	Putative heme-binding protein	2.3E-04	0.00178	0.42
ExbD	Biopolymer transport protein	4.0E-04	0.0027	0.42
YtfJ	Uncharacterized protein Y	1.3E-04	0.00114	0.42
YcaP	UPF0702 transmembrane protein	1.2E-03	0.00587	0.42
YigI	Putative thioesterase	2.0E-03	0.00877	0.42
YdcT	Uncharacterized ABC transporter ATP-binding protein	1.9E-05	0.00035	0.42
YedQ	Probable diguanylate cyclase	3.8E-04	0.00258	0.42
GlnH	Glutamine-binding periplasmic protein	3.0E-05	0.00045	0.42
LsrK	Autoinducer-2 kinase	4.5E-05	0.00057	0.42
MasZ	Malate synthase G	1.9E-05	0.00035	0.42
PrpD	2-methylcitrate dehydratase	6.2E-05	0.00073	0.41
GlcF	Glycolate oxidase iron-sulfur subunit	3.3E-04	0.00233	0.41
YfcG	Disulfide-bond oxidoreductase	1.5E-03	0.00712	0.40
MsrB	Peptide methionine sulfoxide reductase	1.7E-06	8.65E-05	0.40
GlxK2	Glycerate kinase	3.4E-05	0.00048	0.40
DgaL	D-galactose-binding periplasmic protein	5.6E-06	0.00018	0.39
FadB	Fatty acid oxidation complex subunit alpha	3.7E-05	0.0005	0.39
YeeD	UPF0033 protein	4.5E-05	0.00057	0.39
AldA	Lactaldehyde dehydrogenase	5.9E-06	0.00018	0.38
OsmY	Osmotically-inducible protein Y	2.4E-05	0.0004	0.38
GltI	Glutamate/aspartate periplasmic-binding protein	2.7E-06	0.00011	0.38
UbiC	Chorismate pyruvate-lyase	7.1E-05	0.0008	0.38
LivJ	Leu/Ile/Val-binding protein	2.8E-05	0.00044	0.38
YbjX	DUF535 domain-containing protein	7.0E-05	0.0008	0.38
Crl	Sigma factor-binding protein	1.1E-04	0.00103	0.38
AdhP	Alcohol dehydrogenase, propanol-preferring	1.9E-04	0.00158	0.38
PsiF	Phosphate starvation-inducible protein	8.6E-05	0.00089	0.37
DppF	Dipeptide transport ATP-binding protein	1.7E-05	0.00032	0.37
UgpQ	Glycerophosphoryl diester phosphodiesterase	2.0E-05	0.00036	0.37
YjcH	Inner membrane protein	1.2E-04	0.00112	0.37
DlhH	Putative carboxymethylenebutenolidase	3.3E-05	0.00048	0.37
DadA	D-amino acid dehydrogenase	1.6E-05	0.00031	0.37
PuuR	HTH-type transcriptional regulator	1.9E-04	0.00158	0.37
GabT	4-aminobutyrate aminotransferase	1.5E-05	0.00029	0.37
AbdH	Gamma-aminobutyraldehyde dehydrogenase	3.6E-06	0.00013	0.37
OppD	Oligopeptide transport ATP-binding protein	9.3E-06	0.00024	0.37
PaaF	2,3-dehydroadipyl-CoA hydratase	2.7E-05	0.00043	0.37
AroM	Protein	1.2E-05	0.00026	0.37
FadM	Long-chain acyl-CoA thioesterase	2.4E-03	0.01021	0.36
FeaB	Phenylacetaldehyde dehydrogenase	4.3E-05	0.00056	0.36

LsrR	Transcriptional regulator	3.9E-05	0.00052	0.36
YtfQ	ABC transporter periplasmic-binding protein	7.9E-06	0.00022	0.36
GlcC	Glc operon transcriptional activator	9.4E-04	0.00506	0.35
LivK	Leucine-specific-binding protein	3.0E-04	0.00214	0.35
PyrI	Aspartate carbamoyltransferase regulatory chain	3.1E-04	0.00221	0.34
YjgH	RutC family protein	8.8E-05	0.0009	0.34
MtlR	Mannitol operon repressor	2.2E-04	0.0017	0.34
CysI	Sulfite reductase [NADPH] hemoprotein beta-component	1.1E-05	0.00025	0.34
DppA	Periplasmic dipeptide transport protein	2.4E-06	0.00011	0.34
YejG	Uncharacterized protein	6.2E-05	0.00073	0.34
OppA	Periplasmic oligopeptide-binding protein	1.0E-05	0.00024	0.34
PrpB	2-methylisocitrate lyase	6.8E-04	0.004	0.33
YdaM	Probable diguanylate cyclase	9.9E-07	6.04E-05	0.33
BcsE	Protein BcsE homolog	2.1E-04	0.00162	0.33
YdcI	Uncharacterized HTH-type transcriptional regulator	2.4E-05	0.0004	0.33
AstB	N-succinylarginine dihydrolase	2.3E-05	0.00039	0.33
OppF	Oligopeptide transport ATP-binding protein	3.3E-05	0.00048	0.33
Ggt	Gamma-glutamyltranspeptidase	2.4E-04	0.00183	0.33
Cfa	Cyclopropane-fatty-acyl-phospholipid synthase	1.3E-04	0.00114	0.33
PyrB	Aspartate carbamoyltransferase catalytic chain	2.1E-04	0.00165	0.32
YebF	Protein	1.4E-06	8.18E-05	0.32
PdeH	Cyclic di-GMP phosphodiesterase	2.7E-06	0.00011	0.32
LcfA	Long-chain-fatty-acid--CoA ligase	5.6E-06	0.00018	0.32
AstD	N-succinylglutamate 5-semialdehyde dehydrogenase	2.1E-06	9.94E-05	0.31
MetA	Homoserine O-succinyltransferase	3.0E-04	0.00215	0.31
IscR	HTH-type transcriptional regulator	2.8E-07	2.30E-05	0.31
FadA	3-ketoacyl-CoA thiolase	1.0E-05	0.00024	0.31
UgpB	sn-glycerol-3-phosphate-binding periplasmic protein	1.1E-05	0.00025	0.31
ActP	Cation/acetate symporter	1.4E-05	0.00029	0.30
MasY	Malate synthase A	2.9E-06	0.00011	0.30
DmlR	HTH-type transcriptional regulator	1.9E-04	0.00155	0.30
PotF	Putrescine-binding periplasmic protein	6.0E-06	0.00018	0.30
AcsA	Acetyl-coenzyme A synthetase	2.1E-06	9.94E-05	0.30
PaaB	1,2-phenylacetyl-CoA epoxidase, subunit B	2.3E-03	0.00989	0.29
YdjN	L-cystine transporter	4.5E-05	0.00057	0.29
CysH	Phosphoadenosine phosphosulfate reductase	3.5E-06	0.00013	0.29
AmpH	D-alanyl-D-alanine-carboxypeptidase/endopeptidase	2.6E-04	0.00192	0.29
CysP	Thiosulfate-binding protein	1.2E-04	0.00114	0.29
AmiB	N-acetylmuramoyl-L-alanine amidase	8.1E-06	0.00022	0.29
AstA	Arginine N-succinyltransferase	9.1E-06	0.00024	0.28
PhoH	ATP-binding protein	1.8E-04	0.00151	0.28
HisP	Histidine transport ATP-binding protein	3.8E-06	0.00013	0.28

UgpC	sn-glycerol-3-phosphate import ATP-binding protein	1.1E-05	0.00024	0.28
PuuD	Gamma-glutamyl-gamma-aminobutyrate hydrolase	3.2E-05	0.00047	0.27
DdpA	Probable D,D-dipeptide-binding periplasmic protein	2.2E-06	0.0001	0.27
MhpR	Mhp operon transcriptional activator	7.5E-05	0.00082	0.26
PaaK	Phenylacetate-coenzyme A ligase	1.5E-06	8.31E-05	0.26
CsiD	Glutarate hydroxylase	3.6E-05	0.00049	0.26
CsiR	HTH-type transcriptional repressor CsiR	1.7E-05	0.00033	0.26
PaaJ	3-oxoadipyl-CoA/3-oxo-5,6-dehydrosuberyl-CoA thiolase	2.6E-05	0.00042	0.26
FliK	Flagellar hook-length control protein	8.0E-04	0.00449	0.26
RavA	ATPase	4.1E-03	0.01528	0.26
YdeJ	PF02464 family protein	2.1E-03	0.00911	0.26
CycA	D-serine/D-alanine/glycine transporter	8.2E-05	0.00087	0.25
YibI	DUF3302 domain-containing protein	5.0E-06	0.00017	0.25
PuuE	4-aminobutyrate aminotransferase PuuE	7.5E-05	0.00082	0.25
AstE	Succinylglutamate desuccinylase	2.7E-06	0.00011	0.25
DppC	Dipeptide transport system permease protein	4.6E-03	0.01667	0.24
YeaC	DUF1315 domain-containing protein	1.7E-06	8.65E-05	0.24
ArgT	Lysine/arginine/ornithine-binding periplasmic protein	2.7E-06	0.00011	0.24
PaaH	3-hydroxyadipyl-CoA dehydrogenase	1.3E-04	0.00117	0.24
AstC	Succinylornithine transaminase	2.6E-06	0.00011	0.23
PuuC	Aldehyde dehydrogenase	1.4E-05	0.00028	0.23
Pat	Putrescine aminotransferase	4.5E-05	0.00057	0.23
AceK	Isocitrate dehydrogenase kinase/phosphatase	1.8E-04	0.00152	0.21
CysN	Sulfate adenylyltransferase subunit 1	1.2E-05	0.00027	0.21
PotG	Putrescine transport ATP-binding protein	1.1E-05	0.00024	0.20
PrpC	2-methylcitrate synthase	7.1E-05	0.0008	0.20
OppB	Oligopeptide transport system permease protein	8.7E-05	0.00089	0.19
DdpX	D-alanyl-D-alanine dipeptidase	5.2E-07	3.66E-05	0.19
PrpE	Propionate--CoA ligase	5.0E-04	0.00316	0.18
YqeF	Probable acetyl-CoA acetyltransferase	2.8E-05	0.00044	0.16
PuuA	Gamma-glutamylputrescine synthetase	2.3E-05	0.00039	0.15
PuuP	Putrescine importer	8.5E-04	0.00473	0.14
FlgA	Flagella basal body P-ring formation protein	9.2E-05	0.00092	0.14
PaaZ	Oxepin-CoA hydrolase	2.9E-06	0.00011	0.14
LhgO	L-2-hydroxyglutarate oxidase	3.8E-04	0.00261	0.14
FlhD	Flagellar transcriptional regulator	2.6E-03	0.01063	0.13
PaaC	1,2-phenylacetyl-CoA epoxidase, subunit C	6.3E-05	0.00073	0.13
PlaP	Low-affinity putrescine importer	6.3E-08	9.34E-06	0.11
DusB	tRNA-dihydrouridine synthase B	5.1E-07	3.66E-05	0.11
PaaG	1,2-epoxyphenylacetyl-CoA isomerase	2.0E-06	9.85E-05	0.11
PuuB	Gamma-glutamylputrescine oxidoreductase	1.2E-04	0.00112	0.10
AriR	Probable two-component-system connector protein	9.7E-04	0.00517	0.09

CodB	Cytosine permease	1.3E-04	0.00115	0.08
PaaE	1,2-phenylacetyl-CoA epoxidase, subunit E	2.6E-05	0.00042	0.07
YqjA	Inner membrane protein	8.2E-05	0.00087	0.07
YmiA	Uncharacterized protein	5.7E-06	0.00018	0.06
KgtP	Alpha-ketoglutarate permease	3.1E-03	0.01233	0.06
FhuF	Ferric iron reductase protein	3.8E-05	0.00052	0.05
McbR	HTH-type transcriptional regulator	3.9E-06	0.00013	0.04
PaaI	Acyl-coenzyme A thioesterase	1.8E-06	8.96E-05	0.04

Table S3. Differences in Ag43 protein levels. Planktonic cells were harvested at OD_{600} 0.5. Attached cells were scrapped after 5 hours of static attachment.

	Wild-type attached vs wild-type planktonic			
Name	**Description**	**pValue**	**qValue**	**Fold change**
Ag43	Antigen 43	8.3E-02	1.7E-01	0.86
	***ΔmotA* attached vs *ΔmotA* planktonic**			
Ag43	Antigen 43	1.6E-03	7.7E-03	0.66
	***ΔmotA* planktonic vs wild-type planktonic**			
Ag43	Antigen 43	1.5E-08	3.3E-05	0.04
	***ΔmotA* attached vs wild-type attached**			
Ag43	Antigen 43	2.0E-09	4.4E-06	0.03
	***ΔfimA* planktonic vs wild-type planktonic**			
Ag43	Antigen 43	1.5E-08	3.2E-05	0.03
	***ΔmotAΔfimA* planktonic vs *ΔfimA* planktonic**			
Ag43	Antigen 43	8.0E-06	5.9E-04	25.48
	***ΔmotAΔfimA* planktonic vs *ΔfimA* planktonic**			
Ag43	Antigen 43	9.6E-06	4.1E-04	20.88

Table S4. Differences in flagellar protein levels. Planktonic cells were harvested at OD_{600} 0.5. Attached cells were scrapped after 5 hours of static attachment.

	Wild-type attached vs wild-type planktonic			
Name	**Description**	**pValue**	**qValue**	**Fold change**
FliD	Flagellar filament capping protein	0.000241	0.003071	5.34
FlgK	Flagellar hook-filament junction protein 1	0.000229	0.002979	4.64
FlgL	Flagellar hook-filament junction protein 2	0.000072	0.001526	3.66
FlhE	Flagellar protein	0.067516	0.142772	1.40
FliA	RNA polymerase sigma 28 factor	0.001842	0.012139	1.34
FliG	Flagellar motor switch protein	0.055408	0.125204	1.28
FlgC	Flagellar basal-body rod protein	0.949419	0.962915	1.24
FliP	Flagellar biosynthetic protein	0.047479	0.112665	1.22

FlgI	Flagellar P-ring protein	0.033766	0.088384	1.21
FlgM	Anti-sigma factor for FliA	0.147711	0.248639	1.20
FlhA	Flagellar biosynthesis protein	0.059176	0.130572	1.18
FlgH	Flagellar L-ring protein	0.049188	0.115597	1.16
FlgE	Flagellar hook protein	0.326222	0.443380	1.15
FliO	Flagellar biosynthesis protein	0.119754	0.212842	1.15
FliF	Flagellar M-ring protein	0.184744	0.294786	1.12
FliM	Flagellar motor switch protein	0.054257	0.123799	1.10
FliL	Flagellar protein	0.466368	0.578479	1.04
FliC	Flagellin	0.389450	0.508230	1.04
FliH	Flagellar assembly protein	0.824819	0.868751	1.04
FlgG	Flagellar basal-body rod protein	0.305710	0.421676	1.02
FlgF	Flagellar basal-body rod protein	0.536467	0.636924	1.02
FliN	Flagellar motor switch protein	0.898665	0.926959	1.02
FlhB	Flagellar biosynthetic protein	0.923980	0.943758	0.96
FliE	Flagellar hook-basal body complex protein	0.353961	0.472594	0.92
FlgN	Flagella synthesis protein	0.094137	0.181414	0.90
FliS	Flagellar biosynthesis protein	0.731387	0.797118	0.89
FlgB	Flagellar basal body rod protein	0.058047	0.128700	0.83
FliK	Flagellar hook-length control protein	0.149704	0.250143	0.81
MotA	Motility protein A	0.023073	0.067707	0.61
FlhD	Flagellar transcriptional regulator	0.173380	0.281695	0.48
MotB	Motility protein B	0.004391	0.021903	0.29
FlgA	Flagella basal body P-ring formation protein	0.000297	0.003483	0.18
	***ΔmotA* attached vs *ΔmotA* planktonic**			
Name	**Description**	**pValue**	**qValue**	**Fold change**
FlgK	Flagellar hook-filament junction protein 1	0.000212	0.001664	2.17
FliD	Flagellar filament capping protein	0.058232	0.109350	2.17
FlgL	Flagellar hook-filament junction protein 2	0.002890	0.011614	2.08
FlhE	Flagellar protein	0.005644	0.019594	1.43
FliO	Flagellar biosynthesis protein	0.002577	0.010647	1.39
FliG	Flagellar motor switch protein	0.003923	0.014791	1.33
FlhB	Flagellar biosynthetic protein	0.586061	0.667298	1.27
FliA	RNA polymerase sigma 28 factor	0.004918	0.017603	1.25
FlgI	Flagellar P-ring protein	0.019418	0.047744	1.20
FliF	Flagellar M-ring protein	0.166071	0.248136	1.19
FliH	Flagellar assembly protein	0.471549	0.564726	1.18
FlgH	Flagellar L-ring protein	0.031641	0.068395	1.18
FliP	Flagellar biosynthetic protein	0.052872	0.102113	1.17
FliM	Flagellar motor switch protein	0.085329	0.146717	1.16
FlhA	Flagellar biosynthesis protein	0.151856	0.230251	1.15
FliI	Flagellum-specific ATP synthase	0.084630	0.146088	1.12
FlgF	Flagellar basal-body rod protein	0.654246	0.725690	1.12

FliN	Flagellar motor switch protein	0.037477	0.077424	1.10
FlgG	Flagellar basal-body rod protein	0.604751	0.683226	1.06
FlgM	Anti-sigma factor for FliA	0.510442	0.601132	1.02
FliL	Flagellar protein	0.378581	0.474091	1.01
FliE	Flagellar hook-basal body complex protein	0.689280	0.754631	0.91
FlgC	Flagellar basal-body rod protein	0.125406	0.197047	0.87
FlgE	Flagellar hook protein	0.043959	0.087838	0.86
FliC	Flagellin	0.342218	0.438311	0.85
FlgN	Flagella synthesis protein	0.032790	0.070323	0.81
FlgB	Flagellar basal body rod protein	0.023114	0.054179	0.72
FliS	Flagellar biosynthesis protein	0.002862	0.011562	0.60
FliJ	Flagellar biosynthetic protein	0.011675	0.032756	0.26
FliK	Flagellar hook-length control protein	0.000801	0.004492	0.26
FlgA	Flagella basal body P-ring formation protein	0.000092	0.000922	0.14
FlhD	Flagellar transcriptional regulator	0.002567	0.010626	0.13
	Δ*motA* planktonic vs wild-type planktonic			
Name	**Description**	**pValue**	**qValue**	**Fold change**
FlgN	Flagella synthesis protein	0.901353	0.987900	2.38
FlhB	Flagellar biosynthetic protein	0.126914	0.728923	1.49
FlgA	Flagella basal body P-ring formation protein	0.002948	0.342016	1.48
FlgB	Flagellar basal body rod protein	0.063715	0.659895	1.44
FliD	Flagellar filament capping protein	0.508683	0.902563	1.42
FliP	Flagellar biosynthetic protein	0.182244	0.762017	1.28
FlgE	Flagellar hook protein	0.008733	0.469188	1.25
FliN	Flagellar motor switch protein	0.475857	0.883240	1.24
FlgC	Flagellar basal-body rod protein	0.008064	0.469188	1.23
FliS	Flagellar biosynthesis protein	0.040652	0.659895	1.21
FlhE	Flagellar protein	0.703439	0.945864	1.15
FliE	Flagellar hook-basal body complex protein	0.652646	0.945053	1.12
FliM	Flagellar motor switch protein	0.988448	0.996784	1.12
FlgH	Flagellar L-ring protein	0.042262	0.659895	1.11
FliL	Flagellar protein	0.861575	0.987900	1.09
FlgG	Flagellar basal-body rod protein	0.159313	0.739122	1.06
FliC	Flagellin	0.394724	0.856278	1.05
FliH	Flagellar assembly protein	0.344792	0.834835	1.04
FliI	Flagellum-specific ATP synthase	0.980213	0.993821	1.04
FlhD	Flagellar transcriptional regulator	0.024946	0.659895	1.04
FlhA	Flagellar biosynthesis protein	0.250246	0.784651	1.04
FlgL	Flagellar hook-filament junction protein 2	0.794283	0.979278	1.03
FlgI	Flagellar P-ring protein	0.161925	0.739122	1.01
FliG	Flagellar motor switch protein	0.436722	0.869548	1.00
FliO	Flagellar biosynthesis protein	0.541269	0.913116	0.99
FliJ	Flagellar biosynthetic protein	0.596272	0.926222	0.98
FliF	Flagellar M-ring protein	0.901622	0.987900	0.98

FlgM	Anti-sigma factor for FliA	0.062529	0.659895	0.96
FlgF	Flagellar basal-body rod protein	0.008421	0.469188	0.95
FlgK	Flagellar hook-filament junction protein 1	0.227147	0.777334	0.89
FliK	Flagellar hook-length control protein	0.017473	0.600420	0.87
	***ΔmotA* attached vs wild-type attached**			
Name	**Description**	**pValue**	**qValue**	**Fold change**
FlhB	Flagellar biosynthetic protein	0.045376	0.242881	1.51
FlgF	Flagellar basal-body rod protein	0.167127	0.454963	1.37
FlgA	Flagella basal body P-ring formation protein	0.835500	0.933060	1.35
FliI	Flagellum-specific ATP synthase	0.003050	0.060861	1.27
FliH	Flagellar assembly protein	0.714309	0.873487	1.16
FliE	Flagellar hook-basal body complex protein	0.096552	0.352729	1.16
FlgH	Flagellar L-ring protein	0.162211	0.449030	1.13
FlgM	Anti-sigma factor for FliA	0.623640	0.827251	1.13
FlgI	Flagellar P-ring protein	0.252214	0.548447	1.12
FlgG	Flagellar basal-body rod protein	0.396326	0.679716	1.10
FlgB	Flagellar basal body rod protein	0.254103	0.550462	1.06
FliN	Flagellar motor switch protein	0.146906	0.425396	1.05
FliP	Flagellar biosynthetic protein	0.232001	0.523911	1.05
FliO	Flagellar biosynthesis protein	0.463616	0.733697	1.05
FliF	Flagellar M-ring protein	0.925594	0.971166	1.05
FliG	Flagellar motor switch protein	0.250064	0.546077	1.04
FliM	Flagellar motor switch protein	0.999937	0.999937	1.01
FlhA	Flagellar biosynthesis protein	0.516412	0.771533	1.01
FliS	Flagellar biosynthesis protein	0.790761	0.909231	1.00
FlgC	Flagellar basal-body rod protein	0.705847	0.868762	0.99
FliL	Flagellar protein	0.294745	0.587082	0.96
FlgN	Flagella synthesis protein	0.891388	0.959116	0.94
FlhE	Flagellar protein	0.588387	0.812418	0.93
FlgE	Flagellar hook protein	0.700561	0.867587	0.93
FliC	Flagellin	0.543432	0.789956	0.85
FliK	Flagellar hook-length control protein	0.089711	0.341867	0.78
FlgL	Flagellar hook-filament junction protein 2	0.019575	0.159732	0.59
FliJ	Flagellar biosynthetic protein	0.005582	0.088149	0.51
FlgK	Flagellar hook-filament junction protein 1	0.006037	0.089681	0.42
FlhD	Flagellar transcriptional regulator	0.098424	0.357092	0.40
FliD	Flagellar filament capping protein	0.006924	0.092672	0.39
	***ΔfimA* vs wild-type planktonic**			
Name	**Description**	**pValue**	**qValue**	**Fold change**
FlhD	Flagellar transcriptional regulator	0.013308	0.145788	1.98
FliD	Flagellar filament capping protein	0.007683	0.129229	1.97
FliJ	Flagellar biosynthetic protein	0.065123	0.308471	1.93
FliK	Flagellar hook-length control protein	0.009014	0.131727	1.93

FlgC	Flagellar basal-body rod protein	0.000183	0.030077	1.63
FlgK	Flagellar hook-filament junction protein 1	0.002409	0.076496	1.62
FliS	Flagellar biosynthesis protein	0.233862	0.546842	1.46
FlgI	Flagellar P-ring protein	0.006185	0.115252	1.42
FlhE	Flagellar protein	0.394438	0.675696	1.42
FlgE	Flagellar hook protein	0.000828	0.049318	1.39
FlgL	Flagellar hook-filament junction protein 2	0.004820	0.107382	1.32
FlgB	Flagellar basal body rod protein	0.001933	0.069877	1.32
FliC	Flagellin	0.129850	0.420532	1.32
FlhB	Flagellar biosynthetic protein	0.001308	0.056186	1.30
FlgA	Flagella basal body P-ring formation protein	0.012702	0.143457	1.24
FlgM	Anti-sigma factor for FliA	0.010574	0.137589	1.23
FliE	Flagellar hook-basal body complex protein	0.083147	0.347172	1.18
FlgF	Flagellar basal-body rod protein	0.020422	0.189643	1.16
FlgN	Flagella synthesis protein	0.142517	0.439118	1.14
FlhA	Flagellar biosynthesis protein	0.071894	0.318338	1.13
FliL	Flagellar protein	0.063335	0.304984	1.13
FlgH	Flagellar L-ring protein	0.027928	0.222195	1.12
FlgG	Flagellar basal-body rod protein	0.110864	0.391278	1.10
MotB	Motility protein B	0.478612	0.732289	1.08
FliP	Flagellar biosynthetic protein	0.532802	0.770510	1.08
FliH	Flagellar assembly protein	0.570944	0.792737	1.07
FliI	Flagellum-specific ATP synthase	0.769486	0.891632	1.06
FliG	Flagellar motor switch protein	0.266921	0.577649	1.00
FliF	Flagellar M-ring protein	0.914278	0.958766	1.00
FliN	Flagellar motor switch protein	0.313703	0.618652	0.97
FliO	Flagellar biosynthesis protein	0.842392	0.927944	0.95
MotA	Motility protein A	0.822381	0.915044	0.91
FliM	Flagellar motor switch protein	0.163496	0.463476	0.87
	***ΔmotAΔfimA* vs *ΔfimA* planktonic**			
Name	**Description**	**pValue**	**qValue**	**Fold change**
FliS	Flagellar biosynthesis protein	0.079247	0.154616	2.25
FlgA	Flagella basal body P-ring formation protein	0.000924	0.008627	2.03
FlhA	Flagellar biosynthesis protein	0.000509	0.005783	1.50
FliI	Flagellum-specific ATP synthase	0.001692	0.011817	1.50
FlgN	Flagella synthesis protein	0.000933	0.008667	1.46
FliG	Flagellar motor switch protein	0.040596	0.095625	1.42
FliH	Flagellar assembly protein	0.002842	0.016404	1.42
FlhB	Flagellar biosynthetic protein	0.017088	0.051563	1.39
FliM	Flagellar motor switch protein	0.000653	0.006953	1.39
FlgI	Flagellar P-ring protein	0.014881	0.047107	1.33
FlgG	Flagellar basal-body rod protein	0.001264	0.010241	1.29
FliP	Flagellar biosynthetic protein	0.009693	0.035471	1.29
FliN	Flagellar motor switch protein	0.004824	0.023083	1.29

FliL	Flagellar protein	0.017230	0.051691	1.29
FliF	Flagellar M-ring protein	0.013837	0.044823	1.28
FliO	Flagellar biosynthesis protein	0.342021	0.469369	1.24
FliJ	Flagellar biosynthetic protein	0.171117	0.276944	1.21
FlgM	Anti-sigma factor for FliA	0.053378	0.115329	1.17
FlgH	Flagellar L-ring protein	0.061098	0.127607	1.15
FlgL	Flagellar hook-filament junction protein 2	0.640181	0.738327	1.12
FlgE	Flagellar hook protein	0.050979	0.112473	1.12
FliK	Flagellar hook-length control protein	0.640853	0.738513	1.09
FliE	Flagellar hook-basal body complex protein	0.948400	0.970401	1.03
FliD	Flagellar filament capping protein	0.648384	0.743675	1.03
FlhE	Flagellar protein	0.417173	0.541337	1.03
FlgF	Flagellar basal-body rod protein	0.562795	0.672228	1.00
FlhD	Flagellar transcriptional regulator	0.844544	0.894295	0.93
FliC	Flagellin	0.035049	0.085879	0.89
FlgK	Flagellar hook-filament junction protein 1	0.017094	0.051563	0.75
FlgB	Flagellar basal body rod protein	0.006856	0.028372	0.66
FlgC	Flagellar basal-body rod protein	0.001380	0.010620	0.65
	***ΔmotAΔfimA* vs *ΔmotA* planktonic**			
Name	**Description**	**pValue**	**qValue**	**Fold change**
FliS	Flagellar biosynthesis protein	0.135640	0.213668	2.17
FliD	Flagellar filament capping protein	0.238480	0.331332	2.09
FliJ	Flagellar biosynthetic protein	0.131552	0.208259	1.99
FlgI	Flagellar P-ring protein	0.000037	0.000722	1.67
FlgA	Flagella basal body P-ring formation protein	0.007311	0.023558	1.66
FlhA	Flagellar biosynthesis protein	0.000695	0.004689	1.64
FlhE	Flagellar protein	0.002307	0.010487	1.61
FlhB	Flagellar biosynthetic protein	0.031593	0.069151	1.61
FlgN	Flagella synthesis protein	0.000655	0.004516	1.58
FliI	Flagellum-specific ATP synthase	0.002162	0.009993	1.53
FliH	Flagellar assembly protein	0.002151	0.009993	1.50
FliL	Flagellar protein	0.000123	0.001595	1.45
FlgL	Flagellar hook-filament junction protein 2	0.033963	0.072924	1.40
FliG	Flagellar motor switch protein	0.000462	0.003724	1.38
FlgK	Flagellar hook-filament junction protein 1	0.068789	0.127099	1.37
FliO	Flagellar biosynthesis protein	0.121718	0.195373	1.35
FlgG	Flagellar basal-body rod protein	0.009640	0.029051	1.33
FlhD	Flagellar transcriptional regulator	0.315490	0.411696	1.29
FliF	Flagellar M-ring protein	0.020168	0.049818	1.29
FliN	Flagellar motor switch protein	0.001005	0.005966	1.28
FliP	Flagellar biosynthetic protein	0.016806	0.043986	1.27
FliM	Flagellar motor switch protein	0.009830	0.029424	1.25
FlgE	Flagellar hook protein	0.008729	0.026974	1.24
FlgH	Flagellar L-ring protein	0.012269	0.034687	1.15

FlgM	Anti-sigma factor for FliA	0.085241	0.148934	1.11
FliC	Flagellin	0.184282	0.271164	1.09
FliE	Flagellar hook-basal body complex protein	0.230333	0.322672	1.06
FlgF	Flagellar basal-body rod protein	0.728734	0.790033	0.92
FliK	Flagellar hook-length control protein	0.994328	0.994782	0.87
FlgC	Flagellar basal-body rod protein	0.019251	0.048315	0.75
FlgB	Flagellar basal body rod protein	0.051816	0.102370	0.71

Table S5. Differences in chemotaxis protein levels. Planktonic cells were harvested at OD_{600} 0.5. Attached cells were scrapped after 5 hours of static attachment.

	Wild-type attached vs wild-type planktonic			
Name	**Description**	**pValue**	**qValue**	**Fold change**
CheR	Chemotaxis protein methyltransferase	0.349332	0.468209	0.93
CheW	Chemotaxis adaptor protein	0.005151	0.024474	0.78
CheZ	Protein phosphatase	0.253145	0.371643	0.76
CheY	Chemotaxis response regulator	0.018400	0.058450	0.71
CheB	Chemotaxis response regulator protein-glutamate methylesterase	0.000943	0.007516	0.71
CheA	Chemotaxis kinase-phosphotransferase	0.000165	0.002435	0.61
	***ΔmotA* attached vs *ΔmotA* planktonic**			
Name	**Description**	**pValue**	**qValue**	**Fold change**
CheY	Chemotaxis response regulator	0.914745	0.936515	1.13
CheR	Chemotaxis protein methyltransferase	0.724948	0.785681	1.03
CheZ	Protein phosphatase	0.812676	0.855572	0.85
CheB	Chemotaxis response regulator protein-glutamate methylesterase	0.035825	0.074895	0.85
CheW	Chemotaxis adaptor protein	0.076755	0.135261	0.84
CheA	Chemotaxis kinase-phosphotransferase	0.000089	0.000902	0.64
	***ΔmotA* planktonic vs wild-type planktonic**			
Name	**Description**	**pValue**	**qValue**	**Fold change**
CheB	Chemotaxis response regulator protein-glutamate methylesterase	0.162756	0.739831	0.93
CheR	Chemotaxis protein methyltransferase	0.150369	0.728923	0.88
CheW	Chemotaxis adaptor protein	0.027989	0.659895	0.87
CheZ	Protein phosphatase	0.357704	0.843180	0.86
CheY	Chemotaxis response regulator	0.359991	0.845381	0.79
CheA	Chemotaxis kinase-phosphotransferase	0.002157	0.318650	0.77
	***ΔmotA* attached vs wild-type attached**			
Name	**Description**	**pValue**	**qValue**	**Fold change**
CheY	Chemotaxis response regulator	0.073475	0.312554	1.27

CheB	Chemotaxis response regulator protein-glutamate methylesterase	0.121098	0.389749	1.13
CheR	Chemotaxis protein methyltransferase	0.963546	0.983322	0.97
CheZ	Protein phosphatase	0.942361	0.975699	0.96
CheW	Chemotaxis adaptor protein	0.905858	0.961953	0.95
CheA	Chemotaxis kinase-phosphotransferase	0.029358	0.195646	0.81
	***ΔfimA* planktonic vs wild-type planktonic**			
Name	**Description**	**pValue**	**qValue**	**Fold change**
CheY	Chemotaxis response regulator	0.760358	0.889928	1.14
CheW	Chemotaxis adaptor protein	0.536053	0.772692	1.06
CheR	Chemotaxis protein methyltransferase	0.968877	0.983626	0.99
CheA	Chemotaxis kinase-phosphotransferase	0.939664	0.969721	0.97
CheB	Chemotaxis response regulator protein-glutamate methylesterase	0.289979	0.597690	0.89
CheZ	Protein phosphatase	0.656915	0.841205	0.89
	***ΔmotAΔfimA* vs *ΔfimA* planktonic**			
Name	**Description**	**pValue**	**qValue**	**Fold change**
CheB	Chemotaxis response regulator protein-glutamate methylesterase	0.084459	0.161764	1.20
CheZ	Protein phosphatase	0.017326	0.051907	1.16
CheR	Chemotaxis protein methyltransferase	0.138790	0.234332	1.14
CheY	Chemotaxis response regulator	0.588182	0.694980	0.97
CheA	Chemotaxis kinase-phosphotransferase	0.113860	0.203832	0.93
CheW	Chemotaxis adaptor protein	0.074207	0.146214	0.86
	***ΔmotAΔfimA* vs *ΔmotA* planktonic**			
Name	**Description**	**pValue**	**qValue**	**Fold change**
CheY	Chemotaxis response regulator	0.220247	0.313812	1.40
CheR	Chemotaxis protein methyltransferase	0.037077	0.078186	1.26
CheZ	Protein phosphatase	0.030680	0.067830	1.17
CheA	Chemotaxis kinase-phosphotransferase	0.041618	0.085875	1.16
CheB	Chemotaxis response regulator protein-glutamate methylesterase	0.066182	0.123724	1.14
CheW	Chemotaxis adaptor protein	0.149009	0.230239	1.05

Table S6. Differences in c-di-GMP phosphodiesterases and diguanylate cyclases protein levels. Planktonic cells were harvested at OD_{600} 0.5. Attached cells were scrapped after 5 hours of static attachment.

	Wild-type attached vs wild-type planktonic			
Phosphodiesterases				
Name	**Description**	**pValue**	**qValue**	**Fold change**
PdeH	Cyclic di-GMP phosphodiesterase	2.3E-05	8.8E-04	0.49
PdeB	Putative cyclic-di-GMP phosphodiesterase	5.6E-02	1.3E-01	0.21
PdeR	Cyclic-di-GMP phosphodiesterase	8.3E-03	3.4E-02	0.13
Diguanylate cyclases				
Name	**Description**	**pValue**	**qValue**	**Fold change**
DgcJ	Putative diguanylate cyclase	0.007290	0.030633	1.35
DgcE	Diguanylate cyclase	0.008937	0.035344	0.79
YcgR	Flagellar brake protein	0.003546	0.018665	0.76
DosC	Diguanylate cyclase	0.014820	0.050201	0.73
DgcM	Diguanylate cyclase	0.001507	0.010634	0.54
DgcQ	Putative diguanylate cyclase	0.018389	0.058450	0.37
	***ΔmotA* attached vs *ΔmotA* planktonic**			
Phosphodiesterases				
Name	**Description**	**pValue**	**qValue**	**Fold change**
PdeB	Putative cyclic-di-GMP phosphodiesterase	0.478712	0.571744	1.44
PdeH	Cyclic di-GMP phosphodiesterase	0.000003	0.000110	0.32
PdeR	Cyclic-di-GMP phosphodiesterase	0.232301	0.322034	0.24
Diguanylate cyclases				
Name	**Description**	**pValue**	**qValue**	**Fold change**
DgcJ	Putative diguanylate cyclase	0.131426	0.204358	1.33
DgcE	Diguanylate cyclase	0.003954	0.014870	0.75
DosC	Diguanylate cyclase	0.002243	0.009670	0.59
YcgR	Flagellar brake protein	0.000057	0.000680	0.57
DgcQ	Putative diguanylate cyclase	0.000379	0.002584	0.42
DgcM	Diguanylate cyclase	0.000001	0.000060	0.33
	***ΔmotA* planktonic vs wild-type planktonic**			
Phosphodiesterases				
Name	**Description**	**pValue**	**qValue**	**Fold change**
PdeR	Cyclic-di-GMP phosphodiesterase	0.630760	0.934709	1.65
PdeH	Cyclic di-GMP phosphodiesterase	0.314580	0.825312	0.87
PdeB	Putative cyclic-di-GMP phosphodiesterase	0.088874	0.690503	0.64

Diguanylate cyclases				
Name	Description	pValue	qValue	Fold change
DgcM	Diguanylate cyclase	0.088741	0.690503	1.11
DosC	Diguanylate cyclase	0.398114	0.858973	1.05
DgcJ	Putative diguanylate cyclase	0.279157	0.799289	1.03
YcgR	Flagellar brake protein	0.901015	0.987900	1.03
DgcE	Diguanylate cyclase	0.434875	0.869548	1.01
DgcQ	Putative diguanylate cyclase	0.914167	0.987900	0.85
	***ΔmotA* attached vs wild-type attached**			
Phosphodiesterases				
Name	**Description**	**pValue**	**qValue**	**Fold change**
PdeB	Putative cyclic-di-GMP phosphodiesterase	0.124718	0.393193	5.28
PdeR	Cyclic-di-GMP phosphodiesterase	0.103738	0.364107	4.01
PdeH	Cyclic di-GMP phosphodiesterase	0.000213	0.016247	0.57
Diguanylate cyclases				
Name	**Description**	**pValue**	**qValue**	**Fold change**
DgcJ	Putative diguanylate cyclase	0.956730	0.982192	1.02
DgcQ	Putative diguanylate cyclase	0.873208	0.946847	1.00
DgcE	Diguanylate cyclase	0.682259	0.856237	0.97
DosC	Diguanylate cyclase	0.149075	0.429422	0.84
YcgR	Flagellar brake protein	0.018300	0.155690	0.76
DgcM	Diguanylate cyclase	0.007516	0.096829	0.67
	***ΔfimA* vs wild-type planktonic**			
Phosphodiesterases				
Name	**Description**	**pValue**	**qValue**	**Fold change**
PdeH	Cyclic di-GMP phosphodiesterase	0.003225	0.088332	1.24
PdeB	Putative cyclic-di-GMP phosphodiesterase	0.643728	0.836541	0.94
PdeR	Cyclic-di-GMP phosphodiesterase	0.123114	0.409944	0.86
Diguanylate cyclases				
Name	**Description**	**pValue**	**qValue**	**Fold change**
DgcJ	Putative diguanylate cyclase	0.007940	0.129229	1.50
YcgR	Flagellar brake protein	0.879828	0.940802	1.01
DgcE	Diguanylate cyclase	0.659819	0.843937	0.98
DgcQ	Putative diguanylate cyclase	0.376288	0.664341	0.82
DosC	Diguanylate cyclase	0.046731	0.273763	0.81
DgcM	Diguanylate cyclase	0.079858	0.337126	0.76
	***ΔmotAΔfimA* vs *ΔfimA* planktonic**			
Phosphodiesterases				

Name	Description	pValue	qValue	Fold change
PdeH	Cyclic di-GMP phosphodiesterase	0.003241	0.017704	1.28
PdeR	Cyclic-di-GMP phosphodiesterase	0.558327	0.669077	0.73
PdeB	Putative cyclic-di-GMP phosphodiesterase	0.000232	0.003603	0.33
Diguanylate cyclases				
Name	**Description**	**pValue**	**qValue**	**Fold change**
YcgR	Flagellar brake protein	0.039747	0.094540	1.22
DgcJ	Putative diguanylate cyclase	0.723260	0.801591	0.87
DosC	Diguanylate cyclase	0.000499	0.005783	0.70
DgcM	Diguanylate cyclase	0.004994	0.023356	0.66
DgcE	Diguanylate cyclase	0.000072	0.001978	0.50
DgcQ	Putative diguanylate cyclase	0.004672	0.022643	0.46
	***ΔmotAΔfimA* vs *ΔmotA* planktonic**			
Phosphodiesterases				
Name	**Description**	**pValue**	**qValue**	**Fold change**
PdeH	Cyclic di-GMP phosphodiesterase	0.000194	0.002187	1.77
PdeB	Putative cyclic-di-GMP phosphodiesterase	0.013694	0.037645	0.51
PdeR	Cyclic-di-GMP phosphodiesterase	0.778142	0.830447	0.37
Diguanylate cyclases				
Name	**Description**	**pValue**	**qValue**	**Fold change**
DgcJ	Putative diguanylate cyclase	0.483075	0.572737	1.27
YcgR	Flagellar brake protein	0.024006	0.056495	1.16
DosC	Diguanylate cyclase	0.000190	0.002161	0.53
DgcE	Diguanylate cyclase	0.000080	0.001169	0.48
DgcM	Diguanylate cyclase	0.000003	0.000247	0.46
DgcQ	Putative diguanylate cyclase	0.001698	0.008715	0.44

Table S7. Differences in curli protein levels. Planktonic cells were harvested at OD_{600} 0.5. Attached cells were scrapped after 5 hours of static attachment.

	Wild-type attached vs wild-type planktonic			
Name	**Description**	**pValue**	**qValue**	**Fold change**
CsgA	Major curlin subunit	0.104361	0.194790	78.03
CsgD	Curli transcriptional regulator	0.888929	0.918211	1.44
CsgG	Curli secretion channel	0.409690	0.526504	1.16
CsgF	Curli assambly component	0.215840	0.330614	0.77
	***ΔmotA* attached vs *ΔmotA* planktonic**			
Name	**Description**	**pValue**	**qValue**	**Fold change**

CsgG	Curli secretion channel	0.011378	0.032256	0.68
CsgF	Curli assambly component	0.056592	0.10713	0.34
CsgD	Curli transcriptional regulator	0.025286	0.058092	0.20
	***ΔmotA* planktonic vs wild-type planktonic**			
Name	**Description**	**pValue**	**qValue**	**Fold change**
CsgA	Major curlin subunit	0.269317	0.799289	1.00
CsgD	Curli transcriptional regulator	0.005763	0.420865	0.69
CsgG	Curli secretion channel	3.13E-05	0.013731	0.20
CsgF	Curli assambly component	0.001192	0.290244	0.17
	***ΔmotA* attached vs wild-type attached**			
Name	**Description**	**pValue**	**qValue**	**Fold change**
CsgG	Curli secretion channel	4.62E-05	0.008442	0.10
CsgD	Curli transcriptional regulator	0.045973	0.243161	0.09
CsgF	Curli assambly component	0.000919	0.032912	0.06
CsgA	Major curlin subunit	0.058497	0.280585	0.01
	***ΔfimA* vs wild-type planktonic**			
Name	**Description**	**pValue**	**qValue**	**Fold change**
CsgA	Major curlin subunit	0.092887	0.359566	3.61
CsgF	Curli assambly component	0.663052	0.846096	1.59
CsgG	Curli secretion channel	0.386897	0.669754	1.12
CsgD	Curli transcriptional regulator	0.400632	0.680312	0.56
	***ΔmotAΔfimA* vs *ΔfimA* planktonic**			
Name	**Description**	**pValue**	**qValue**	**Fold change**
CsgF	Curli assambly component	0.010784	0.037747	0.19
CsgA	Major curlin subunit	0.003105	0.017284	0.16
CsgD	Curli transcriptional regulator	0.000233	0.003603	0.14
CsgG	Curli secretion channel	2.75E-05	0.001119	0.06
	***ΔmotAΔfimA* vs *ΔmotA* planktonic**			
Name	**Description**	**pValue**	**qValue**	**Fold change**
CsgF	Curli assambly component	0.13985	0.219015	2.01
CsgG	Curli secretion channel	0.009366	0.028462	0.46
CsgD	Curli transcriptional regulator	1.26E-06	0.000243	0.12

Table S8. Differences in type 1 fimbriae protein levels. Planktonic cells were harvested at OD_{600} 0.5. Attached cells were scrapped after 5 hours of static attachment.

	Wild-type attached vs wild-type planktonic			
Name	**Description**	**pValue**	**qValue**	**Fold change**
FimG	Type 1 fimbriae minor subunit	0.000169	0.002435	30.48
FimH	Type 1 fimbriae D-mannose specific adhesin	0.077477	0.157318	28.27
FimC	Chaperone protein	0.000000	0.000088	16.26
	***ΔmotA* attached vs *ΔmotA* planktonic**			
Name	**Description**	**pValue**	**qValue**	**Fold change**
FimC	Chaperone protein	0.817622	0.859129	1.05
FimG	Type 1 fimbriae minor subunit	0.230268	0.320157	0.74
FimH	Type 1 fimbriae D-mannose specific adhesin	0.366482	0.461838	0.46
	***ΔmotA* planktonic vs wild-type planktonic**			
Name	**Description**	**pValue**	**qValue**	**Fold change**
FimH	Type 1 fimbriae D-mannose specific adhesin	0.186515	0.764334	2.99
FimG	Type 1 fimbriae minor subunit	0.073459	0.665076	2.00
FimC	Chaperone protein	0.000215	0.067201	1.71
	***ΔmotA* attached vs wild-type attached**			
Name	**Description**	**pValue**	**qValue**	**Fold change**
FimC	Chaperone protein	0.000003	0.002334	0.11
FimG	Type 1 fimbriae minor subunit	0.000065	0.009644	0.04
FimH	Type 1 fimbriae D-mannose specific adhesin	0.120394	0.389197	0.04

Table S9. Chemicals used in this work

Chemicals	Company
4-Methylumbelliferyl α-D-mannopyranoside	Sigma-Aldrich
1 Kb Plus DNA Ladder	Inviitrogen
Agar bacteriology	Applichem
Agarose ultra-pure	Biozym,
Albumin Fraktion V (BSA)	Carl Roth
Ampicillin	Applichem
L-(+)-Arabinose	Roth
BactoTM Tryptone	BD Biosciences
BactoTM Yeast extract	BD Biosciences
$CaCl_2$ x 2 H_2O	Carl Roth
Chloramphenicol	Applichem
EDTA	Merck
Ethanol	Applichem
D-Glucose	Applichem
Glycerol	GERBU Biotechnik
HEPES	Sigma-Aldrich
Isopropyl-β-D-thiogalactoside (IPTG)	Carl Roth
Kanamycin sulphate	Sigma-Aldrich
L-Serine	Acros Organics
Lithium acetate	Sigma-Aldrich
Magnesium sulfate ($MgSO_4$)	Sigma-Aldrich
Manganese (II) chloride ($MnCl_2$)	Sigma-Aldrich
α-Methyl-DL-aspartate (MeAsp)	Sigma-Aldrich
Potassium phosphate dibasic (K_2HPO_4)	Sigma-Aldrich
Potassium chloride (KCl)	Sigma-Aldrich
Potassium phosphate monobasic (KH_2PO_4)	Sigma-Aldrich
2-Propanol	Carl Roth
Sodium chloride (NaCl)	Carl Roth
Yeast Extract	Applichem

Table S10. Strains used in this work

Strains	Relevant genotype	Source
W3110 *rpoS*$^-$	Wild-type W3110, *rpoS*$^-$(Am)	(Hayashi *et al.*, 2006)
VM35	W3110 *rpoS*$^-$ *ΔfliC*	This work
VM114	W3110 *rpoS*$^-$ *ΔcheZ*	This work
VM321	W3110 *rpoS*$^-$ *ΔmotA*	This work
VM270	W3110 *rpoS*$^-$ *ΔcheA*	This work
VM108	W3110 *rpoS*$^-$ *ΔcheY*	This work
VM28	W3110 *rpoS*$^-$ *ΔdgcE*	This work
VM38	W3110 *rpoS*$^-$ *ΔpdeH*	This work
VM194	W3110 *rpoS*$^-$ *ΔycgR::* Kan^R	This work
ME21	W3110 *rpoS*$^-$ *ΔycgR*	This work
VM196	W3110 *rpoS*$^-$ *ΔdgcEΔycgR::* Kan^R	This work
VM198	W3110 *rpoS*$^-$ *ΔpdeHΔycgR::* Kan^R	This work
VM274	W3110 *rpoS*$^-$ *ΔdgcZ*	This work
VM314	W3110 *rpoS*$^-$ *ΔdgcM*	This work
VM125	W3110 *rpoS*$^-$ *ΔcsgA*	This work
OB475	W3110 *rpoS*$^-$ *ΔfimA*	This work
OB477	W3110 *rpoS*$^-$ *ΔfimAΔycgR*	This work
ME120	W3110 *rpoS*$^-$ *ΔcheYΔfliC::*Kan^R	This work
ME124	W3110 *rpoS*$^-$ *ΔcheYΔfimA::*Kan^R	This work
ME147	W3110 *rpoS*$^-$ *ΔcheYΔfimA*	This work
ME119	W3110 *rpoS*$^-$ *ΔcheYΔycgR::*Kan^R	This work
ME151	W3110 *rpoS*$^-$ *ΔcheYΔycgR*	This work
W3110 *rpoS*$^+$	W3110 derivative *rpoS*+	(Serra *et al.*, 2013)
ME69	W3110 *rpoS*+ *ΔfimA*	This work
VM335	W3110 *rpoS*+ *ΔfliC*	From V. Suchanek
ME103	W3110 *rpoS*+ *ΔcsgA*	This work
ME52	W3110 *rpoS*+ *ΔfimH*	This work
ME17	W3110 *rpoS*+ *ΔfliCΔfimA::KanR*	This work
ME149	W3110 *rpoS*+ *ΔfliCΔfimA*	This work
ME48	W3110 *rpoS*+ *ΔfimAΔcsgA::*Kan^R	This work
ME150	W3110 *rpoS*+ *ΔfimAΔcsgA*	This work
ME112	W3110 *rpoS*+ *ΔmotAΔfimA*	This work

Table S11. Plasmids used in this work

Plasmid	Resistance	Induction	Description	Source
pTrc99a	Amp^R	IPTG	Expression vector; *trc* promotor.	(Amann *et al.*, 1988)
pVS147 (pTrc99a-yfp)	Amp^R	IPTG	*eyfp* A206K	(Earhart, 2000)
pVS130 pTrc99a-cfp)	Amp^R	IPTG	*ecfp* A206K	(Earhart, 2000)
pVM42 (pTrc99a- gfp)	Amp^R	IPTG	*egfp* A206K	(Besharova *et al.*, 2016)
pOB2 (pTrc99a-mch)	Amp^R	IPTG	mcherry	(Besharova *et al.*, 2016)
pTrc99a-fliC	Amp^R	ITPG	*fliC* under the control of *trc* promoter	Received from B. Ni
pTrc99a-fliA	Amp^R	ITPG	*fliA* under the control of *trc* promoter	Received from B. Ni
pTrc99a-flhDC	Amp^R	ITPG	*flhDC* under the control of *trc* promoter	Received from B. Ni
pCP20	Cm^R, Amp^R		*FLP recombinase*	(Cherepanov & Wackernagel, 1995)
pME7 (pBAD-*fimA*)	Amp^R	IPTG	*fimA* under control pBAD promoter	This study
pBAD33	Amp^R	IPTG	Expression vector; pACYC184 ori,	V. Sourjik collection
pOSK237 (pBAD-mch)	Kan^R	Arabinose	*lacI, araC*, pBAD promotor, *mCherry*	Received from O. Schauer
pOSK239 (pBad-gfp)	Kan^R	Arabinose	*lacI, araC*, pBAD promotor, *gfp*	(Schauer *et al.*, 2018)
pUA66-*fimD*	Kan^R		*gfpmut2* under control of fimD promoter	(Zaslaver *et al.*, 2006)
pUA66-*fliC*	Amp^R		*gfpmut2* under control of fliC promoter	(Zaslaver *et al.*, 2006)

Table S12. Primers used in this work

Primers	Target	Nucleotide Sequence (5'-3')
ME1	fimA_XbaI_fwd	CAATCTAGAAAAACTGTGCAGTGTTGGC
ME2	fimA_HindIII_rev	GTTAAGCTTTTATTGATACTGAACCTTGAA
ME3	egfp-139-rev	ACTTCAGGGTCAGCTTG
VM8	pUA66_gfp_rev	CAAACTAGCAACACCAGAAC
VM84	ycgR_fw_check_ko	GTTAACTGTGACCGATAAACC
VM85	ycgR_rev_check_ko	GATGCTGACGAGTTCCTCGA
VM103	csgA_fw_check_ko	GAGAGAGGTTGTTGCGCAAGAAGGTAG
VM104	csgA_rev_check_ko	GAGAGACAAAGCAATGGGTTGATTAGCAG
VM109	fliC_fw_check_ko	GAGAGAGACCCGACTCCCAGCGATG
VM110	fliC_rev_check_ko	GAGAGAGAGTTATCGGCATGATTATCC
OB315	fimA_fw_check_ko	AAAAAGAGAA GAGGTTTGATTTAACT
OB316	fimA_rev_check_ko	TGCCAGCAAGCAGAATGTTATTTC
OB317	fimH_fw_check_ko	TGTATTGGCGGCAATATTGGCGCTC
OB318	fimH_rev_check_ko	AAAGCGCGGTGAAGAGTATTGCAAT

References

Abdallah, M., Benoliel, C., Drider, D., Dhulster, P., & Chihib, N. E. (2014). Biofilm formation and persistence on abiotic surfaces in the context of food and medical environments. *Archives of Microbiology, 196*(7), 453-472.

Aberg, A., Shingler, V., & Balsalobre, C. (2006). (p)ppGpp regulates type 1 fimbriation of *Escherichia coli* by modulating the expression of the site-specific recombinase FimB. *Molecular microbiology, 60*(6), 1520-1533.

Abraham, J. M., Freitag, C. S., Clements, J. R., & Eisenstein, B. I. (1985). An invertible element of DNA controls phase variation of type 1 fimbriae of *Escherichia coli*. *Proceedings of the National Academy of Sciences of the United States of America, 82*(17), 5724-5727.

Aldridge, P. D., Karlinsey, J. E., Aldridge, C., Birchall, C., Thompson, D., Yagasaki, J., & Hughes, K. T. (2006). The flagellar-specific transcription factor, sigma28, is the Type III secretion chaperone for the flagellar-specific anti-sigma28 factor FlgM. *Genes & development, 20*(16), 2315-2326.

Alon, U., Surette, M. G., Barkai, N., & Leibler, S. (1999). Robustness in bacterial chemotaxis. *Nature, 397*(6715), 168-171.

Amann, E., Ochs, B., & Abel, K. J. (1988). Tightly regulated *tac* promoter vectors useful for the expression of unfused and fused proteins in *Escherichia coli*. *Gene, 69*(2), 301-315.

Amin, D. N., & Hazelbauer, G. L. (2010). The chemoreceptor dimer is the unit of conformational coupling and transmembrane signaling. *Journal of bacteriology, 192*(5), 1193-1200.

Anderson, B. N., Ding, A. M., Nilsson, L. M., Kusuma, K., Tchesnokova, V., Vogel, V.*, et al.* (2007). Weak rolling adhesion enhances bacterial surface colonization. *Journal of bacteriology, 189*(5), 1794-1802.

Aprikian, P., Interlandi, G., Kidd, B. A., Le Trong, I., Tchesnokova, V., Yakovenko, O.*, et al.* (2011). The bacterial fimbrial tip acts as a mechanical force sensor. *PLoS Biology, 9*(5), e1000617.

Arnold, J. W., & Bailey, G. W. (2000). Surface finishes on stainless steel reduce bacterial attachment and early biofilm formation: scanning electron and atomic force microscopy study. *Poultry science, 79*(12), 1839-1845.

Arnqvist, A., Olsen, A., & Normark, S. (1994). Sigma S-dependent growth-phase induction of the csgBA promoter in *Escherichia coli* can be achieved in vivo by sigma 70 in the absence of the nucleoid-associated protein H-NS. *Molecular microbiology, 13*(6), 1021-1032.

Austin, J. W., Sanders, G., Kay, W. W., & Collinson, S. K. (1998). Thin aggregative fimbriae enhance Salmonella enteritidis biofilm formation. *FEMS microbiology letters, 162*(2), 295-301.

Barnhart, M. M., Lynem, J., & Chapman, M. R. (2006). GlcNAc-6P levels modulate the expression of Curli fibers by *Escherichia coli*. *Journal of bacteriology, 188*(14), 5212-5219.

Belisle, J. M., Correia, J. P., Wiseman, P. W., Kennedy, T. E., & Costantino, S. (2008). Patterning protein concentration using laser-assisted adsorption by photobleaching, LAPAP. *Methods in Cell Biology, 8*(12), 2164-2167.

Beloin, C., Roux, A., & Ghigo, J.-M. (2008). *Escherichia coli* biofilms. *Current Topics in Microbiology and Immunology, 322*, 249-289.

Berg, H. C. (2003). The rotary motor of bacterial flagella. *Annual review of biochemistry, 72*, 19-54.

Berke, A. P., Turner, L., Berg, H. C., & Lauga, E. (2008). Hydrodynamic attraction of swimming microorganisms by surfaces. *Physical Review Letters, 101*(3), 038102.

Bernbom, N., Ng, Y. Y., Jorgensen, R. L., Arpanaei, A., Meyer, R. L., Kingshott, P.*, et al.* (2009). Adhesion of food-borne bacteria to stainless steel is reduced by food conditioning films. *Journal of applied microbiology, 106*(4), 1268-1279.

Berne, C., Ducret, A., Hardy, G. G., & Brun, Y. V. (2015). Adhesins Involved in Attachment to Abiotic Surfaces by Gram-Negative Bacteria. *Microbiology spectrum, 3*(4).

Berne, C., Ellison, C. K., Ducret, A., & Brun, Y. V. (2018). Bacterial adhesion at the single-cell level. *Nature reviews. Microbiology, 16*(10), 616-627.

Besharova, O., Suchanek, V. M., Hartmann, R., Drescher, K., & Sourjik, V. (2016). Diversification of Gene Expression during Formation of Static Submerged Biofilms by *Escherichia coli*. *Frontiers in microbiology, 7*, 1568.

Bhomkar, P., Materi, W., Semenchenko, V., & Wishart, D. S. (2010). Transcriptional response of *E. coli* upon FimH-mediated fimbrial adhesion. *Gene regulation and systems biology, 4*, 1-17.

Bian, Z., Brauner, A., Li, Y., & Normark, S. (2000). Expression of and cytokine activation by *Escherichia coli* curli fibers in human sepsis. *The Journal of infectious diseases, 181*(2), 602-612.

Boehm, A., Kaiser, M., Li, H., Spangler, C., Kasper, C. A., Ackermann, M.*, et al.* (2010). Second messenger-mediated adjustment of bacterial swimming velocity. *Cell, 141*(1), 107-116.

Bolster, C. H., Haznedaroglu, B. Z., & Walker, S. L. (2009). Diversity in cell properties and transport behavior among 12 different environmental *Escherichia coli* isolates. *Journal of environmental quality, 38*(2), 465-472.

Boyer, R. R., Sumner, S. S., Williams, R. C., Pierson, M. D., Popham, D. L., & Kniel, K. E. (2007). Influence of curli expression by *Escherichia coli* 0157:H7 on the cell's overall hydrophobicity, charge, and ability to attach to lettuce. *Journal of food protection, 70*(6), 1339-1345.

Briegel, A., Li, X., Bilwes, A. M., Hughes, K. T., Jensen, G. J., & Crane, B. R. (2012). Bacterial chemoreceptor arrays are hexagonally packed trimers of receptor dimers networked by rings of kinase and coupling proteins. *Proceedings of the National Academy of Sciences of the United States of America, 109*(10), 3766-3771.

Brown, P. K., Dozois, C. M., Nickerson, C. A., Zuppardo, A., Terlonge, J., & Curtiss, R., 3rd. (2001). MlrA, a novel regulator of curli (AgF) and extracellular matrix synthesis by *Escherichia coli* and Salmonella enterica serovar Typhimurium. *Molecular microbiology, 41*(2), 349-363.

Busscher, H. J., & van der Mei, H. C. (2012). How do bacteria know they are on a surface and regulate their response to an adhering state? *PLoS pathogens, 8*(1), e1002440.

Chao, Y., & Zhang, T. (2011). Probing roles of lipopolysaccharide, type 1 fimbria, and colanic acid in the attachment of *Escherichia coli* strains on inert surfaces. *Langmuir, 27*(18), 11545-11553.

Chawla, R., Ford, K. M., & Lele, P. P. (2017). Torque, but not FliL, regulates mechanosensitive flagellar motor-function. *Scientific reports, 7*(1), 5565.

Cherepanov, P. P., & Wackernagel, W. (1995). Gene disruption in *Escherichia coli*: TcR and KmR cassettes with the option of Flp-catalyzed excision of the antibiotic-resistance determinant. *Gene, 158*(1), 9-14.

Chevance, F. F., & Hughes, K. T. (2008). Coordinating assembly of a bacterial macromolecular machine. *Nature reviews. Microbiology, 6*(6), 455-465.

Chilcott, G. S., & Hughes, K. T. (2000). Coupling of flagellar gene expression to flagellar assembly in *Salmonella enterica serovar typhimurium* and *Escherichia coli*. *Microbiology and molecular biology reviews : MMBR, 64*(4), 694-708.

Claret, L., Miquel, S., Vieille, N., Ryjenkov, D. A., Gomelsky, M., & Darfeuille-Michaud, A. (2007). The flagellar sigma factor FliA regulates adhesion and invasion of Crohn disease-associated *Escherichia coli* via a cyclic dimeric GMP-dependent pathway. *The Journal of biological chemistry, 282*(46), 33275-33283.

Clarke, E. J., & Voigt, C. A. (2011). Characterization of combinatorial patterns generated by multiple two-component sensors in *E. coli* that respond to many stimuli. *Biotechnology and bioengineering, 108*(3), 666-675.

Dai, X., Boll, J., Hayes, M. E., & Aston, D. E. (2004). Adhesion of *Cryptosporidium parvum* and *Giardia lamblia* to solid surfaces: the role of surface charge and hydrophobicity. *Colloids and surfaces. B, Biointerfaces, 34*(4), 259-263.

Danese, P. N., Pratt, L. A., Dove, S. L., & Kolter, R. (2000). The outer membrane protein, antigen 43, mediates cell-to-cell interactions within *Escherichia coli* biofilms. *Molecular microbiology, 37*(2), 424-432.

Darnton, N. C., Turner, L., Rojevsky, S., & Berg, H. C. (2007). On torque and tumbling in swimming *Escherichia coli*. *Journal of bacteriology, 189*(5), 1756-1764.

Datsenko, K. A., & Wanner, B. L. (2000). One-step inactivation of chromosomal genes in *Escherichia coli* K-12 using PCR products. *Proceedings of the National Academy of Sciences of the United States of America, 97*(12), 6640-6645.

Dickson, J. S., & Koohmaraie, M. (1989). Cell surface charge characteristics and their relationship to bacterial attachment to meat surfaces. *Applied and environmental microbiology, 55*(4), 832-836.

Dorman, C. J., & Higgins, C. F. (1987). Fimbrial phase variation in *Escherichia coli*: dependence on integration host factor and homologies with other site-specific recombinases. *Journal of bacteriology, 169*(8), 3840-3843.

Dove, S. L., Smith, S. G., & Dorman, C. J. (1997). Control of *Escherichia coli* type 1 fimbrial gene expression in stationary phase: a negative role for RpoS. *Molecular & general genetics : MGG, 254*(1), 13-20.

Drescher, K., Dunkel, J., Cisneros, L. H., Ganguly, S., & Goldstein, R. E. (2011). Fluid dynamics and noise in bacterial cell-cell and cell-surface scattering. *Proceedings of the National Academy of Sciences of the United States of America, 108*(27), 10940-10945.

Du, M., Yuan, Z., Yu, H., Henderson, N., Sarowar, S., Zhao, G.*, et al.* (2018). Handover mechanism of the growing pilus by the bacterial outer-membrane usher FimD. *Nature, 562*(7727), 444-447.

Duan, Q., Zhou, M., Zhu, X., Yang, Y., Zhu, J., Bao, W.*, et al.* (2013). Flagella from F18+*Escherichia coli* play a role in adhesion to pig epithelial cell lines. *Microbial Pathogenesis, 55*, 32-38.

Dudin, O., Geiselmann, J., Ogasawara, H., Ishihama, A., & Lacour, S. (2014). Repression of flagellar genes in exponential phase by CsgD and CpxR, two crucial

modulators of *Escherichia coli* biofilm formation. *Journal of bacteriology, 196*(3), 707-715.

Earhart, C. F. (2000). Use of an Lpp-OmpA fusion vehicle for bacterial surface display. *Methods in enzymology, 326*, 506-516.

El-Labany, S., Sohanpal, B. K., Lahooti, M., Akerman, R., & Blomfield, I. C. (2003). Distant cis-active sequences and sialic acid control the expression of *fimB* in *Escherichia coli* K-12. *Molecular microbiology, 49*(4), 1109-1118.

Fang, X., & Gomelsky, M. (2010). A post-translational, c-di-GMP-dependent mechanism regulating flagellar motility. *Molecular Microbiology, 76*(5), 1295-1305.

Feenstra, T., Thogersen, M. S., Wieser, E., Peschel, A., Ball, M. J., Brandes, R.*, et al.* (2017). Adhesion of *Escherichia coli* under flow conditions reveals potential novel effects of FimH mutations. *European journal of clinical microbiology & infectious diseases : official publication of the European Society of Clinical Microbiology, 36*(3), 467-478.

Fink, R. C., Black, E. P., Hou, Z., Sugawara, M., Sadowsky, M. J., & Diez-Gonzalez, F. (2012). Transcriptional responses of *Escherichia coli* K-12 and O157:H7 associated with lettuce leaves. *Applied and environmental microbiology, 78*(6), 1752-1764.

Fletcher, M. (1976). The effects of proteins on bacterial attachment to polystyrene. *Journal of general microbiology, 94*(2), 400-404.

Francez-Charlot, A., Castanie-Cornet, M. P., Gutierrez, C., & Cam, K. (2005). Osmotic regulation of the *Escherichia coli* bdm (biofilm-dependent modulation) gene by the RcsCDB His-Asp phosphorelay. *Journal of bacteriology, 187*(11), 3873-3877.

Friedlander, R. S., Vlamakis, H., Kim, P., Khan, M., Kolter, R., & Aizenberg, J. (2013). Bacterial flagella explore microscale hummocks and hollows to increase adhesion. *Proceedings of the National Academy of Sciences of the United States of America, 110*(14), 5624-5629.

Friedlander, R. S., Vogel, N., & Aizenberg, J. (2015). Role of Flagella in Adhesion of *Escherichia coli* to Abiotic Surfaces. *Langmuir, 31*(22), 6137-6144.

Frymier, P. D., Ford, R. M., Berg, H. C., & Cummings, P. T. (1995). Three-dimensional tracking of motile bacteria near a solid planar surface. *Proceedings of the National Academy of Sciences of the United States of America, 92*(13), 6195-6199.

Gally, D. L., Bogan, J. A., Eisenstein, B. I., & Blomfield, I. C. (1993). Environmental regulation of the *fim* switch controlling type 1 fimbrial phase variation in *Escherichia coli* K-12: effects of temperature and media. *Journal of bacteriology, 175*(19), 6186-6193.

Gannon, J. T., Manilal, V. B., & Alexander, M. (1991). Relationship between Cell Surface Properties and Transport of Bacteria through Soil. *Applied and environmental microbiology, 57*(1), 190-193.

Gebbink, M. F., Claessen, D., Bouma, B., Dijkhuizen, L., & Wosten, H. A. (2005). Amyloids-a functional coat for microorganisms. *Nature reviews. Microbiology, 3*(4), 333-341.

Girgis, H. S., Liu, Y., Ryu, W. S., & Tavazoie, S. (2007). A comprehensive genetic characterization of bacterial motility. *PLoS Genetics, 3*(9), 1644-1660.

Glatter, T., Ludwig, C., Ahrne, E., Aebersold, R., Heck, A. J., & Schmidt, A. (2012). Large-scale quantitative assessment of different in-solution protein digestion protocols reveals superior cleavage efficiency of tandem Lys-C/trypsin proteolysis over trypsin digestion. *Journal of proteome research, 11*(11), 5145-5156.

Gonzalez Barrios, A. F., Zuo, R., Hashimoto, Y., Yang, L., Bentley, W. E., & Wood, T. K. (2006). Autoinducer 2 controls biofilm formation in *Escherichia coli* through a novel motility quorum-sensing regulator (MqsR, B3022). *Journal of bacteriology, 188*(1), 305-316.

Gophna, U., Barlev, M., Seijffers, R., Oelschlager, T. A., Hacker, J., & Ron, E. Z. (2001). Curli fibers mediate internalization of *Escherichia coli* by eukaryotic cells. *Infection and immunity, 69*(4), 2659-2665.

Gophna, U., Oelschlaeger, T. A., Hacker, J., & Ron, E. Z. (2002). Role of fibronectin in curli-mediated internalization. *FEMS microbiology letters, 212*(1), 55-58.

Guttenplan, S. B., & Kearns, D. B. (2013). Regulation of flagellar motility during biofilm formation. *FEMS Microbiology Reviews, 37*(6), 849-871.

Hahn, E., Wild, P., Hermanns, U., Sebbel, P., Glockshuber, R., Haner, M.*, et al.* (2002). Exploring the 3D molecular architecture of *Escherichia coli* type 1 pili. *Journal of molecular biology, 323*(5), 845-857.

Haiko, J., & Westerlund-Wikstrom, B. (2013). The role of the bacterial flagellum in adhesion and virulence. *Biology (Bassel), 2*(4), 1242-1267.

Hammar, M. R., Arnqvist, A., Bian, Z., Olsen, A., & Normark, S. (1995). Expression of two *csg* operons is required for production of fibronectin- and Congo red-binding curli polymers in *Escherichia coli* K-12. *Molecular microbiology, 18*(4), 661-670.

Harapanahalli, A. K., Younes, J. A., Allan, E., van der Mei, H. C., & Busscher, H. J. (2015). Chemical Signals and Mechanosensing in Bacterial Responses to Their Environment. *PLoS pathogens, 11*(8), e1005057.

Hasman, H., Chakraborty, T., & Klemm, P. (1999). Antigen-43-mediated autoaggregation of *Escherichia coli* is blocked by fimbriation. *Journal of bacteriology, 181*(16), 4834-4841.

Hayashi, K., Morooka, N., Yamamoto, Y., Fujita, K., Isono, K., Choi, S.*, et al.* (2006). Highly accurate genome sequences of *Escherichia coli* K-12 strains MG1655 and W3110. *Molecular Systems Biology, 2*, 2006 0007.

Hazelbauer, G. L., Falke, J. J., & Parkinson, J. S. (2008). Bacterial chemoreceptors: high-performance signaling in networked arrays. *Trends in biochemical sciences, 33*(1), 9-19.

Hazelbauer, G. L., & Lai, W. C. (2010). Bacterial chemoreceptors: providing enhanced features to two-component signaling. *Current opinion in microbiology, 13*(2), 124-132.

He, X., Liu, Y., Huang, J., Chen, X., Ren, K., & Li, H. (2015). Adsorption of alginate and albumin on aluminum coatings inhibits adhesion of *Escherichia coli* and enhances the anti-corrosion performances of the coatings. (332), 89-96.

Henderson, B., Nair, S., Pallas, J., & Williams, M. A. (2011). Fibronectin: a multidomain host adhesin targeted by bacterial fibronectin-binding proteins. *FEMS microbiology reviews, 35*(1), 147-200.

Hengge, R. (2009). Principles of c-di-GMP signalling in bacteria. *Nature Reviews. Microbiology, 7*(4), 263-273.

Hengge, R., Galperin, M. Y., Ghigo, J. M., Gomelsky, M., Green, J., Hughes, K. T.*, et al.* (2016). Systematic Nomenclature for GGDEF and EAL Domain-Containing Cyclic Di-GMP Turnover Proteins of *Escherichia coli*. *Journal of bacteriology, 198*(1), 7-11.

Hong, Y., & Brown, D. G. (2009). Variation in bacterial ATP level and proton motive force due to adhesion to a solid surface. *Applied and environmental microbiology, 75*(8), 2346-2353.

Hou, Y. J., Yang, W. S., Hong, Y., Zhang, Y., Wang, D. C., & Li, D. F. (2020). Structural insights into the mechanism of c-di-GMP-bound YcgR regulating flagellar motility in *Escherichia coli*. *The Journal of biological chemistry, 295*(3), 808-821.

Hsu, L. C., Fang, J., Borca-Tasciuc, D. A., Worobo, R. W., & Moraru, C. I. (2013). Effect of micro- and nanoscale topography on the adhesion of bacterial cells to solid surfaces. *Applied and environmental microbiology, 79*(8), 2703-2712.

Husmark, U., & Ronner, U. (1990). Forces involved in adhesion of *Bacillus cereus* spores to solid surfaces under different environmental conditions. *The Journal of applied bacteriology, 69*(4), 557-562.

Itoh, Y., Rice, J. D., Goller, C., Pannuri, A., Taylor, J., Meisner, J.*, et al.* (2008). Roles of pgaABCD genes in synthesis, modification, and export of the *Escherichia coli* biofilm adhesin poly-beta-1,6-N-acetyl-D-glucosamine. *Journal of bacteriology, 190*(10), 3670-3680.

Jenal, U., & Malone, J. (2006). Mechanisms of cyclic-di-GMP signaling in bacteria. *Annual Review of Genetics, 40*, 385-407.

Jenal, U., Reinders, A., & Lori, C. (2017). Cyclic di-GMP: second messenger extraordinaire. *Nature reviews. Microbiology, 15*(5), 271-284.

Jubelin, G., Vianney, A., Beloin, C., Ghigo, J. M., Lazzaroni, J. C., Lejeune, P., & Dorel, C. (2005). CpxR/OmpR interplay regulates curli gene expression in response to osmolarity in *Escherichia coli*. *Journal of bacteriology, 187*(6), 2038-2049.

Karatan, E., & Michael, A. J. (2013). A wider role for polyamines in biofilm formation. *Biotechnology letters, 35*(11), 1715-1717.

Karlinsey, J. E., Tanaka, S., Bettenworth, V., Yamaguchi, S., Boos, W., Aizawa, S. I., & Hughes, K. T. (2000). Completion of the hook-basal body complex of the *Salmonella typhimurium* flagellum is coupled to FlgM secretion and *fliC* transcription. *Molecular microbiology, 37*(5), 1220-1231.

Keilberg, D., & Ottemann, K. M. (2016). How *Helicobacter pylori* senses, targets and interacts with the gastric epithelium. *Environmental Microbiology, 18*(3), 791-806.

Khan, S., Dapice, M., & Reese, T. S. (1988). Effects of *mot* gene expression on the structure of the flagellar motor. *Journal of molecular biology, 202*(3), 575-584.

Kimkes, T. E. P., & Heinemann, M. (2020). How bacteria recognise and respond to surface contact. *FEMS microbiology reviews, 44*(1), 106-122.

Klemm, P., & Schembri, M. (2004). Type 1 Fimbriae, Curli, and Antigen 43: Adhesion, Colonization, and Biofilm Formation. *EcoSal Plus, 1*(1).

Klemm, P., & Schembri, M. A. (2000). Bacterial adhesins: function and structure. *290*(1), 27-35.

Korea, C. G., Badouraly, R., Prevost, M. C., Ghigo, J. M., & Beloin, C. (2010). *Escherichia coli* K-12 possesses multiple cryptic but functional chaperone-usher fimbriae with distinct surface specificities. *Environmental microbiology, 12*(7), 1957-1977.

Korea, C. G., Ghigo, J. M., & Beloin, C. (2011). The sweet connection: Solving the riddle of multiple sugar-binding fimbrial adhesins in *Escherichia coli*: Multiple *E. coli* fimbriae

form a versatile arsenal of sugar-binding lectins potentially involved in surface-colonisation and tissue tropism. *BioEssays, 33*(4), 300-311.

Kumar, C. G., & Anand, S. K. (1998). Significance of microbial biofilms in food industry: a review. *International journal of food microbiology, 42*(1-2), 9-27.

Larsen, S. H., Adler, J., Gargus, J. J., & Hogg, R. W. (1974). Chemomechanical coupling without ATP: the source of energy for motility and chemotaxis in bacteria. *Proceedings of the National Academy of Sciences of the United States of America, 71*(4), 1239-1243.

Lejeune, P. (2003). Contamination of abiotic surfaces: what a colonizing bacterium sees and how to blur it. *Trends in microbiology, 11*(4), 179-184.

Lele, P. P., Hosu, B. G., & Berg, H. C. (2013). Dynamics of mechanosensing in the bacterial flagellar motor. *Proceedings of the National Academy of Sciences of the United States of America, 110*(29), 11839-11844.

Lindenberg, S., Klauck, G., Pesavento, C., Klauck, E., & Hengge, R. (2013). The EAL domain protein YciR acts as a trigger enzyme in a c-di-GMP signalling cascade in E. coli biofilm control. *The EMBO journal, 32*(14), 2001-2014.

Liu, Y., Yang, S. F., Li, Y., Xu, H., Qin, L., & Tay, J. H. (2004). The influence of cell and substratum surface hydrophobicities on microbial attachment. *Journal of biotechnology, 110*(3), 251-256.

Liu, Z., Niu, H., Wu, S., & Huang, R. (2014). CsgD regulatory network in a bacterial trait-altering biofilm formation. *Emerging microbes & infections, 3*(1), e1.

Lloyd, S. A., Tang, H., Wang, X., Billings, S., & Blair, D. F. (1996). Torque generation in the flagellar motor of *Escherichia coli*: evidence of a direct role for FliG but not for FliM or FliN. *Journal of bacteriology, 178*(1), 223-231.

Lopes, J. G., & Sourjik, V. (2018). Chemotaxis of *Escherichia coli* to major hormones and polyamines present in human gut. *The ISME journal, 12*(11), 2736-2747.

Macarisin, D., Patel, J., Bauchan, G., Giron, J. A., & Sharma, V. K. (2012). Role of curli and cellulose expression in adherence of *Escherichia coli* O157:H7 to spinach leaves. *Foodborne pathogens and disease, 9*(2), 160-167.

Macnab, R. M., & Koshland, D. E., Jr. (1972). The gradient-sensing mechanism in bacterial chemotaxis. *Proceedings of the National Academy of Sciences of the United States of America, 69*(9), 2509-2512.

Majdalani, N., & Gottesman, S. (2006). The Rcs phosphorelay: a complex signal transduction system. (187), 6770-6778.

Manson, M. D., Tedesco, P., Berg, H. C., Harold, F. M., & Van der Drift, C. (1977). A protonmotive force drives bacterial flagella. *Proceedings of the National Academy of Sciences of the United States of America, 74*(7), 3060-3064.

Marshall, K. C. (1988). Adhesion and growth of bacteria at surfaces in oligotrophic habitats. (34), 503-506.

McCarter, L. L. (2006). Regulation of flagella. *Current opinion in microbiology, 9*(2), 180-186.

McClain, M. S., Blomfield, I. C., Eberhardt, K. J., & Eisenstein, B. I. (1993). Inversion-independent phase variation of type 1 fimbriae in Escherichia coli. *Journal of bacteriology, 175*(14), 4335-4344.

McCrate, O. A., Zhou, X., Reichhardt, C., & Cegelski, L. (2013). Sum of the parts: composition and architecture of the bacterial extracellular matrix. *Journal of molecular biology, 425*(22), 4286-4294.

Merritt, P. M., Danhorn, T., & Fuqua, C. (2007). Motility and chemotaxis in *Agrobacterium tumefaciens* surface attachment and biofilm formation. *Journal of Bacteriology, 189*(22), 8005-8014.

Mewborn, L., Benitez, J. A., & Silva, A. J. (2017). Flagellar motility, extracellular proteases and *Vibrio cholerae* detachment from abiotic and biotic surfaces. *Microbial pathogenesis, 113*, 17-24.

Michaux, C., Verneuil, N., Hartke, A., & Giard, J. C. (2014). Physiological roles of small RNA molecules. *Microbiology, 160*(Pt 6), 1007-1019.

Mika, F., & Hengge, R. (2014). Small RNAs in the control of RpoS, CsgD, and biofilm architecture of *Escherichia coli. RNA biology, 11*(5), 494-507.

Misselwitz, B., Barrett, N., Kreibich, S., Vonaesch, P., Andritschke, D., Rout, S.*, et al.* (2012). Near surface swimming of *Salmonella typhimurium* explains target-site selection and cooperative invasion. *PLoS Pathogens, 8*(7), e1002810.

Monroe, D. (2007). Looking for Chinks in the Armor of Bacterial Biofilms. *PLoS Biology, 5*(11).

Monteiro, C., Papenfort, K., Hentrich, K., Ahmad, I., Le Guyon, S., Reimann, R.*, et al.* (2012). Hfq and Hfq-dependent small RNAs are major contributors to multicellular development in *Salmonella enterica serovar Typhimurium*. *RNA biology, 9*(4), 489-502.

Morimoto, Y. V., & Minamino, T. (2014). Structure and function of the bi-directional bacterial flagellar motor. *Biomolecules, 4*(1), 217-234.

Mydock-McGrane, L. K., Cusumano, Z. T., & Janetka, J. W. (2016). Mannose-derived FimH antagonists: a promising anti-virulence therapeutic strategy for urinary tract infections and Crohn's disease. *Expert opinion on therapeutic patents, 26*(2), 175-197.

Nord, A. L., Gachon, E., Perez-Carrasco, R., Nirody, J. A., Barducci, A., Berry, R. M., & Pedaci, F. (2017). Catch bond drives stator mechanosensitivity in the bacterial flagellar motor. *Proceedings of the National Academy of Sciences of the United States of America, 114*(49), 12952-12957.

O'Toole, G., Kaplan, H., & Kolter, R. (2000). Biofilm formation as microbial development. *Annual Review of Microbiology, 54*, 49-79.

Ogasawara, H., Yamada, K., Kori, A., Yamamoto, K., & Ishihama, A. (2010). Regulation of the Escherichia coli *csgD* promoter: interplay between five transcription factors. *Microbiology, 156*(Pt 8), 2470-2483.

Oh, Y. J., Cui, Y., Kim, H., Li, Y., Hinterdorfer, P., & Park, S. (2012). Characterization of curli A production on living bacterial surfaces by scanning probe microscopy. *Biophysical journal, 103*(8), 1666-1671.

Olsen, P. B., & Klemm, P. (1994). Localization of promoters in the fim gene cluster and the effect of H-NS on the transcription of *fimB* and *fimE*. *FEMS microbiology letters, 116*(1), 95-100.

Olsen, P. B., Schembri, M. A., Gally, D. L., & Klemm, P. (1998). Differential temperature modulation by H-NS of the *fimB* and *fimE* recombinase genes which control the orientation of the type 1 fimbrial phase switch. *FEMS microbiology letters, 162*(1), 17-23.

Orndorff, P. E., Devapali, A., Palestrant, S., Wyse, A., Everett, M. L., Bollinger, R. R., & Parker, W. (2004). Immunoglobulin-mediated agglutination of and biofilm formation by *Escherichia coli* K-12 require the type 1 pilus fiber. *Infection and immunity, 72*(4), 1929-1938.

Otto, K., Norbeck, J., Larsson, T., Karlsson, K. A., & Hermansson, M. (2001). Adhesion of type 1-fimbriated *Escherichia coli* to abiotic surfaces leads to altered composition of outer membrane proteins. *Journal of bacteriology, 183*(8), 2445-2453.

Otto, K., & Silhavy, T. J. (2002). Surface sensing and adhesion of *Escherichia coli* controlled by the Cpx-signaling pathway. *Proceedings of the National Academy of Sciences of the United States of America, 99*(4), 2287-2292.

Parsek, M. R., & Greenberg, E. P. (2005). Sociomicrobiology: the connections between quorum sensing and biofilms. *Trends in microbiology, 13*(1), 27-33.

Paul, K., Nieto, V., Carlquist, W. C., Blair, D. F., & Harshey, R. M. (2010). The c-di-GMP binding protein YcgR controls flagellar motor direction and speed to affect chemotaxis by a "backstop brake" mechanism. *Molecular Cell, 38*(1), 128-139.

Paul, R., Weiser, S., Amiot, N. C., Chan, C., Schirmer, T., Giese, B., & Jenal, U. (2004). Cell cycle-dependent dynamic localization of a bacterial response regulator with a novel di-guanylate cyclase output domain. *Genes & development, 18*(6), 715-727.

Pawar, D. M., Rossman, M. L., & Chen, J. (2005). Role of curli fimbriae in mediating the cells of enterohaemorrhagic *Escherichia coli* to attach to abiotic surfaces. *Journal of applied microbiology, 99*(2), 418-425.

Pesavento, C., Becker, G., Sommerfeldt, N., Possling, A., Tschowri, N., Mehlis, A., & Hengge, R. (2008). Inverse regulatory coordination of motility and curli-mediated adhesion in Escherichia coli. *Genes & development, 22*(17), 2434-2446.

Pesavento, C., & Hengge, R. (2009). Bacterial nucleotide-based second messengers. *Current opinion in microbiology, 12*(2), 170-176.

Pratt, L. A., & Kolter, R. (1998). Genetic analysis of *Escherichia coli* biofilm formation: roles of flagella, motility, chemotaxis and type I pili. *Molecular Microbiology, 30*(2), 285-293.

Prigent-Combaret, C., Vidal, O., Dorel, C., & Lejeune, P. (1999). Abiotic surface sensing and biofilm-dependent regulation of gene expression in *Escherichia coli*. *Journal of bacteriology, 181*(19), 5993-6002.

Pruss, B. M., Campbell, J. W., Van Dyk, T. K., Zhu, C., Kogan, Y., & Matsumura, P. (2003). FlhD/FlhC is a regulator of anaerobic respiration and the Entner-Doudoroff pathway through induction of the methyl-accepting chemotaxis protein Aer. *Journal of bacteriology, 185*(2), 534-543.

Pruss, B. M., Liu, X., Hendrickson, W., & Matsumura, P. (2001). FlhD/FlhC-regulated promoters analyzed by gene array and lacZ gene fusions. *FEMS microbiology letters, 197*(1), 91-97.

Raivio, T. L. (2014). Everything old is new again: an update on current research on the Cpx envelope stress response. *Biochimica et biophysica acta, 1843*(8), 1529-1541.

Raivio, T. L., Leblanc, S. K., & Price, N. L. (2013). The *Escherichia coli* Cpx envelope stress response regulates genes of diverse function that impact antibiotic resistance and membrane integrity. *Journal of bacteriology, 195*(12), 2755-2767.

Reisner, A., Maierl, M., Jorger, M., Krause, R., Berger, D., Haid, A.*, et al.* (2014). Type 1 fimbriae contribute to catheter-associated urinary tract infections caused by Escherichia coli. *Journal of bacteriology, 196*(5), 931-939.

Ridgway, H. G., Silverman, M., & Simon, M. I. (1977). Localization of proteins controlling motility and chemotaxis in Escherichia coli. *Journal of bacteriology, 132*(2), 657-665.

Roesch, P. L., & Blomfield, I. C. (1998). Leucine alters the interaction of the leucine-responsive regulatory protein (Lrp) with the fim switch to stimulate site-specific recombination in Escherichia coli. *Molecular microbiology, 27*(4), 751-761.

Romling, U. (2012). Cyclic di-GMP, an established secondary messenger still speeding up. *Environmental microbiology, 14*(8), 1817-1829.

Romling, U. (2013). Microbiology: bacterial communities as capitalist economies. *Nature, 497*(7449), 321-322.

Romling, U., Bian, Z., Hammar, M., Sierralta, W. D., & Normark, S. (1998). Curli fibers are highly conserved between *Salmonella typhimurium* and *Escherichia coli* with respect to operon structure and regulation. *Journal of bacteriology, 180*(3), 722-731.

Romling, U., Galperin, M. Y., & Gomelsky, M. (2013). Cyclic di-GMP: the first 25 years of a universal bacterial second messenger. *Microbiology and Molecular Biology Reviews 77*(1), 1-52.

Ryjenkov, D. A., Simm, R., Romling, U., & Gomelsky, M. (2006). The PilZ domain is a receptor for the second messenger c-di-GMP: the PilZ domain protein YcgR controls motility in enterobacteria. *The Journal of biological chemistry, 281*(41), 30310-30314.

Sakamoto, A., Terui, Y., Yamamoto, T., Kasahara, T., Nakamura, M., Tomitori, H.*, et al.* (2012). Enhanced biofilm formation and/or cell viability by polyamines through stimulation of response regulators UvrY and CpxR in the two-component signal transducing systems, and ribosome recycling factor. *The international journal of biochemistry & cell biology, 44*(11), 1877-1886.

Saldana, Z., Xicohtencatl-Cortes, J., Avelino, F., Phillips, A. D., Kaper, J. B., Puente, J. L., & Giron, J. A. (2009). Synergistic role of curli and cellulose in cell adherence and biofilm formation of attaching and effacing *Escherichia coli* and identification of Fis as a negative regulator of curli. *Environmental microbiology, 11*(4), 992-1006.

Samatey, F. A., Matsunami, H., Imada, K., Nagashima, S., Shaikh, T. R., Thomas, D. R.*, et al.* (2004). Structure of the bacterial flagellar hook and implication for the molecular universal joint mechanism. *Nature, 431*(7012), 1062-1068.

Samuelsson, M. O., & Kirchman, D. L. (1990). Degradation of adsorbed protein by attached bacteria in relationship to surface hydrophobicity. *Applied and environmental microbiology, 56*(12), 3643-3648.

Sarenko, O., Klauck, G., Wilke, F. M., Pfiffer, V., Richter, A. M., Herbst, S.*, et al.* (2017). More than Enzymes That Make or Break Cyclic Di-GMP-Local Signaling in the Interactome of GGDEF/EAL Domain Proteins of Escherichia coli. *mBio, 8*(5).

Sauer, M. M., Jakob, R. P., Eras, J., Baday, S., Eris, D., Navarra, G.*, et al.* (2016). Catch-bond mechanism of the bacterial adhesin FimH. *Nature Communications, 7*, 10738.

Schauer, O., Mostaghaci, B., Colin, R., Hurtgen, D., Kraus, D., Sitti, M., & Sourjik, V. (2018). Motility and chemotaxis of bacteria-driven microswimmers fabricated using antigen 43-mediated biotin display. *Scientific reports, 8*(1), 9801.

Schembri, M. A., Kjaergaard, K., & Klemm, P. (2003). Global gene expression in Escherichia coli biofilms. *Molecular microbiology, 48*(1), 253-267.

Schirmer, T., & Jenal, U. (2009). Structural and mechanistic determinants of c-di-GMP signalling. *Nature reviews. Microbiology, 7*(10), 724-735.

Schneider, B. L., Hernandez, V. J., & Reitzer, L. (2013). Putrescine catabolism is a metabolic response to several stresses in *Escherichia coli*. *Molecular microbiology, 88*(3), 537-550.

Schniederberend, M., Williams, J. F., Shine, E., Shen, C., Jain, R., Emonet, T., & Kazmierczak, B. I. (2019). Modulation of flagellar rotation in surface-attached bacteria: A pathway for rapid surface-sensing after flagellar attachment. *PLoS pathogens, 15*(11), e1008149.

Schwan, W. R., Lee, J. L., Lenard, F. A., Matthews, B. T., & Beck, M. T. (2002). Osmolarity and pH growth conditions regulate fim gene transcription and type 1 pilus expression in uropathogenic Escherichia coli. *Infection and immunity, 70*(3), 1391-1402.

Segall, J. E., Block, S. M., & Berg, H. C. (1986). Temporal comparisons in bacterial chemotaxis. *Proceedings of the National Academy of Sciences of the United States of America, 83*(23), 8987-8991.

Segall, J. E., Manson, M. D., & Berg, H. C. (1982). Signal processing times in bacterial chemotaxis. *Nature, 296*(5860), 855-857.

Serra, D. O., & Hengge, R. (2019). A c-di-GMP-Based Switch Controls Local Heterogeneity of Extracellular Matrix Synthesis which Is Crucial for Integrity and Morphogenesis of Escherichia coli Macrocolony Biofilms. *Journal of molecular biology*.

Serra, D. O., Richter, A. M., Klauck, G., Mika, F., & Hengge, R. (2013). Microanatomy at cellular resolution and spatial order of physiological differentiation in a bacterial biofilm. *mBio, 4*(2), e00103-00113.

Sharma, G., Sharma, S., Sharma, P., Chandola, D., Dang, S., Gupta, S., & Gabrani, R. (2016). *Escherichia coli* biofilm: development and therapeutic strategies. *Journal of applied microbiology, 121*(2), 309-319.

Sharma, S., Jaimes-Lizcano, Y. A., McLay, R. B., Cirino, P. C., & Conrad, J. C. (2016). Subnanometric Roughness Affects the Deposition and Mobile Adhesion of *Escherichia coli* on Silanized Glass Surfaces. *Langmuir : the ACS journal of surfaces and colloids, 32*(21), 5422-5433.

Sherlock, O., Schembri, M. A., Reisner, A., & Klemm, P. (2004). Novel roles for the AIDA adhesin from diarrheagenic Escherichia coli: cell aggregation and biofilm formation. *Journal of bacteriology, 186*(23), 8058-8065.

Sherlock, O., Vejborg, R. M., & Klemm, P. (2005). The TibA adhesin/invasin from enterotoxigenic *Escherichia coli* is self recognizing and induces bacterial aggregation and biofilm formation. *Infection and immunity, 73*(4), 1954-1963.

Sherman, E., Bayles, K., Moormeier, D., Endres, J., & Wei, T. (2019). Observations of Shear Stress Effects on *Staphylococcus aureus* Biofilm Formation. *mSphere, 4*(4).

Sohanpal, B. K., El-Labany, S., Lahooti, M., Plumbridge, J. A., & Blomfield, I. C. (2004). Integrated regulatory responses of *fimB* to N-acetylneuraminic (sialic) acid and GlcNAc in Escherichia coli K-12. *Proceedings of the National Academy of Sciences of the United States of America, 101*(46), 16322-16327.

Sommerfeldt, N., Possling, A., Becker, G., Pesavento, C., Tschowri, N., & Hengge, R. (2009). Gene expression patterns and differential input into curli fimbriae regulation of all GGDEF/EAL domain proteins in *Escherichia coli*. *Microbiology, 155*(Pt 4), 1318-1331.

Sourjik, V., & Wingreen, N. S. (2012). Responding to chemical gradients: bacterial chemotaxis. *Current Opinion in Cell Biology, 24*(2), 262-268.

Stafford, G. P., Ogi, T., & Hughes, C. (2005). Binding and transcriptional activation of non-flagellar genes by the Escherichia coli flagellar master regulator FlhD2C2. *Microbiology, 151*(Pt 6), 1779-1788.

Suchanek, V. M., Esteban-Lopez, M., Colin, R., Besharova, O., Fritz, K., & Sourjik, V. (2020). Chemotaxis and cyclic-di-GMP signalling control surface attachment of *Escherichia coli*. *Mol Microbiol.* 113(4):728-739.

Tagliabue, L., Maciag, A., Antoniani, D., & Landini, P. (2010). The yddV-dos operon controls biofilm formation through the regulation of genes encoding curli fibers' subunits in aerobically growing *Escherichia coli*. *FEMS Immunology and Medical Microbiology, 59*(3), 477-484.

Thomason, L. C., Costantino, N., & Court, D. L. (2007). *E. coli* genome manipulation by P1 transduction. *Current protocols in molecular biology, Chapter 1*, Unit 1 17.

Thomen, P., Robert, J., Monmeyran, A., Bitbol, A. F., Douarche, C., & Henry, N. (2017). Bacterial biofilm under flow: First a physical struggle to stay, then a matter of breathing. *PloS one, 12*(4), e0175197.

Tindall, M. J., Gaffney, E. A., Maini, P. K., & Armitage, J. P. (2012). Theoretical insights into bacterial chemotaxis. *Wiley interdisciplinary reviews. Systems biology and medicine, 4*(3), 247-259.

Tipping, M. J., Delalez, N. J., Lim, R., Berry, R. M., & Armitage, J. P. (2013). Load-dependent assembly of the bacterial flagellar motor. *mBio, 4*(4).

Tschauner, K., Hornschemeyer, P., Muller, V. S., & Hunke, S. (2014). Dynamic interaction between the CpxA sensor kinase and the periplasmic accessory protein CpxP mediates signal recognition in *E. coli*. *PloS one, 9*(9), e107383.

Turner, L., Ryu, W. S., & Berg, H. C. (2000). Real-time imaging of fluorescent flagellar filaments. *Journal of bacteriology, 182*(10), 2793-2801.

Tuson, H. H., & Weibel, D. B. (2013). Bacteria-surface interactions. *Soft Matter, 9*(18), 4368-4380.

Ulett, G. C., Webb, R. I., & Schembri, M. A. (2006). Antigen-43-mediated autoaggregation impairs motility in *Escherichia coli*. *Microbiology, 152*(Pt 7), 2101-2110.

Valenski, M. L., Harris, S. L., Spears, P. A., Horton, J. R., & Orndorff, P. E. (2003). The Product of the fimI gene is necessary for *Escherichia coli* type 1 pilus biosynthesis. *Journal of bacteriology, 185*(16), 5007-5011.

van der Velden, A. W., Baumler, A. J., Tsolis, R. M., & Heffron, F. (1998). Multiple fimbrial adhesins are required for full virulence of *Salmonella typhimurium* in mice. *Infection and immunity, 66*(6), 2803-2808.

van der Woude, M. W., & Henderson, I. R. (2008). Regulation and function of Ag43 (flu). *Annual review of microbiology, 62*, 153-169.

Vidal, O., Longin, R., Prigent-Combaret, C., Dorel, C., Hooreman, M., & Lejeune, P. (1998). Isolation of an *Escherichia coli* K-12 mutant strain able to form biofilms on inert surfaces: involvement of a new ompR allele that increases curli expression. *Journal of bacteriology, 180*(9), 2442-2449.

Vigeant, M. A., Ford, R. M., Wagner, M., & Tamm, L. K. (2002). Reversible and irreversible adhesion of motile *Escherichia coli* cells analyzed by total internal reflection aqueous fluorescence microscopy. *Applied and Environmental Microbiology, 68*(6), 2794-2801.

Vladimirov, N., & Sourjik, V. (2009). Chemotaxis: how bacteria use memory. *Biological chemistry, 390*(11), 1097-1104.

Wadhams, G. H., & Armitage, J. P. (2004). Making sense of it all: bacterial chemotaxis. *Nature Reviews. Molecular Cell Biology, 5*(12), 1024-1037.

Wang, H., Wilksch, J. J., Chen, L., Tan, J. W., Strugnell, R. A., & Gee, M. L. (2017). Influence of Fimbriae on Bacterial Adhesion and Viscoelasticity and Correlations of the Two Properties with Biofilm Formation. *Langmuir: the ACS journal of surfaces and colloids, 33*(1), 100-106.

Wang, L., Keatch, R., Zhao, Q., Wright, J. A., Bryant, C. E., Redmann, A. L., & Terentjev, E. M. (2018). Influence of Type I Fimbriae and Fluid Shear Stress on Bacterial Behavior and Multicellular Architecture of Early *Escherichia coli* Biofilms at Single-Cell Resolution. *Applied and environmental microbiology, 84*(6).

Wang, X., Dubey, A. K., Suzuki, K., Baker, C. S., Babitzke, P., & Romeo, T. (2005). CsrA post-transcriptionally represses pgaABCD, responsible for synthesis of a biofilm polysaccharide adhesin of *Escherichia coli*. *Molecular microbiology, 56*(6), 1648-1663.

Wang, Z., Banerjee, S., Ahmad, A., Li, Y., Azmi, A. S., Gunn, J. R.*, et al.* (2011). Activated K-ras and INK4a/Arf deficiency cooperate during the development of pancreatic cancer by activation of Notch and NF-kappaB signaling pathways. *PloS one, 6*(6), e20537.

Whittaker, C. J., Klier, C. M., & Kolenbrander, P. E. (1996). Mechanisms of adhesion by oral bacteria. *Annual review of microbiology, 50*, 513-552.

Wilson, L. G., Martinez, V. A., Schwarz-Linek, J., Tailleur, J., Bryant, G., Pusey, P. N., & Poon, W. C. (2011). Differential dynamic microscopy of bacterial motility. *Physical Review Letters, 106*(1), 018101.

Wong, A. C. (1998). Biofilms in food processing environments. *Journal of dairy science, 81*(10), 2765-2770.

Wood, T. K., Gonzalez Barrios, A. F., Herzberg, M., & Lee, J. (2006). Motility influences biofilm architecture in *Escherichia coli*. *Applied microbiology and biotechnology, 72*(2), 361-367.

Wurpel, D. J., Beatson, S. A., Totsika, M., Petty, N. K., & Schembri, M. A. (2013). Chaperone-usher fimbriae of *Escherichia coli*. *PloS one, 8*(1), e52835.

Xie, Y., Yao, Y., Kolisnychenko, V., Teng, C. H., & Kim, K. S. (2006). HbiF regulates type 1 fimbriation independently of FimB and FimE. *Infection and immunity, 74*(7), 4039-4047.

Zaslaver, A., Bren, A., Ronen, M., Itzkovitz, S., Kikoin, I., Shavit, S.*, et al.* (2006). A comprehensive library of fluorescent transcriptional reporters for *Escherichia coli*. *Nature Methods, 3*(8), 623-628.

Zhao, R., Amsler, C. D., Matsumura, P., & Khan, S. (1996a). FliG and FliM distribution in the *Salmonella typhimurium* cell and flagellar basal bodies. *Journal of bacteriology, 178*(1), 258-265.

Zhao, R., Pathak, N., Jaffe, H., Reese, T. S., & Khan, S. (1996b). FliN is a major structural protein of the C-ring in the Salmonella typhimurium flagellar basal body. *Journal of molecular biology, 261*(2), 195-208.

Zhou, M., Duan, Q., Zhu, X., Guo, Z., Li, Y., Hardwidge, P. R., & Zhu, G. (2013). Both flagella and F4 fimbriae from F4ac+ enterotoxigenic *Escherichia coli* contribute to attachment to IPEC-J2 cells in vitro. *Veterinary Research, 44*, 30.

Zita, A., & Hermansson, M. (1997). Effects of bacterial cell surface structures and hydrophobicity on attachment to activated sludge flocs. *Applied and environmental microbiology, 63*(3), 1168-1170.

Zoltai, P. T., Zottola, E. A., & McKay, L. L. (1981). Scanning Electron Microscopy of Microbial Attachment to Milk Contact Surfaces (1). *Journal of food protection, 44*(3), 204-208.

Acknowledgements

“Nada que valga la pena en esta vida es fácil.”

Carlos Ruiz Zafón, La sombra del viento

Erklärung

Hiermit erkläre ich, dass ich die vorliegende Dissertation mit dem Titel:

„**Role of chemotaxis, cyclic-di-GMP and type 1 fimbriae in *Escherichia coli* surface attachment**“

selbstständig verfasst, keine anderen als die im Text angegebenen Hilfsmittel verwendet und sämtliche Stellen, die im Wortlaut oder dem Sinn nach anderen Werken entnommen sind, mit Quellenangaben kenntlich gemacht habe.

Die Arbeit wurde in dieser oder ähnlicher Form noch keiner Prüfungskommission vorgelegt.

Marburg,_____

_____

(María Esteban López)